ANALYSIS AND TESTING OF A WINTER OROGRAPHIC PRECIPITATION MODEL

by Mark D. Branson

Colorado State University

DEPARTMENT OF ATMOSPHERIC SCIENCE

PAPER NO. 505

ANALYSIS AND TESTING OF A WINTER OROGRAPHIC PRECIPITATION MODEL

(Thesis title: An Historical Evaluation of a Winter Orographic Precipitation Model)

Mark D. Branson

This report was prepared with support provided by
National Science Foundation Grants ATM-8813345,
ATM-8704776, ATM-8519370, and the Colorado
Agricultural Experiment Station, Hydrometeorology COL00113

Department of Atmospheric Science
Colorado State University
Fort Collins, Colorado 80523

May 1991

Atmospheric Science Paper 505

ABSTRACT

ANALYSIS AND TESTING OF A WINTER OROGRAPHIC PRECIPITATION MODEL

In the mid-1970's, an orographic precipitation model was developed by J. Owen Rhea in an effort to determine the ability to diagnose the effect of topography on winter precipitation for western Colorado. The model was tested for various time periods for differing wind regimes using upper air data and a fine-mesh topographic grid. The model is two-dimensional, steady state and multi-layer. Computations follow parcels at layer mid-points through topographically-induced moist adiabatic ascents and descents. The Lagrangian coordinate system allows for consideration of precipitation shadowing effects by upstream barriers.

The model was originally tested for 13 winter seasons and the results were well correlated to observed values of snowpack water equivalent and spring and summer runoff. Although large discrepancies often existed between model and observations on a daily basis, the model frequency distribution of daily precipitation totals was realistic.

This study attempted to update and improve the historical comparisons of model calculations to observations and also investigate the application of the model to current-season snowpack diagnosis and prediction. Model calculations were performed for the most recent 15

years of upper air data in addition to the 12 original seasons previously analyzed by Rhea (1978), and the correlation coefficients for model calculated precipitation values and the three observational types maintained good agreement throughout the 27 year historical period. Model calculations using an extended model winter season for the same 27 year period improved these comparisons for the precipitation gauges but had a slightly negative effect on the snowcourse and streamflow runoff relationships. When pre-model and post-model season observed precipitation data were included in the regression analysis for small basin streamflow runoff, some dramatic improvement in the correlations were noted in a few cases. The application of the model for "real-time" diagnosis of the seasonal snowpack was tested in the 1989-90 season and the results were comparable to the Soil Conservation Service predictions. Model calculations utilizing National Meteorological Center (NMC) gridded data as input were performed as a case study and the results were similar to the model calculations utilizing upper air data as well as to the observed precipitation values.

The positive results of this study encourage further use of the model for "real-time" snowpack monitoring. Further case studies should be performed to test the model's ability as a predictive tool. The application of interfacing the model to a hydrological process model coupled with improvements such as the use of finer scale topography might further improve spring and summer runoff predictions.

Mark Douglas Branson
Atmospheric Science Department
Colorado State University
Fort Collins, CO 80523
Spring 1991

ACKNOWLEDGEMENTS

I would like to thank my advisor, Professor Lewis Grant, for his helpful suggestions and for giving me the opportunity to work on this project. I would also like to extend my thanks to committee members Dr. William R. Cotton and Dr. Paul W. Mielke for their advice and encouragement.

I am also deeply indebted to the following individuals: Dr. David C. Rogers for his invaluable aid and support throughout the study; Kelley Wittmeyer for her indispensable assistance with the model code improvements; Dr. J. Owen Rhea for his patience in answering my numerous questions; Lucy McCall for drafting some of the figures and always willing to lend a hand; Jan Davis for her help in assembling the manuscript; and my parents, Garl and Mary Branson, for their enduring support and encouragement.

The funding for this research was provided by National Science Foundation Grants ATM-8813345, ATM-8704776 and ATM-8519370, and the Colorado Agricultural Experiment Station.

TABLE OF CONTENTS

1.0 INTRODUCTION

Accurate prediction and diagnosis of winter precipitation distribution in mountainous regions is of vital importance for avalanche prediction, highway maintenance, and water supply forecasting. The influence of terrain on precipitation in mountainous regions has been readily recognized but difficult to quantify.

In the mid 1970's, an orographic precipitation model was formulated by Owen Rhea as part of his dissertation (1978), the main objective of which was to determine the ability to diagnose the magnitude of topographic effects on winter precipitation for Colorado under varying wind regimes, using routinely available upper air data and a fine-mesh topographic grid. The model design was kept sufficiently simplistic to ensure quick computer execution time, which allows for processing of numerous historical cases for climatological purposes, and also allows the model to be used as an objective short-term forecasting aid.

In the original study the model was run for each of the winter seasons 1961-62 through 1973-74 from October 15 to April 30 (Rhea, 1978). The computations showed strong positive correlations with observed runoff and snowcourse water equivalent measurements. This led to the use of the model for such endeavors as avalanche forecasting in the Colorado Rockies as well as the adaptation of the model for other mountainous regions such as the Sierra Nevada of California and the Atlas Mountains of Morocco (El Majdoub, 1989).

The main objective of the research described in this paper is to improve the scientific understanding and diagnostic capabilities of predicting winter orographic precipitation. The first step toward this objective involved the installation of a current version of Rhea's model on a VaxStation 2000 computer system. Next, historical computations were performed and the resulting values were compared to observed records of snowcourse water equivalent, spring and summer runoff and precipitation gauge measurements. The period of record began with the 1961-62 winter season and continued through the 1987-88 season. This effectively extended the historical period of record from the 12 years of Rhea's original study (1978) to a total of 27 years. The historical computations were also performed with the winter season period redefined as September 1 to April 30 in an attempt to improve the correlations between model precipitation and the three aforementioned observational data types. Observed precipitation data for the early fall as well as late spring and early summer periods was combined with the model's October 15 through April 30 winter season calculations as a second method to try to improve the regression relationships to small basin streamflow runoff. Then, for the 1989-90 winter season, the model was run on a continuous basis and monthly reports were compiled coinciding with Soil Conservation Service Water Supply Outlooks to monitor the snowpack status. An investigation into the model's potential use as a forecast product was also undertaken using Nested Grid Model (NGM) gridded data as input as a substitute for the rawinsonde data.

2.0 OBJECTIVES

The specific objectives of this research are to (1) update the model historical computations as well as the comparisons of the model values to observed snowcourse, runoff and precipitation gauge data, (2) characterize the model's climatological distribution of precipitation with respect to time and space, (3) investigate the effects of extending the model run period and including the pre- and post-model season observed conditions on the historical statistical correlations, (4) study the potential for operating the model in a "real-time" mode to monitor the current year's snowpack during the course of a winter season, and (5) investigate the model's forecasting potential using Nested Grid Model (NGM) data as input.

3.0 BACKGROUND

For mountainous terrain, the total precipitation, R_T, can be broken down into 3 component processes via the equation

$$R_T = R_d + R_c + R_o$$

where

R_d = large-scale vertical motion precipitation component

R_c = convective precipitation component

R_o = orographic (forced lifting) precipitation component

These component processes have been discussed by Elliott and Shaffer (1962), Hjermstad (1970), Chappell (1970), and others. The following discussion provides a review of orographic precipitation studies and ways to quantitatively estimate the separate contributions of these three components.

In general, a most favorable condition for substantial orographic precipitation consists of strong winds moving deep layers of moist air up steeply sloping terrain. In terms of a generalized precipitation formula, the amount of precipitation is directly proportional to the vertical motion (w). While orographic vertical motion (10-100 cm/s) is generally an order of magnitude greater than large-scale vertical motion associated with baroclinic waves (1-10 cm/s), vertical motion in

embedded convection frequently exceeds 100 cm/s. However, orographic and convective element vertical motions are short time scale processes, whereas the large-scale vertical motion field slowly displaces large volumes of air for extended periods of time. Thus, each of the three components may have a considerable influence on the total precipitation process.

In most complex terrain areas, the topography tends to be the dominant factor because it provides a more persistent orographic vertical motion field and a forced lifting zone for release of convection. This effect is evidenced by ridge-to-valley precipitation ratios observed in western U.S. mountainous regions in the range of 2:1 to 10:1 (Hjermstad, 1970; Rogers, 1970; Rhea, et al. 1969; Elliott and Shaffer, 1962; Peck and Williams, 1962). The high variability in these ratios is partially due to periodic passage of meso-scale convergence bands (Elliott and Hovind, 1964; Rhea, et al. 1969) and varying wind direction effects on orographic precipitation patterns. Other complicating factors that arise in attempting to specify point precipitation amounts using a generalized formula such as the one above include "rain shadowing" effects of upstream topography, the complex and variable nature of the precipitation efficiency, and difficulties in model calibration due to increased errors in observed historical values of snowfall amount with increased wind speed.

Despite these and many other complexities inherent in attempting to quantify mountain precipitation, the design goal in the Rhea model was to concentrate on the effects of the dominant control factor, topography.

Many hydrologic studies in the mountainous western U.S. have utilized the observed precipitation increase with increasing elevation to develop local linear regression relationships between these two variables (Peck and Brown, 1962; Schermerhorn, 1967). Another study by Spreen (1947) used graphical multiple correlation of the terrain factors of elevation, slope and exposure to explain up to 88 percent of the variance in winter precipitation between selected stations in western Colorado. However, none of these studies attempted to directly relate these factors to any meteorological variables. In a study by Elliott and Shaffer (1962) in the Santa Ynez and San Gabriel Mountains of southern California, the correlation coefficients between observed and calculated hourly precipitation increased when such factors as stability, temperature (and therefore condensate supply rate) and wind speed and direction were included in a multiple regression formula as independent variables as a replacement for a theoretical equation.

Prior to the development of the Rhea model, a number of other orographic precipitation models had been developed. Many were two-dimensional with flow in the x-z plane (Myers, 1962; Sarker, 1967; Willis, 1970; Fraser et al., 1973; Plooster and Fukuta, 1974; and Young, 1974), a few were three-dimensional (Colton, 1975; Nickerson, et al., 1975) and at least one (Elliott, 1969) consisted of both two- and three-dimensional versions. Most of these two-dimensional models were steady-state and obtained a flow solution using perturbation theory with some basic assumptions (adiabatic flow, frictionless flow over a sinusoidal barrier, lower boundary streamline follows surface of ideal mountain). Exceptions are the solutions found in the Myers (1962) and Elliott (1969) two-dimensional models, which use the Bernoulli, mass

continuity, hydrostatic and thermodynamic energy equations to provide streamline configurations over barriers of arbitrary shape. The three-dimensional models have the advantage of more realistic simulation of the overall topographic effects of the flow, but have the disadvantage of computer execution times ranging from 10 to 100 times longer than most of the two-dimensional models which reduce their operational effectiveness.

The treatment of atmospheric water substance in these models varies from the assumption that all water which condenses also precipitates (Myers, 1962; Sarker, 1967; Colton, 1975) to rather complex cloud physics considerations (Young, 1974; Nickerson and Chappell, 1975). All of these models with the exception of those by Sarker (1967), Myers (1962) and Colton (1975) were primarily constructed as aids to physical understanding or weather modification research.

Both the Myers and (1962) Sarker (1967) models had good correlations of model computed to observed precipitation using upper air sounding data as input. In preliminary tests using the two-dimensional version of the Colton (1976) model, precipitation amounts computed for a watershed agreed well with observations.

Some more recent models have been developed since the completion of the Rhea model. A notable one is the Regional Atmospheric Modelling System (RAMS) currently in use at Colorado State University (CSU) (Cotton et al., 1986). The RAMS model performs explicit calculations of the precipitation physics. The RAMS' preprocessor software package allows for one, two or three dimensional use as well as various model physics options. Meyers (1989) used RAMS with full dynamics and

explicit microphysics to simulate an orographic precipitation event in the Sierra Nevada as part of the Sierra Cooperative Pilot Project (SCPP). Rauber (1981) developed a two-dimensional trajectory model as well as a crystal trajectory model to study the microphysical processes in two stably stratified orographic cloud system in the Park Range of Colorado as part of the Colorado Orographic Seeding Experiment (COSE). Cotton et al. (1982) also applied the CSU RAMS model to the same cloud system as Rauber (1981).

Research that directly lead to the development of the Rhea model included an empirical study by Wilson and Atwater (1972) that showed the importance of wind direction at hill-top level on precipitation patterns in Connecticut. A similar study by Rhea (1973) also demonstrated this effect for portions of mountainous southwest Colorado. A study by Rhea et. al. (1969) of western Colorado and extreme eastern Utah implied significant "rain-shadowing" effects of upstream barriers on downstream mountains and valleys for certain 700mb level (near mountain top) wind directions. Finally, a study preliminary to Rhea's dissertation (Rhea and Grant, 1974) demonstrated that a high correlation exits between certain western Colorado snowcourse water equivalent measurements and the influencing factors of upstream topographic slope, 700mb wind direction, and the number of upstream "shadowing" barriers. Hence, the original goal in developing the model was to determine the potential ability to quantify mountain precipitation in Colorado using only twice-daily upper air data and a fine mesh topographic grid as input.

4.0 MODEL DESCRIPTION

4.1 Guidelines

In keeping with the objectives to develop an operationally-oriented computational scheme for orographic precipitation for hydrological and/or climatological use, the key considerations in the design process were simplicity, quick computer execution time, and usage of routinely available data for model input. Highly realistic topography was also desired to adequately describe the marked variations in average precipitation that occur in regions of complex terrain over very short distances.

In choosing the coordinate system to be used for the model, the "rain-shadowing" effect of successive downstream barriers (Rhea and Grant, 1974) was an important consideration. Therefore, to monitor the atmospheric water budget, a Lagrangian coordinate system was adopted which follows the air parcels using steady-state, two-dimensional flow (i.e., horizontal flow only along the major current direction with vertical displacement by the underlying topography). While this choice for a coordinate system simplifies the water budget-keeping task, it also requires that the model's topography consists of grids unique to each 10° interval in wind direction for the entire grid area and that the model uses only one wind direction for the entire domain.

4.2 General Model Description

The model follows the interactions of air layers with the underlying topography by allowing forced vertical displacements of the

air column, keeping track of the resulting condensate or evaporation. The lifting process is assumed to be moist adiabatic. The lifting due to the large scale vertical motion is considered to be linearly additive to the topographic lift. As the layers flow across the region, part of the condensate precipitates. Evaporation of falling precipitation is taken into account in regions of subsidence and precipitation falling into subsaturated layers. This effectively decreases the amount of precipitation reaching the ground and also moistens the subsaturated strata. Eventually, a fraction of the precipitation generated in the highest layers, given by the efficiency factor E, reaches the ground provided it does not totally evaporate. The remainder of the condensate that does not precipitate is advected downwind where it is added to the locally produced condensate.

Using steady-state, two-dimensional flow and the spatially constant precipitation efficiency, E, the computational formula for the precipitation rate, r, along grid interval x is:

$$(r_{I,I+1})_{\ell} = \frac{EV_{\ell}\Delta P_{\ell}}{\rho_w g \Delta x} (Q_I + \Delta C_{I,I+1})_{\ell} , \qquad (4\text{-}1)$$

where

ℓ = computation layer index

V_{ℓ} = the horizontal wind speed in the x direction at the upwind edge of the computational area

ΔP_{ℓ} = pressure thickness of the inflowing layer at the upwind edge of the computational grid

Q_I = cloud water content (mixing ratio) of liquid or solid at grid point I

$\Delta C_{I,I+1}$ = additional condensation (or evaporation) due to

vertical displacement between points I and I+1. In the event that this term is evaporation and is numerically greater than Q_I, precipitation is zero.

E = precipitation efficiency

ρ_w = density of water (1 g cm^{-3})

This formulation combined with separate topographic grids for each wind direction allows for the "rain-shadowing" effects of upstream barriers. A more detailed description of each of the terms in the equation is seen below.

4.3 Topography, Study Area and Data Input

Figure 1 displays the study area, upper air sounding station locations and the border interpolation points. Upper air sounding data are taken from the six stations shown in Figure 1: Denver, CO; Grand Junction, CO; Lander, WY; Salt Lake City, UT; Albuquerque, NM; and Winslow, AZ. Pressure height, temperature and relative humidity along with wind speed and direction are input at 50mb intervals from 850mb to 300mb for each station, and values are interpolated using the method of Panofsky (1949) for the 10 border points of the study area and an additional point located at the center of the study area. The wind direction at the center determines the topographic grid for the current sounding period. Before the interpolation procedure, some of the humidity values must be adjusted due to lag effects of the various sensing elements used in the rawinsondes in the early 1960's.

The topographic grids cover the 60,000 square mile area from 105 to 109 degrees west longitude and 37 to 41 degrees latitude. A 2.5 km horizontal resolution elevation grid was constructed from 1/500,000 or 1/250,000 scale topographic maps, with elevation values estimated to

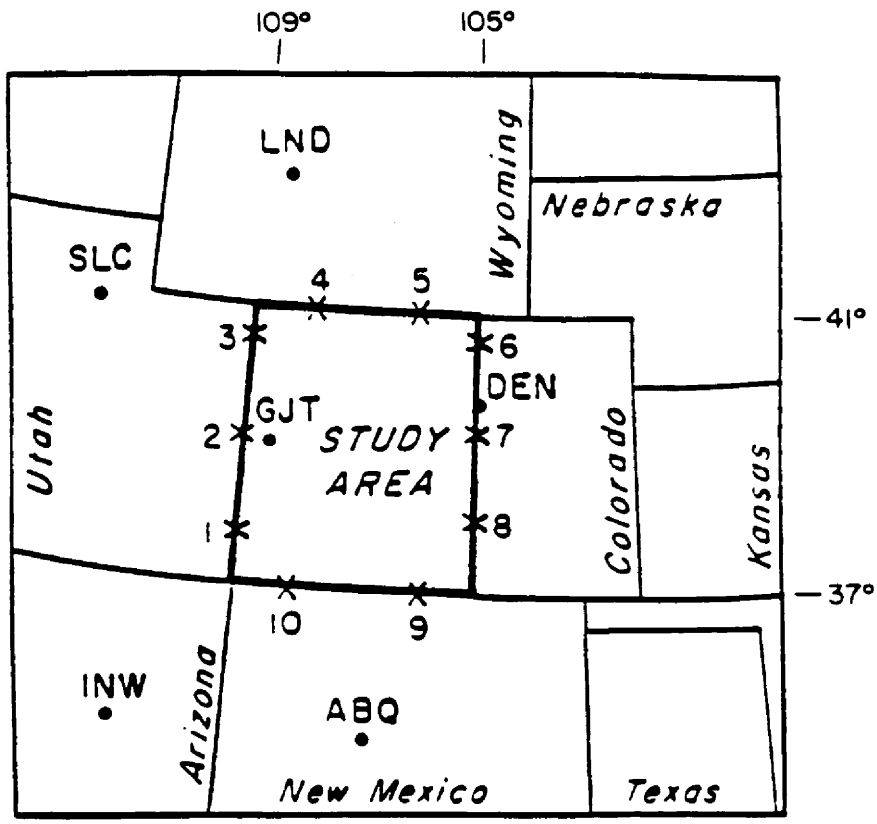

Figure 1. The study area, border interpolation points and available upper air stations (Rhea, 1978)

the nearest 100 feet. The 36 rotated grids for each 10 degrees of wind direction were made by overlaying the original 2.5 x 2.5 km elevation grid and using inverse distance squared interpolation (see Figure 2). 5 x 5 km grids were then constructed by taking the average of the 9 values of elevation from the 2.5 x 2.5 km grid points. Similarly, the 10 x 10 km grids were made by averaging the 25 values of elevation from the 2.5 x 2.5 km grid points. Figure 3 shows the model topography using the 10km by 10km grid spacing. The model produces a precipitation grid for this area defined by 35 points east-west and 45 points north-south. The marginal gain in overall areal-total precipitation accuracy using the 5 x 5 km grids was overshadowed by the quadrupled computer execution time as compared to the 10 x 10 km grids, so the 10 x 10 km grids were used for the model computations.

Since total precipitation at a point results from the combination of orographic effects, convective release, and large scale vertical motion, the large scale vertical motion values for each sounding period are estimated using the Bellamy technique (Bellamy, 1949). This technique uses the areas of five triangles formed by the six sounding stations. The resulting vertical motion profiles are corrected by the method of O'Brien (1970).

4.4 Model Physics

This section describes the development of the general precipitation formula from section 4.2. The major components are discussed in detail along with some parameter sensitivity and calibration tests.

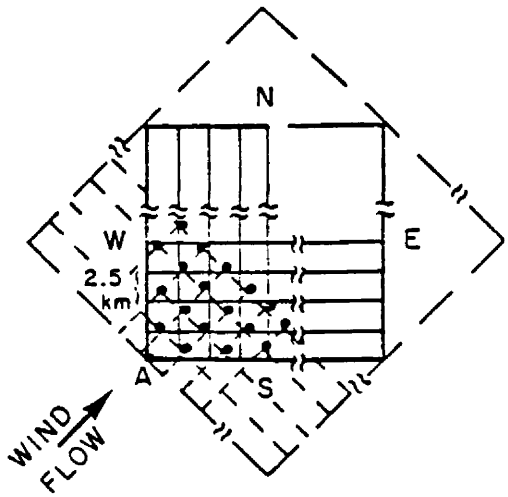

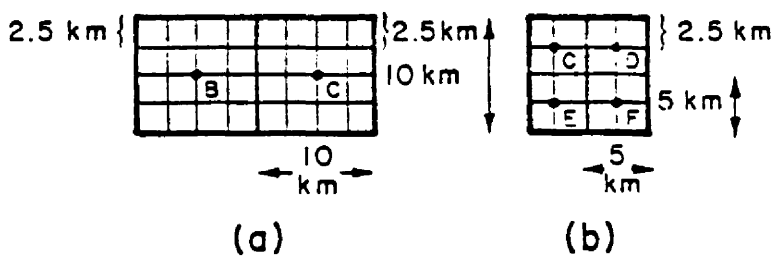

Figure 2. The averaging method for generating 10 x 10 km and 5 x 5 km elevation grids (Rhea, 1978)

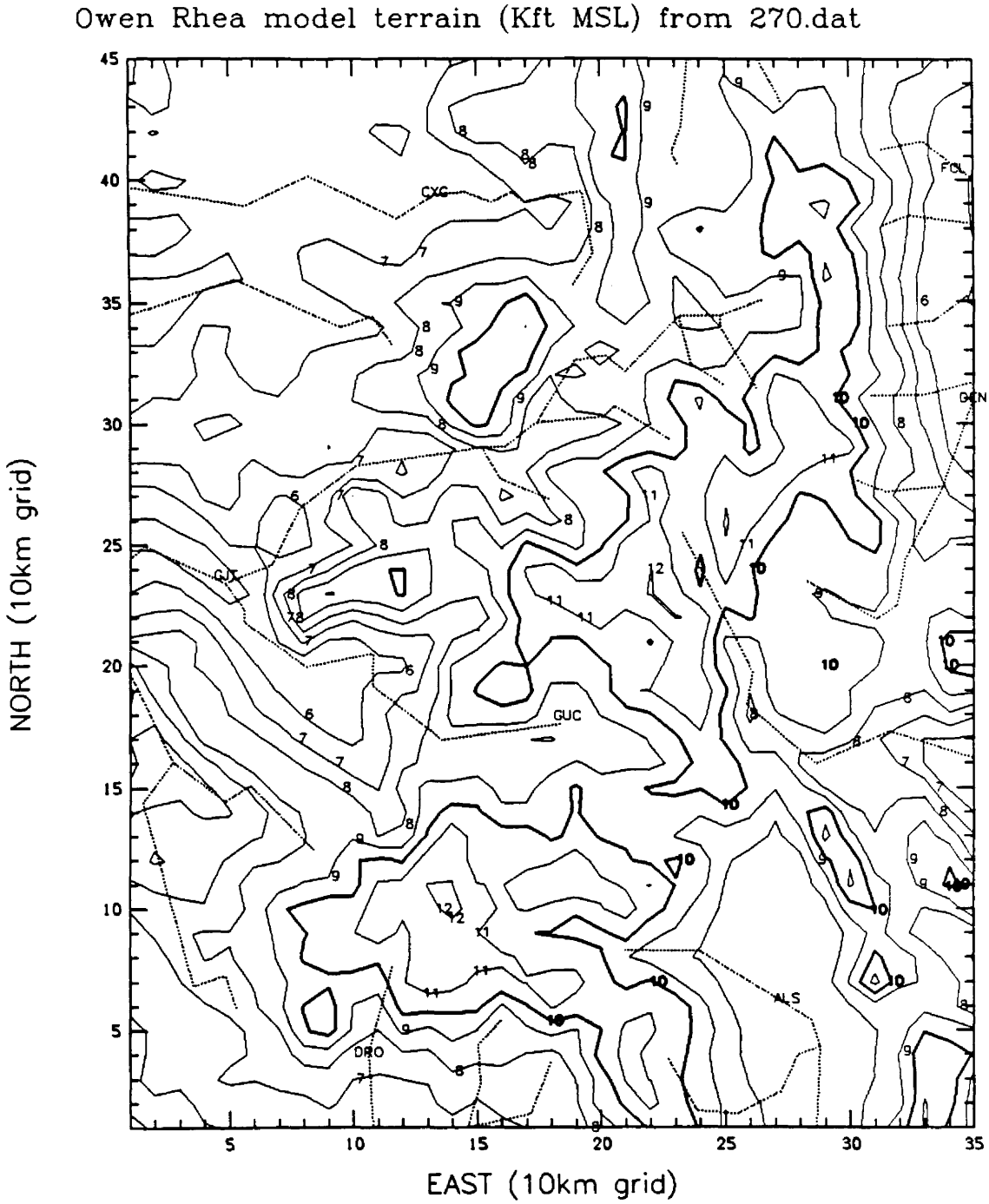

Figure 3. Model topography with 10 km grid interval (thousands of feet)

4.4.1 Flow Direction

For each 12 hour sounding period, the model selects one topographic grid to be used for the calculations by rounding the 700mb wind direction interpolated at the center of the study area to the nearest 10 degrees. The air streams are then assumed to flow along the grid lines of the topographic grid selected with no cross-current deflection allowed. To account for directional shear with height, only the component of the wind at each 50mb level that is along the direction of the topographic grid being used is considered in the model calculations.

4.4.2 Blocking

When a stable air mass flows toward a major barrier, the flow in the lower layers is often observed to turn and flow either parallel to the barrier or in the reverse direction. This has the effect of producing a stagnant or "blocked" layer with respect to the transbarrier wind component in the two-dimensional flow.

Elliott (1969) referred to such blocked strata as "dead" layers where either inversions existed over a 50mb layer or the transbarrier wind component was less than or equal to zero. For the Rhea model, a "dead" layer was designated when either the mean layer transbarrier wind was less than 2.5 m/s or $\partial T/\partial P$ less than (0.4K / 50mb) and all lower layers also met these criteria. Tests for these conditions were made for 25mb thick layers starting with the surface-based layer and working upward.

In parameter sensitivity testing of these conditions, it was found necessary to make two modifications to the testing criteria. The first was to always consider the layer below 800mb level to be blocked in all

cases. Most of the upper air sounding stations are at approximately the 840mb level during the winter. Without this additional criteria, overprediction of precipitation occurred on barriers rising abruptly from deep, broad river valleys such as the Grand Mesa in Figure 3. The second modification was to always set the blocked layer top at 800mb for interpolation points 3, 4 and 5 in west to west-northwest flow. Under these flow conditions, a moderate to strong sea-level pressure gradient is typically observed to develop across Wyoming and extends into northern Colorado while very weak flow is observed over central and southern Colorado. Consequently, the Grand Junction (GJT) radiosonde frequently indicates either temperature inversions or isothermal vertical structure with light and variable winds to approximately 700mb under these conditions. The upper air interpolation scheme weighs this stagnant GJT condition too heavily when computing the wind and temperature profiles for border points 3, 4 and 5, resulting in unrealisitically deep blocked layers.

4.4.3 Streamline Vertical Displacement

When stable air is forced to rise over a barrier, a wave disturbance is created whereby the induced vertical motion decreases with height, possibly even reversing in sign. Formulations derived to quantitatively describe the resulting vertical displacement of streamlines (Elliott, 1969; Myers, 1962; Fraser et al., 1973) are quite sensitive to the static stability profile (i.e., whether the air stream is dry or saturated). This sensitivity is critical when dealing with moist winter air masses flowing across complex terrain because of their nearly moist adiabatic lapse rates (i.e., moist static stability near zero). Some exhibit slight conditional instability, in which case

lifting over the higher terrain may release convection and thus invalidate the forced wave mode equations for the streamline vertical displacement.

Despite the complicated nature of streamline vertical displacement, some simple criteria were adopted in the development of the Rhea model to be consistent with the operationally-oriented goal of the model design. Three classes of streamline vertical displacement were defined based on certain stability and humidity characteristics of the "undisturbed" air stream.

Upper air and precipitation data for one winter season (1970-71) were studied for Colorado to help develop the criteria. It was found that virtually no precipitation occurred even at high mountain locations if the maximum relative humidity on the Grand Junction sounding was less than 65 percent. The amount of terrain relief between the typical top of the blocked layer and mountain top level is 1500 meters, whereas only approximately 600 meters of lifting is required to bring air of 65 percent relative humidity to saturation. Based on these data, the highest potentially precipitating cloud layer (ℓ_T) was defined as the highest layer with $\geq$ 65 percent relative humidity which is also not undercut by any lower layer of $<$ 50 percent relative humidity, and the vertical displacement of that layer streamline, Δh_T, is 600/1500 (or 0.4) of the surface streamline displacement (Δh_o). The surface streamline is assumed to follow either the terrain or the upper surface of the dead layer, whichever is highest. Two exceptions were allowed to this basic criterion. First, if an inversion exists above layer ℓ_T, the streamline displacement of ℓ_T was assumed to be zero ($\Delta h_T = 0$). Second, if no inversion exists

above layer ℓ_T and the temperature difference between 500mb and 700mb (i.e., the environmental lapse rate) is near the moist adiabatic value, the streamline vertical displacement Δh_T was set to 0.7 Δh_o except over the the highest terrain, where $\Delta h_T = 1.2\ \Delta h_o$ to crudely simulate convective release over the highest terrain.

Displacement Δh_i of the intermediate layers was assumed to vary linearly with pressure between Δh_T and Δh_o

$$\Delta h_i = \Delta h_o \left[1 - \left[1 - \frac{\Delta h_T}{\Delta h_o} \right] \left[\frac{P_o - P_i}{P_o - P_T} \right] \right] . \qquad (4\text{-}2)$$

Since $\Delta h_o = Z_{I+1} - Z_I$, we can simplify by writing

$$\Delta h_i = (Z_{I+1} - Z_I)d , \qquad (4\text{-}3)$$

where

$$d = 1 - \left[1 - \frac{\Delta h_T}{\Delta h_o} \right] \left[\frac{P_o - P_i}{P_o - P_T} \right] . \qquad (4\text{-}4)$$

Table 1 summarizes the three criteria.

The difference in precipitation between the three classes for streamline vertical displacement is shown in Figure 4 using the same atmospheric sounding (Figure 5). Also shown for comparison is a run with d = 1 (no damping) for all levels. This figure shows that the inversion case results in much lower precipitation amounts over the higher terrain when compared to the stable with no inversion case, whereas the unstable case increases the high mountain precipitation to nearly the amounts achieved with the d = 1 case.

4.4.4 Orographic Precipitation Computation

A schematic diagram of steady-state, two-dimensional flow over a barrier with streamlines N_1 and N_2 is shown in Figure 6. The atmospheric water balance equation for the region between x_o and x_1

Table 1

Streamline Vertical Displacement Classes

STABILITY CLASS	DISPLACEMENT OF "CLOUD TOP" STEAMLINE (Δh_T)
(a) INVERSION ABOVE "CLOUD TOP"	0
(b) STABLE 500MB - 700MB TEMPERATURE NO INVERSION ABOVE CLOUD TOP	$0.4\Delta h_o$
(c) APPROXIMATELY NEUTRAL STABILITY 500MB TO 700MB LAYER NO INVERSION ABOVE CLOUD TOP	$0.7\Delta h_o$ ($1.2\Delta h_o$ OVER HIGHEST TERRAIN)

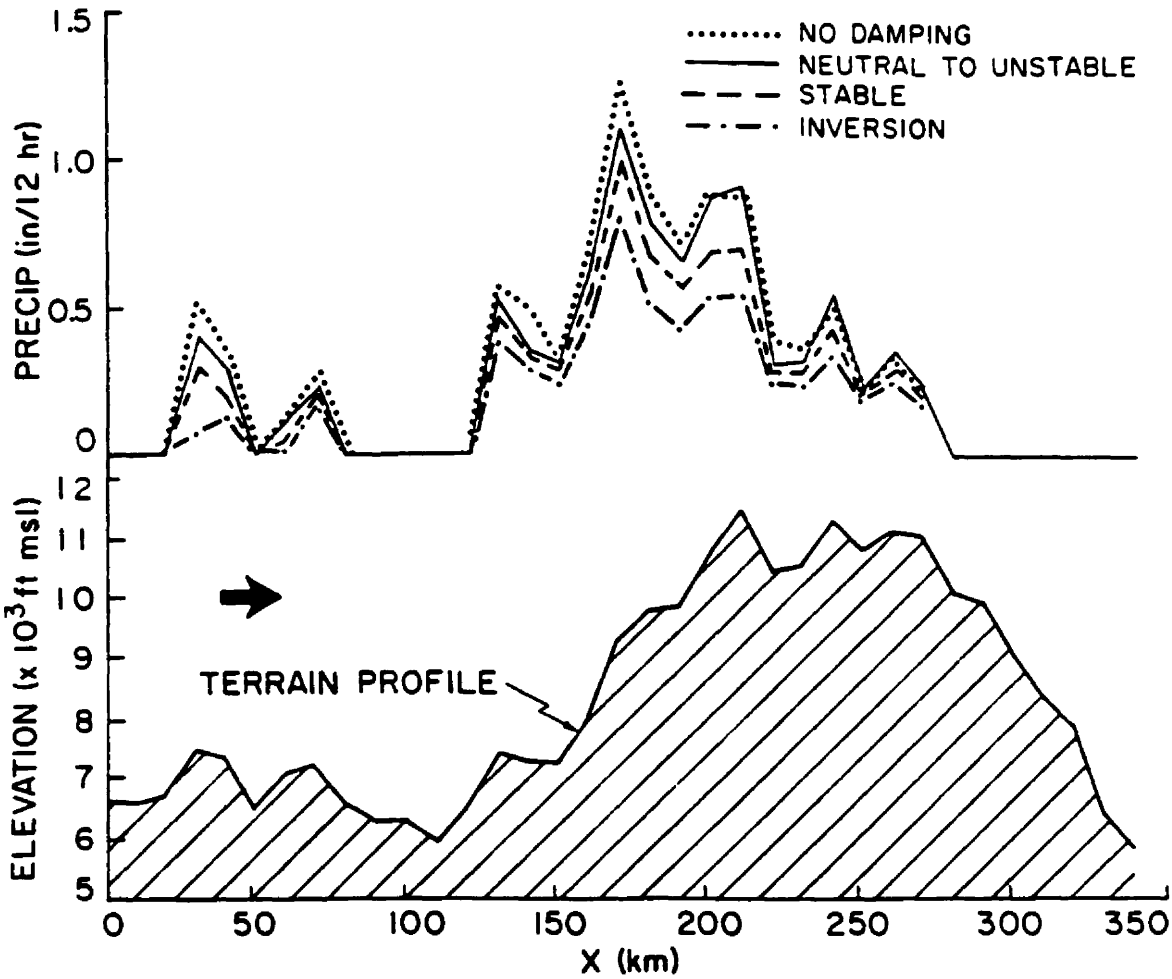

Figure 4. Examples of model sensitivity to streamline vertical displacement classes (Rhea, 1978)

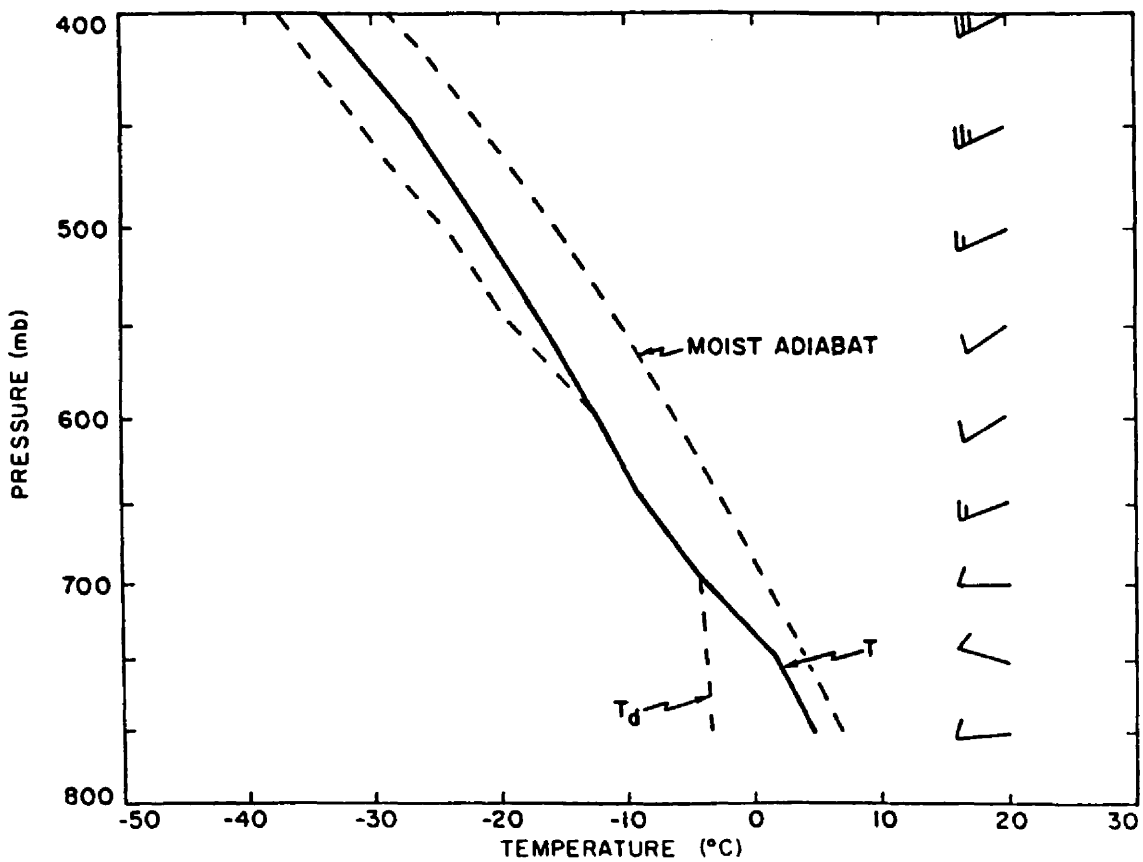

Figure 5. Hypothetical sounding used to make sensitivity tests (Rhea, 1978)

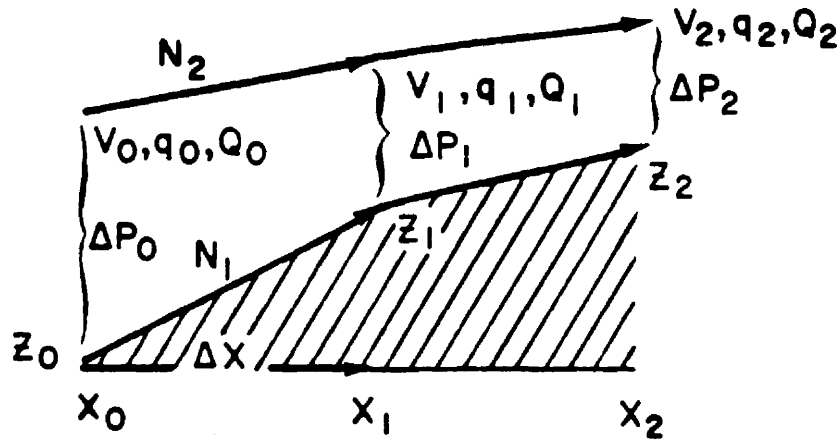

Figure 6. Symbolic two-dimensional flow across a barrier (Rhea, 1978)

(Rhea, 1978) can be written as

$$r_{o,1} = \frac{1}{\rho_w g \Delta x}\left[(q_o + Q_o)\frac{\Delta P_o V_o}{g} - (q_1 + Q_1)\frac{\Delta P_1 V_1}{g}\right] \qquad (4\text{-}5)$$

where surface evaporation has been neglected and where

$r_{o,1}$ = average precipitation rate over the distance, Δx, between grid points 0 and 1

q = layer mean water vapor specific humidity ($\approx$ mixing ratio)

Q = layer mean cloud water (liquid or solid) specific humidity ($\approx$ mixing ratio)

ΔP = layer thickness (in pressure units)

V = mean horizontal velocity of layer

g = gravity

ρ_w = density of water (1 g cm^{-3})

Neglecting water substance changes, the continuity equation for two-dimensional, steady-state, hydrostatic flow can be written

$$\frac{\Delta P_o V_o}{g} = \frac{\Delta P_1 V_1}{g} = \frac{\Delta P_2 V_2}{g} . \qquad (4\text{-}6)$$

Therefore, in general, equation (4-5) can be written

$$r_{o,1} = \frac{\Delta P_o V_o}{\rho_w g \Delta x}\left[(q_o + Q_o) - (q_1 + Q_1)\right] . \qquad (4\text{-}7)$$

The lifting process is assumed to be moist adiabatic, so as the parcel moves from point I to I+1

$$q_{I+1} - q_I = \frac{dq_s}{dz} d(Z_{I+1} - Z_I) , \qquad (4\text{-}8)$$

where

$\frac{dq_s}{dz}$ = the rate of change of parcel saturation water vapor mixing ratio per unit of lift

$d(Z_{I+1} - Z_I)$ = the parcel vertical displacement between point I and I+1.

From the streamline vertical displacement equation (4-3)

$$\Delta h_{I,I+1} = d(Z_{I+1} - Z_I) \quad . \tag{4-9}$$

By continuity, the condensation per unit mass ($\Delta C_{I,I+1}$) that occurs as the parcel moves from I to I+1 can be defined as

$$\Delta C_{I,I+1} = q_I - q_{I-1} = - \frac{dq_s}{dz} (\Delta h_{I,I+1}) \quad . \tag{4-10}$$

By specifying that a constant fraction, E, of the sum of the condensate formed ($\Delta C_{I,I+1}$) and imported (Q_I) precipitates over the distance Δx, the remaining cloud water (Q_{I+1}) at point I+1 is

$$Q_{I+1} = (1 - E)Q_I + (1 - E)\Delta C_{I,I+1} \quad . \tag{4-11}$$

Substitution of equations (4-10) and (4-11) into equation (4-7) yields

$$r_{I,I+1} = \frac{\Delta P_o V_o}{\rho_w g \Delta x} \left[E(Q_I + \Delta C_{I,I+1}) \right] \quad . \tag{4-12}$$

For parcel descent, water saturation is maintained by evaporating cloud water contained in the layer into the parcel as long as (Q_I + $\Delta C_{I,I+1}$) ≥ 0. If the descent is sufficient to evaporate all of the imported cloud water, further descent is still done moist adiabatically and a saturation deficit or negative cloud water content is generated. If this occurs, then

$$r_{I,I+1} = 0 \tag{4-13}$$

$$Q_{I+1} = Q_I + \Delta C_{I,I+1} \tag{4-14}$$

The computations are made using the three equations (4-12), (4-13), and (4-14) following the parcel for the pressure midpoint of

each layer by iterating the horizontal index I to move to each successive grid point.

These equations allow for the partial removal of the parcel water over each barrier which effectively raises the cloud base over successive downstream barriers (i.e., greater vertical displacement is required to attain saturation). Thus, the "shadowing" effect is taken into account quantitatively in the model.

4.4.5 Large Scale Vertical Motion

For the Rhea model, the large scale vertical motion was considered to be linearly additive to the topographically-induced vertical motion. Thus, in equation (4-9), the vertical displacement due to large scale vertical motion ($\Delta Z_{\ell.s.}$) that occurs in the region Δx is added to the topographic displacement ($\Delta h_{I,I+1}$), with the result

$$Q_{I+1} = (1 - E)\left[-\frac{dq_s}{dz}(\Delta h_{I,I+1} + \Delta Z_{\ell.s.}) + (1 - E)Q_I\right] \qquad (4\text{-}15)$$

when using equations. (4-10) and (4-11). Values for large scale vertical motion were estimated from the sounding data using the Bellamy (1949) technique.

Figure 7 shows the effect of large scale vertical motion on precipitation profiles. With regards to the orographic precipitation equation, the large scale vertical motion had to be less effective in minimizing "shadowing" effects for strong wind as compared to slow wind cases. Downward values of w would not only intensify the "shadowing" effect but also present the problem of potential subterranean sinking parcels. Thus, the w values are restricted to be greater than or equal to zero.

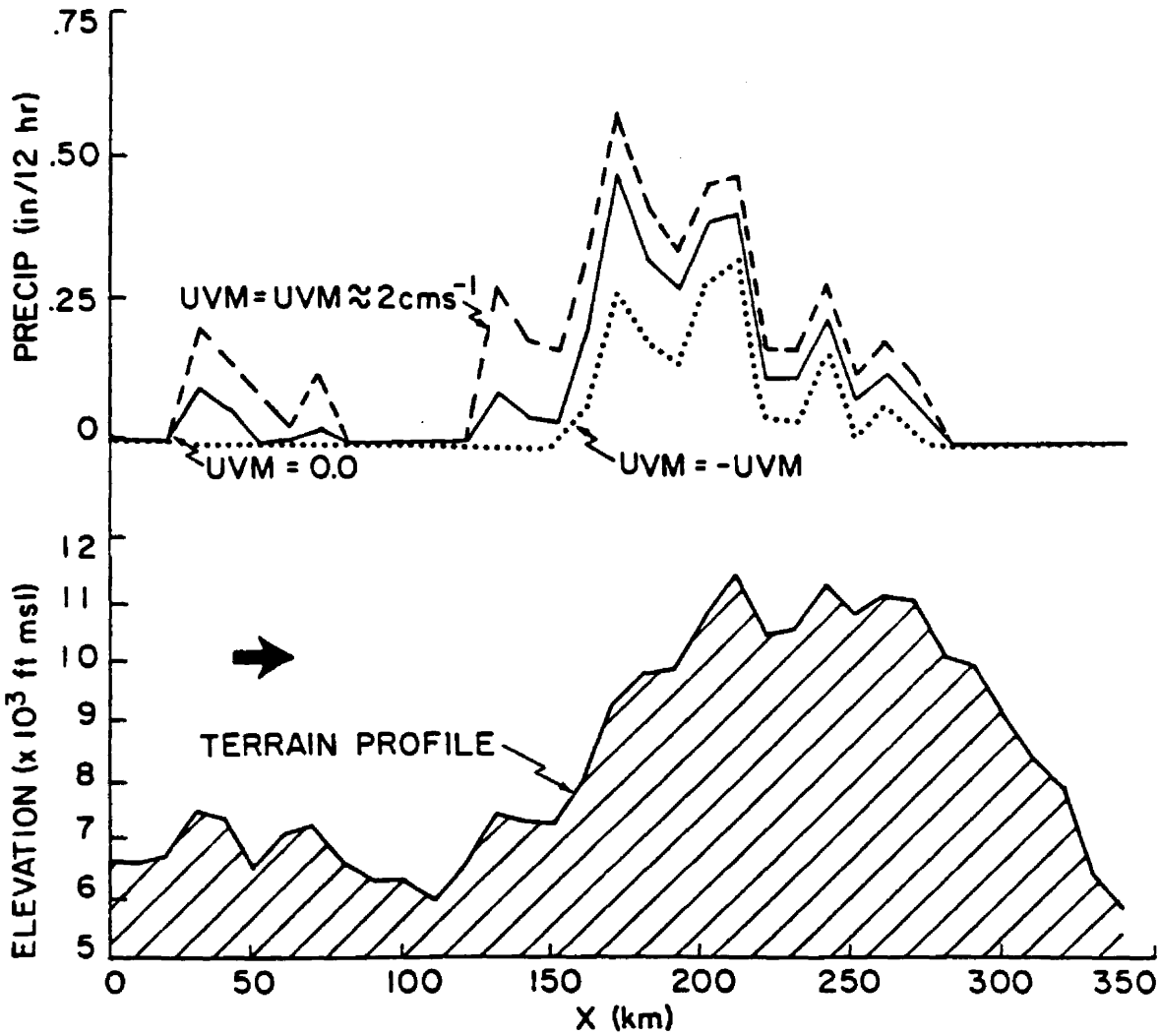

Figure 7. Examples of model sensitivity to large-scale vertical motion (UVM = upward vertical motion) (Rhea, 1978)

As a sensitivity test, model-calculated precipitation amounts in 19 small basins for the 1965-66 winter season using the vertical motion values obtained with the Bellamy technique (with the criteria $w \geq 0$) were compared with the precipitation amounts for the same season when forcing $w = 0$. The result was an average precipitation decrease of 23 percent for the $w = 0$ case. Thus, for the Rhea model, the large scale vertical motion field is quite important in lifting parcels back to saturation following passage of the airstream over an initial high barrier.

4.4.6 Precipitation Efficiency

Natural precipitation efficiency (E) is a complex and elusive factor to quantitatively determine. It is as dependent on the temporal and spatial dimensions of the saturated flow and the mountain geometry as well as on the microphysical properties of the cloud. Representative values of E have been intensively sought in a number of studies to assess weather modification potential, and the resultant values have ranged from near zero to one (Elliott and Hovind, 1964; Auer and Veal, 1970; Chappell, 1970; Dirks, 1973; Young, 1974; Hindman, 1982). For this model, the input data is upper air soundings, which are of such coarse spatial and temporal resolution that they cannot accurately specify cloud microphysical characteristics or cloud geometry.

However, two macrophysical parameters that influence E that the upper air data provide are wind speed and temperature. For clouds of limited geographical extent, E should be negatively correlated to cloud top temperature T_c (i.e., the colder the temperature, the greater number of active ice nuclei). However, the wind speed dependence is not so clear-cut. On the one hand, it seems that E should be inversely

proportional to V, because as the wind speed increases, there is less crystal residence time available in the cloud. On the other hand, other studies (Rhea, 1973; Elliott and Shaffer, 1962; Nielsen, 1966) suggest that E should have no dependence on the wind speed, since condensate supply rate is directly proportional to V. Since not enough cases were available to empirically study the dependence of E on both T_c and V, the calibration of E was restricted to the temperature effects alone.

Various precipitation functions were tested using two years worth of data (1965-66 and 1970-71). Some sample output for various E values are shown in Figure 8. The precipitation "shadowing" effect by the upstream barriers becomes rather severe for the higher efficiency values. For the two test seasons, the equation

$$E = -0.01\ T_c \qquad (4\text{-}16)$$

(where T_c is in degrees Celsius) gave the best areal distribution of seasonal precipitation for all regions of the study area on comparison to a group of snowcourse values. Therefore, this equation is used in the model with the sole limitation that $E \leq 0.25$ to prevent over-shadowing effects at colder cloud top temperatures.

4.4.7 Layer Computations

The individual layers can moisten or dry by vertical displacement as a result of the topography and large scale vertical motion field. They can also moisten by precipitation that falls from higher layers above. This effect is taken into account in the vertical layer computations for each grid point by working downward from the highest layer to the lowest.

Figure 8. Examples of model sensitivity to precipitation efficiency (Rhea, 1978)

Under this scheme, evaporation of falling precipitation into unsaturated lower layers (i.e., subsaturated with respect to water) moistens these strata and decreases the precipitation reaching the ground. If the lower layer saturation deficit is large enough to evaporate all the precipitation falling into it, the change in that layer's vapor mixing ratio is given by

$$(\Delta q_{I,I+1})_{evap_1} = \frac{EV_2\Delta P_2}{V_1\Delta P_1}\left[Q_{I_2} + (\Delta C_{I,I+1})_2\right] , \tag{4-17}$$

where the subscript "2" refers to the higher layer and "1" to the subsaturated lower layer. The ratio V_2/V_1 corrects to unit mass of air for layers moving at different speeds because the upper precipitating layer will more effectively moisten the subsaturated lower layer if $V_2 > V_1$ than if $V_2 = V_1$ (assuming laminar flow). The ratio $\Delta P_2/\Delta P_1$ corrects to unit mass of air for layers of different thickness. In this case,

$$(Q_{I+1})_1 = (Q_I)_1 + (\Delta C_{I,I+1})_1 + (\Delta q_{I,I+1})_{evap_1} \tag{4-18}$$

$$(r_{I,I+1})_{BASE_1} = 0 . \tag{4-19}$$

On the other hand, if $(r_{I,I+1})_2$ is more than sufficient to saturate layer 1, then the precipitation falling through the base of layer 1 is given by

$$(r_{I,I+1})_{BASE_1} = (r_{I,I+1})_2 + \frac{V_1\Delta P_1}{\rho_w g\Delta x}\left[Q_{I_1} + (\Delta C_{I,I+1})_1\right] . \tag{4-20}$$

After this computation is made, $(Q_{I+1})_1$ is set to zero because the precipitation from layer 2 has saturated layer 1, thereby removing its saturation deficit at I+1.

4.4.8 Initialization at the Upwind Borders

Before beginning the precipitation computation for each line of topography, each layer's initial saturation content or deficit has to be determined. For each layer, a minimum elevation (MELV) over which the air parcel would be required to flow was defined by computing the lifting condensation level (LCL) and adding to it the elevation of the top of the blocked layer.

If the elevation of the first point of topography was less than MELV, an initial negative amount of condensate (saturation deficit) was computed for such a layer, ℓ, as

$$(Q_o)_\ell = - \frac{dq_s}{dz} (z_o - \text{MELV}) \qquad (4\text{-}21)$$

However, if the elevation of the first point of topography was greater than MELV, the amount of condensate present in the layer was computed by assuming an arbitrary terrain upslope of 0.01 to exist upwind of the border which generates condensate as the air climbs the slope. For certain border points of the study area, this method of computation sometimes produced large, unrealistic amounts of precipitation along the upwind edge of the computational area.

5.0 MODEL EVALUATION

5.1 Research Approach/Analysis Procedures

For this portion of the study, upper air sounding data (0000 UTC and 1200 UTC) for the six upper air stations (ABQ, DEN, GJT, INW, LND, SLC) were obtained from the National Center for Atmospheric Research (NCAR) data archives for the study period (1961-62 to 1987-88). The model was run from October 15 through April 30 for each of the 27 seasons at each sounding time. To avoid overprediction, the period of representativeness of each sounding was taken to be 10 hours, as was done in Rhea's original study.

Note that the original study years (1961-62 through 1973-74) from Rhea's dissertation (1978) are included as part of this study for the purpose of obtaining consistent results for the entire 27 year period. Also, some minor changes have been made in the model code since the original results were published, but the effect of these coding changes on the resulting precipitation grids was expected to be small, showing only a slight increase in the total precipitation amount (personal communication with O. Rhea, 1989). Thus, comparison of the isohyetal plots shown in the dissertation to the ones obtained in this study is possible for verification of proper model performance, while any effects of the coding changes can still be accounted for.

Three observational data types were available to evaluate the model performance for the 27 year study:

1) Daily precipitation gauges

2) United States Department of Agriculture (USDA) Soil Conservation Service (SCS) Snow Survey snowcourse water equivalent records (Feb 1, Mar 1, Apr 1, May 1)

3) United States Geological Survey (USGS) Streamgauge records

Model computations for point locations (snowcourses and precipitation gauges) were performed by first converting the site's latitude and longitude into model specific coordinates. Inverse-distance-squared interpolation of the four surrounding model grid points was then used to determine the precipitation amount. Computations for watershed and snowcourse areas within the model domain were calculated by areally integrating the model calculations for a specified group of grid points with attached weighting factors yielding both a precipitation depth and volume amount.

5.2 Historical Computations

Isohyetal plots were constructed from the 35 x 45 grids for each of the 27 winter seasons' cumulative (October 15 - April 30) precipitation. The grid values for the initial study years exhibited the slight expected increase in total precipitation as mentioned above, but otherwise were in good agreement with Rhea's (1978) plots. This provided assurance that the improved version of the model was working properly.

Figure 9 displays the record of cumulative precipitation in monthly increments over the entire model domain for each water year in the study period (1961-62 to 1987-88). The x-axis values indicate the water year end (i.e. 62 = 1961-62 water year). October and November precipitation were combined since October is normally a relatively dry month and only the last half of it (October 15-31) is included in a

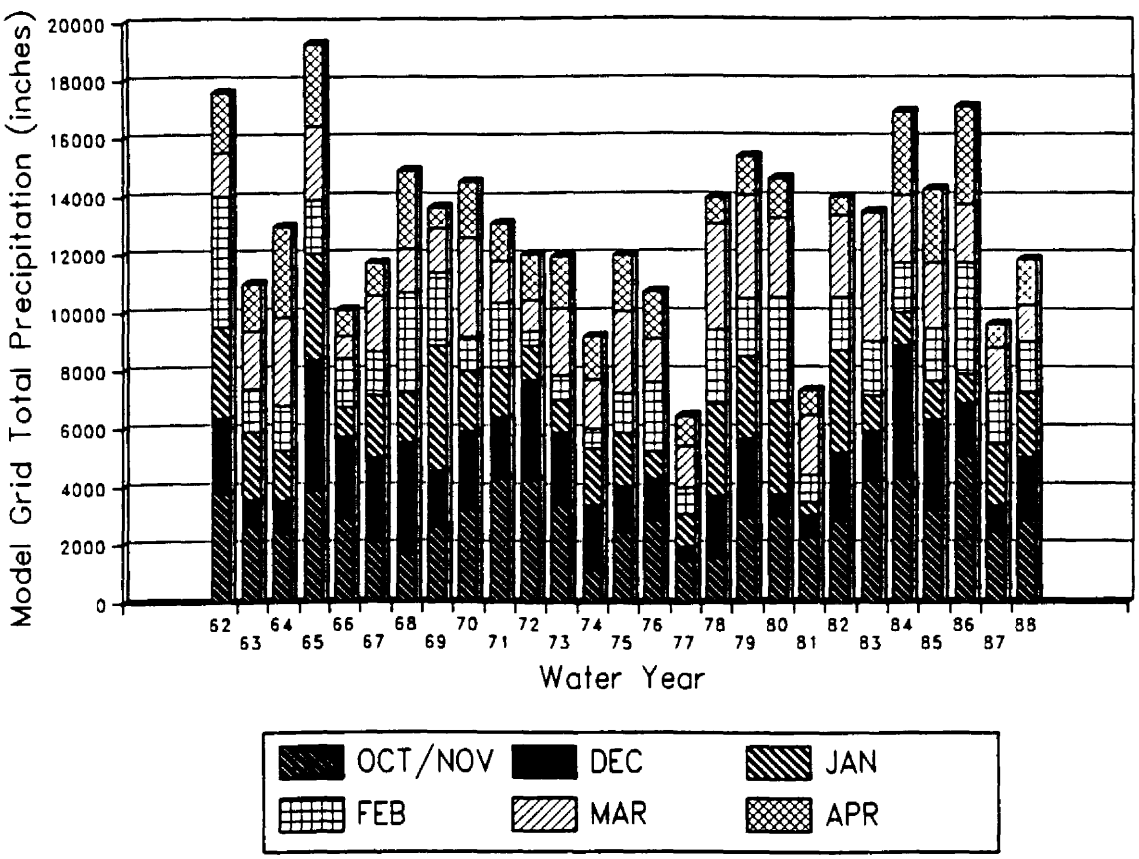

Figure 9. Model grid total precipitation shown in monthly increments for the 27 year study period

model run period. The annual grid total average for the 27 year period is 13,048 inches.

Table 2 displays the model averages and standard deviations for each month's grid total precipitation. According to the model, December is the wettest month on average with 2241 inches but it also has the greatest variability with a standard deviation of 1066 inches. The next wettest month is March with 2218 inches, followed by November with 2035 inches and January with 2032 inches. The driest month (not including October since only half of this month is included in the water year period) is April, which received only 1654 inches on average.

Examples of isohyetal water year plots of model precipitation for 1984-85, 1985-86 and 1986-87 are shown in Figures 10 through 12. Seasonal variations for the entire study area as well as regional differences are evident in these figures. Figure 9 shows that the 1985-86 and 1986-87 consecutive water years were somewhat extreme relative to the other years of the study. 1985-86 was wet and 1986-87 dry. The grid total precipitation for the 1985-86 season was 16,590 inches which is 22% above normal, whereas only 9165 inches were tallied for the 1986-87 season, which is 32% below normal. The model's results are consistent with the SCS measurements, as reported in Colorado-New Mexico Water Supply Outlook: "statewide snowpack is 26 percent above normal" (1986), and "Colorado's snowpack figures decreased ... to only 74 percent of average" (1987). These figures confirm the model's ability to predict inter-seasonal changes as had been shown in the original study. An example showing areal differences can be seen by comparing the isohyetal plots from 1984-85 and 1985-86,

Table 2

Model Precipitation Statistical Summary

Month	Average	Standard Deviation	Maximum	Minimum
OCT	918"	955"	2333" (1971-72)	121" (1977-78)
NOV	2035	916"	4555" (1985-86)	878" (1980-81)
DEC	2241"	1066"	4557" (1983-84)	523" (1976-77)
JAN	2032"	971"	4359" (1968-69)	478" (1980-81)
FEB	1952"	954"	4520" (1961-62)	539" (1971-72)
MAR	2219"	878"	4517" (1982-83)	797" (1965-66)
APR	1654"	832"	3423" (1985-86)	651" (1981-82)
total	13050"	2955"	19323" (1964-65)	6585" (1976-77)

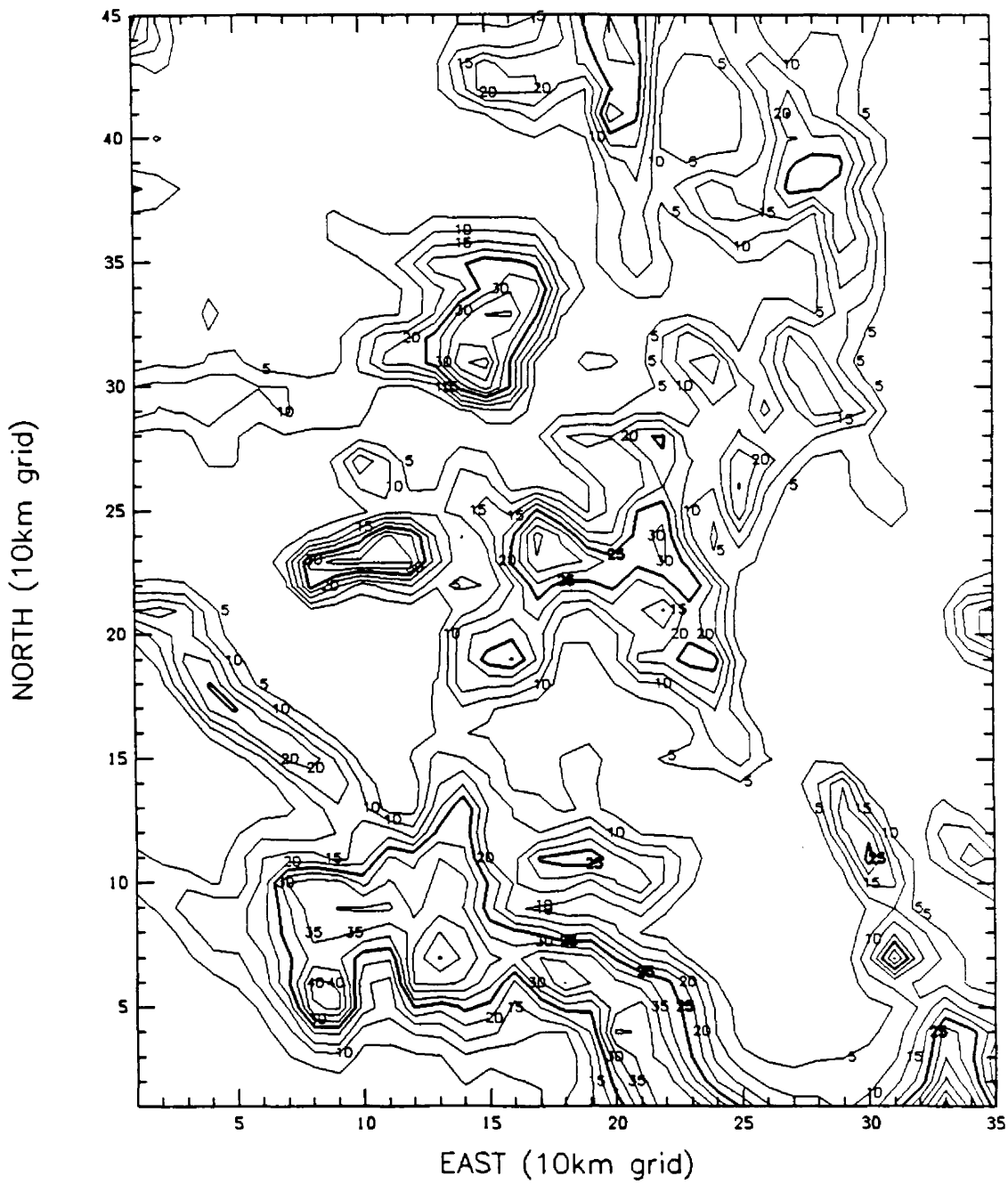

Figure 10. Isohyetal map of model precipitation for the 1984-85 season (inches).

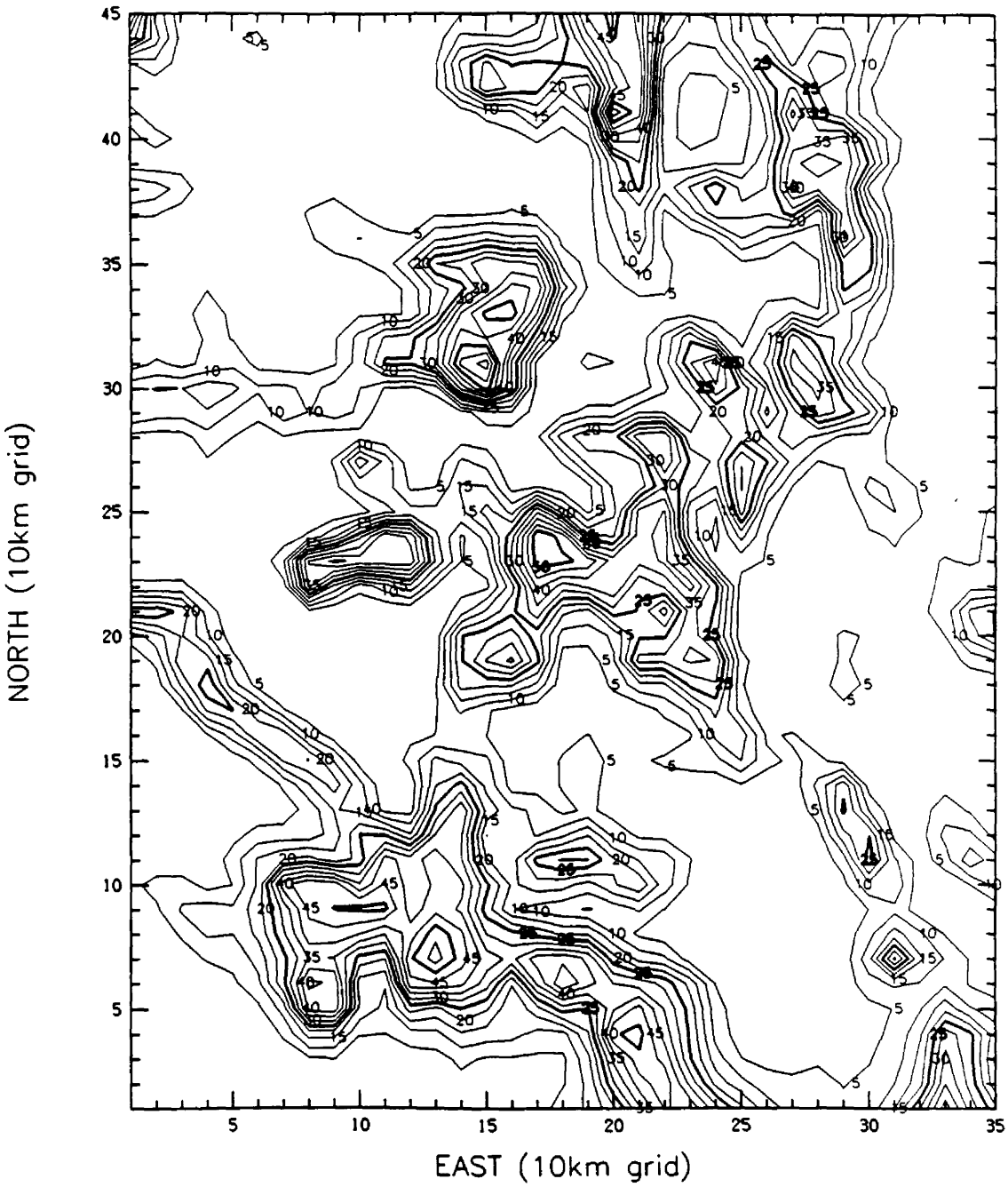

Figure 11. Isohyetal map of model precipitation for the 1985-86 season (inches).

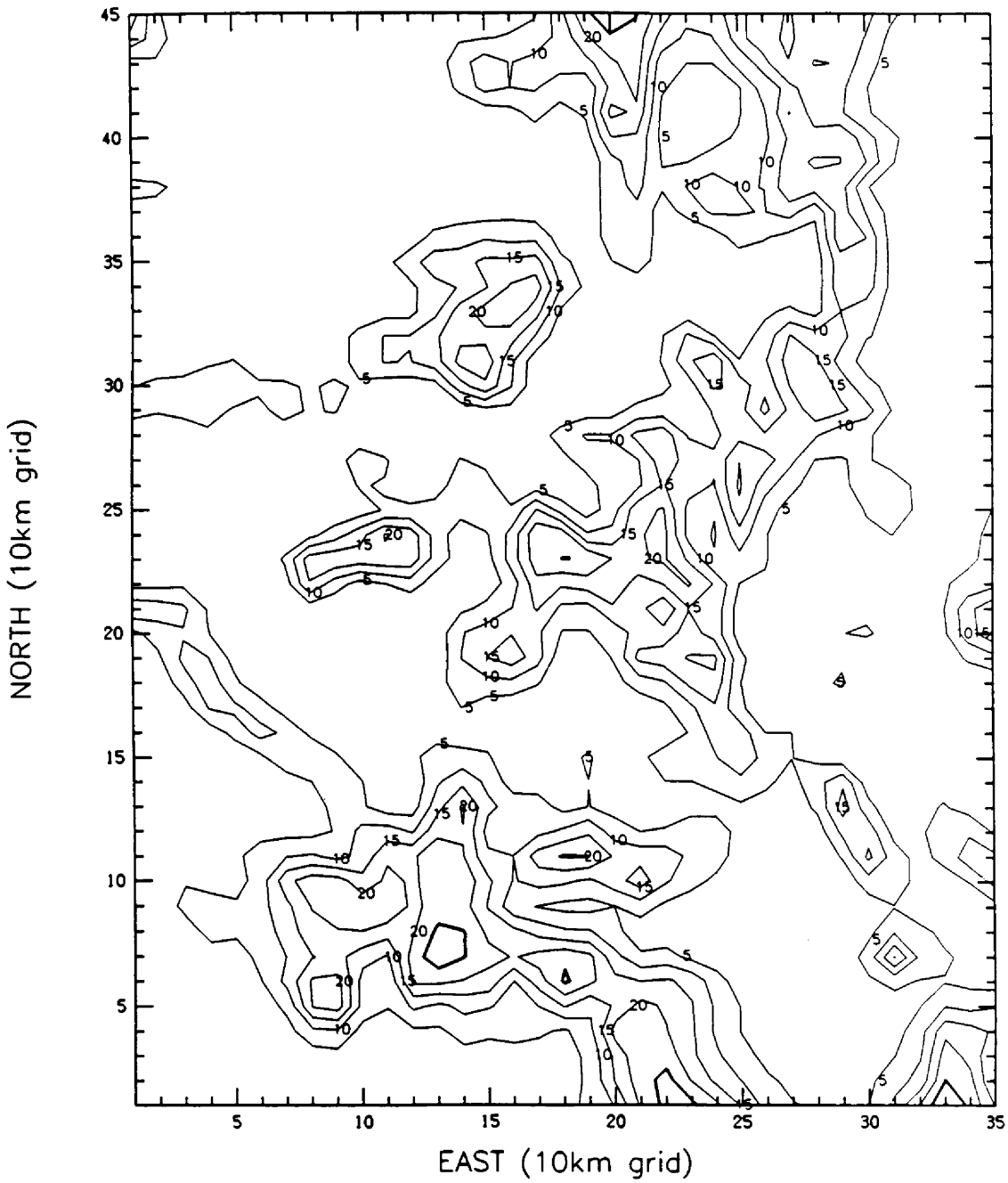

Figure 12. Isohyetal map of model precipitation for the 1986-87 season (inches).

Figures 10 and 11, respectively. Note that the isohyetal contours show similar values of precipitation in the southern regions of both grids, but the northern values are much lower for 1984-85 than for 1985-86.

Referring to Figure 9 again, note that the trend of cumulative grid total precipitation at the end of each month is similar to the annual grid total precipitation. This suggests the possibility of using the cumulative grid precipitation values at the end of each month to predict what the grid total precipitation will be on April 30, the end of winter snowpack in the water year. This would be particularly useful when the model is run in real-time during a winter season.

To assess this predictive potential, cumulative end-of-January grid total precipitation values were compared with the end-of-April values. The results are shown in Figure 13. The correlation coefficient is 0.87. Similar calculations were performed for each month, and the results are shown in Figure 14.

Slope values from the regression analyses are shown in Figure 15. They represent the average fraction of model-predicted total snowpack as a function of time. The results in Figure 15 show that for December, already 40% of the total season snowpack has fallen on average, while Figure 14 shows that the snowpack through the end of December has a correlation coefficient of 0.73 with the April 30 total. Thus, even by the end of December, there is some skill in predicting the total seasonal snowpack. These figures also show that this potential predictive ability increases with the fraction of season snowpack, both of these parameters being functions of time. Therefore, when the model is used in a real-time mode, these regression analysis

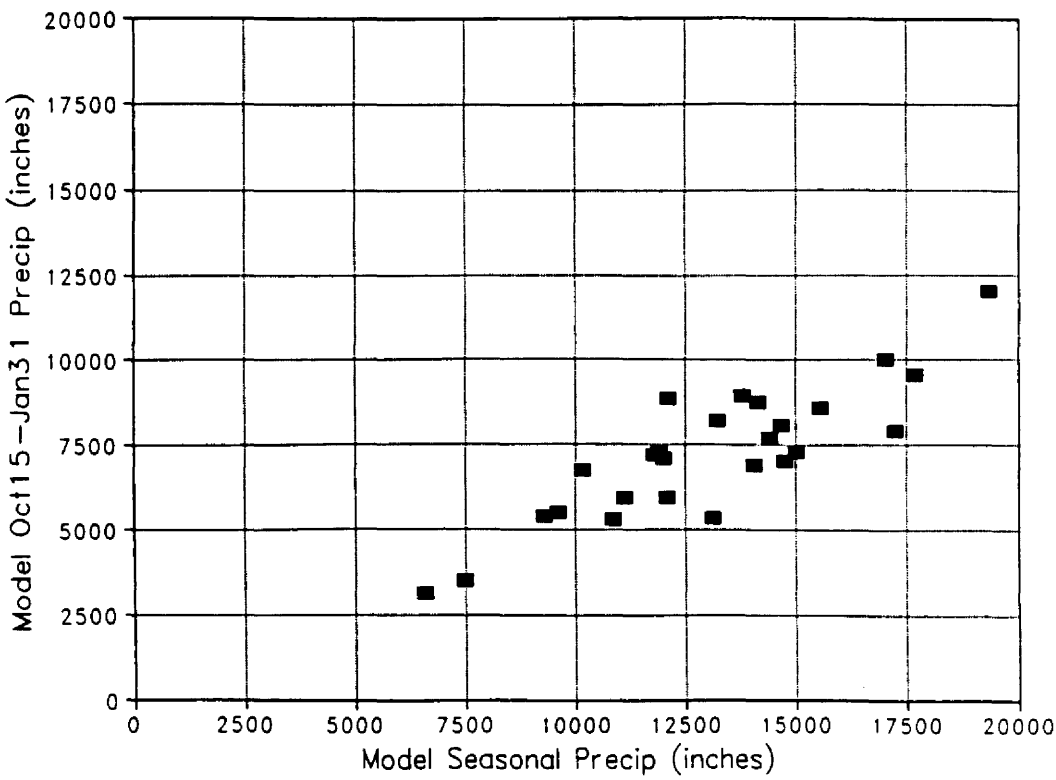

Figure 13. Scatterplot of model cumulative January precipitation versus model cumulative April (seasonal) precipitation for the 27 year study period (r =+0.87)

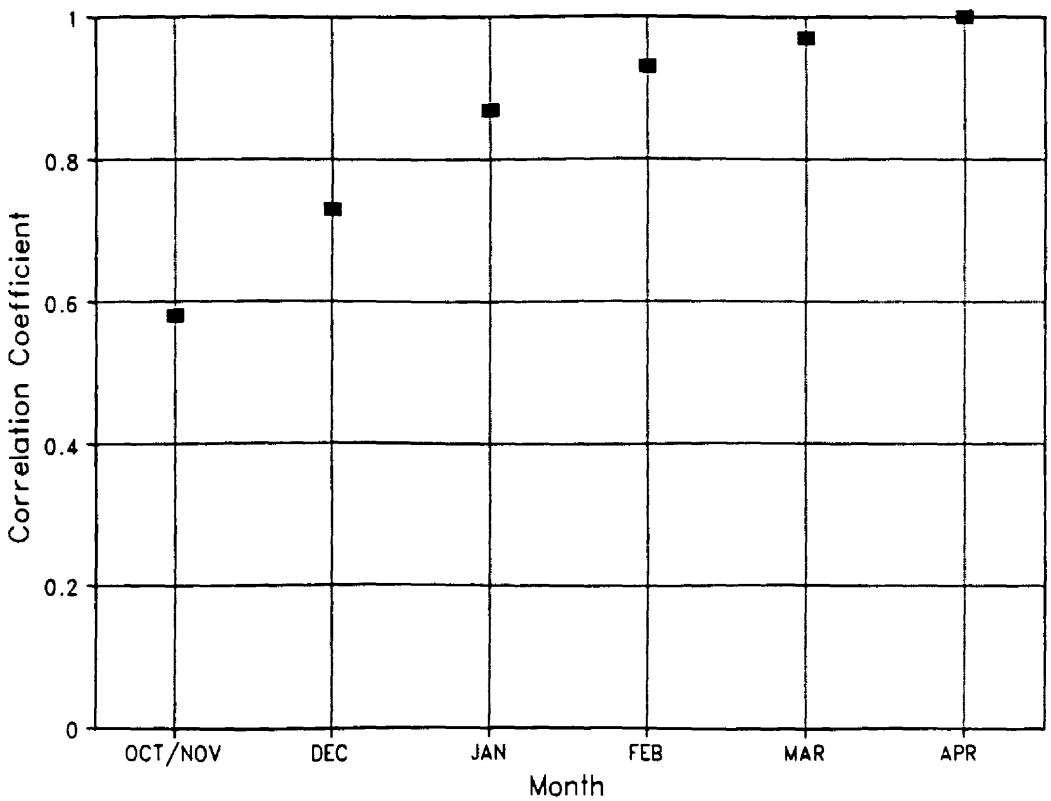

Figure 14. Plot of correlation coefficient values between model cumulative monthly precipitation and model seasonal precipitation

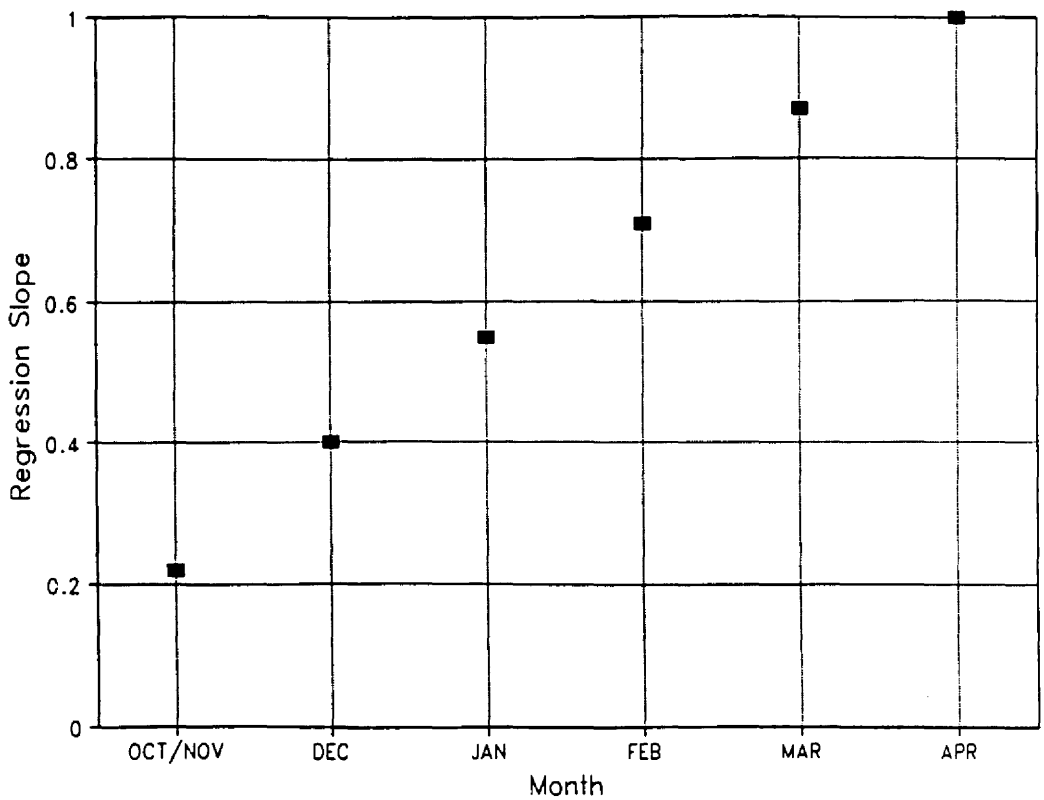

Figure 15. Plot of regression slope values between model cumulative monthly precipitation and model seasonal precipitation

results can be used to predict the total seasonal snowpack and this predictive skill will increase with time into a water year season.

The frequency and duration of model calculated precipitation events over the entire study area were in good agreement with previous observational studies. The number of 12 hour sounding events in a water year (October 15 to April 30) is 396 (398 in a leap year), and 51.4 percent of these, or 204 events, produced at least 0.01 inches of precipitation over the study area on average for the 27 years. Observations from mountain precipitation gauges show that approximately 50 percent of the winter days have snowfall at elevations above 9,000 to 10,000 feet at any one location (Hurley, 1972). A scatterplot of the percentage of events with precipitation versus grid total precipitation for each of the 27 seasons is shown in Figure 16. The linear correlation coefficient is 0.80. This figure shows that it snows more frequently in wet years than in dry years and, on average, it snows about half or 50 percent of the time. For an extremely dry year, the frequency drops to roughly 33 percent of the time, while for an extremely wet year, the frequency increases to approximately 66 percent of the time. In the Colorado River Basin Pilot Project, precipitation was measured at one or more measurement sites on 57 percent of the days with yearly averages ranging from a minimum of 47 percent to a maximum of 73 percent (Hartzell and Crow, 1976).

The most noticeable outlier in Figure 16 is the 1972-73 point, which had 62.1 percent of its events produce precipitation but had a grid total precipitation value of 12,002 inches. The explanation for its anomalous value is probably the record October, 1972 precipitation in the San Juan Mountains and Grand Mesa area. Much of this

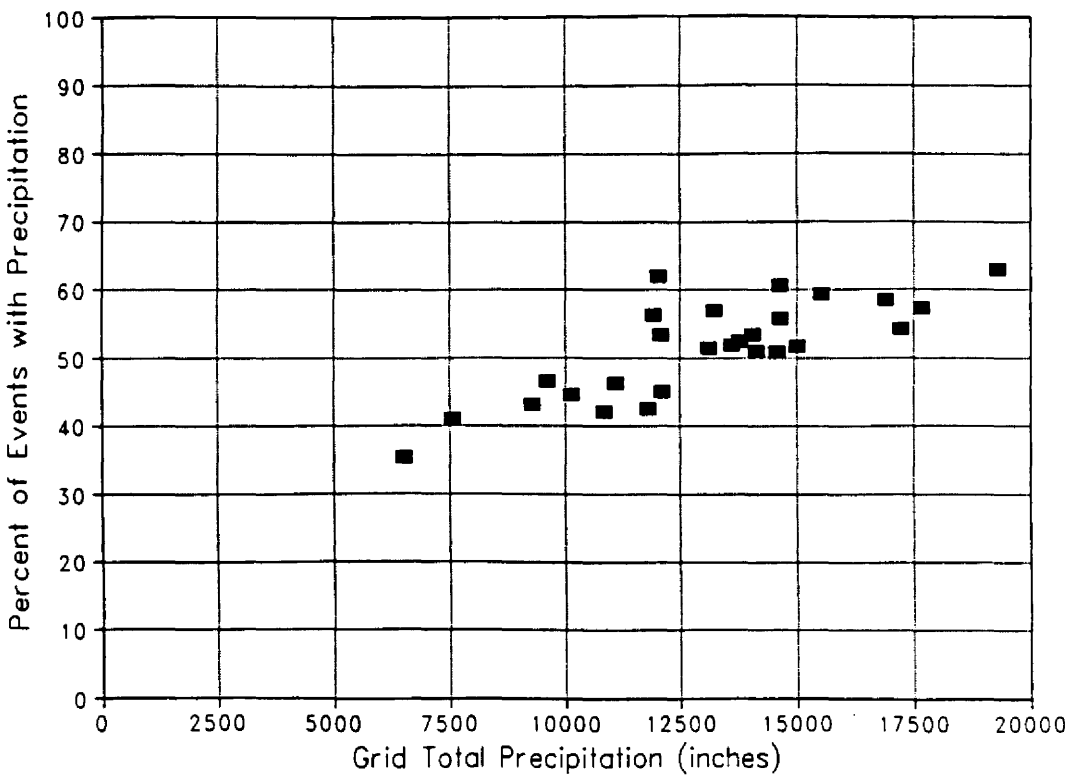

Figure 16. Scatterplot of percentage of 12 hour sounding events that produced at least 0.01" of model grid precipitation versus model seasonal precipitation total for all 27 years

precipitation was convective in nature and thus is not adequately simulated by the model. The linear correlation coefficient for Figure 16 increases to 0.86 when the 1972-73 point is left out of the analysis.

An example of the history of model precipitation in 12 hour sounding increments for the 1984-85 season is shown in Figure 17. Notice that in most cases the precipitation events are clustered, consisting of several consecutive 12 hour sounding periods. In fact, the average duration of a precipitation event for all 27 winter seasons was 4.1 consecutive 12 hour periods.

The model calculations of precipitation event duration demonstrated good agreement with a study by Hindman (1981) of observed mountain precipitation data in Colorado. This study found that more long-duration storms occur during "wet" winters than "dry" winters. Using data from 1959 to 1978, the average number of precipitation events lasting 3 or more days was 13 for the five "wettest" years and 5 for the five driest years. For the 27 seasons of model calculations, the averages were 13.8 events for the 5 wettest years and 7.6 for the 5 driest years.

The model's climatology also shows that the number of precipitation events varies with wind direction. The distribution of these 204 events for each of the 36 steps of 10° wind direction is shown in Figure 18. The maximum number of events is 14.8 for a wind direction of 260 degrees, and the minimum is 0.3 events for 100 degrees. The distribution is highly skewed toward southwesterly flow with 50.8 percent of the precipitation events occurring between 180 and 270 degrees inclusive in the mean.

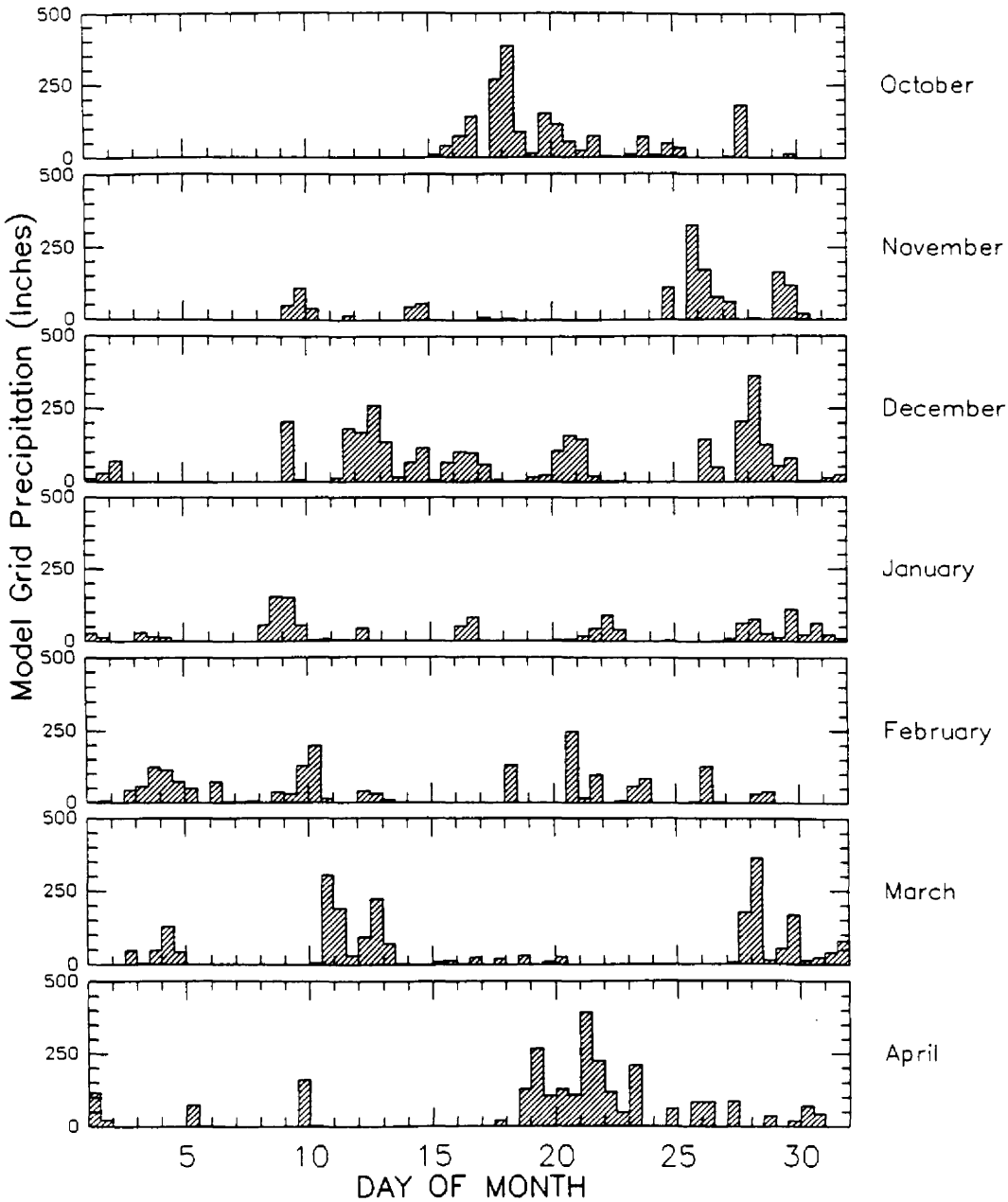

Figure 17. Grid total precipitation for each 12 hour sounding period for the 1984-85 winter season

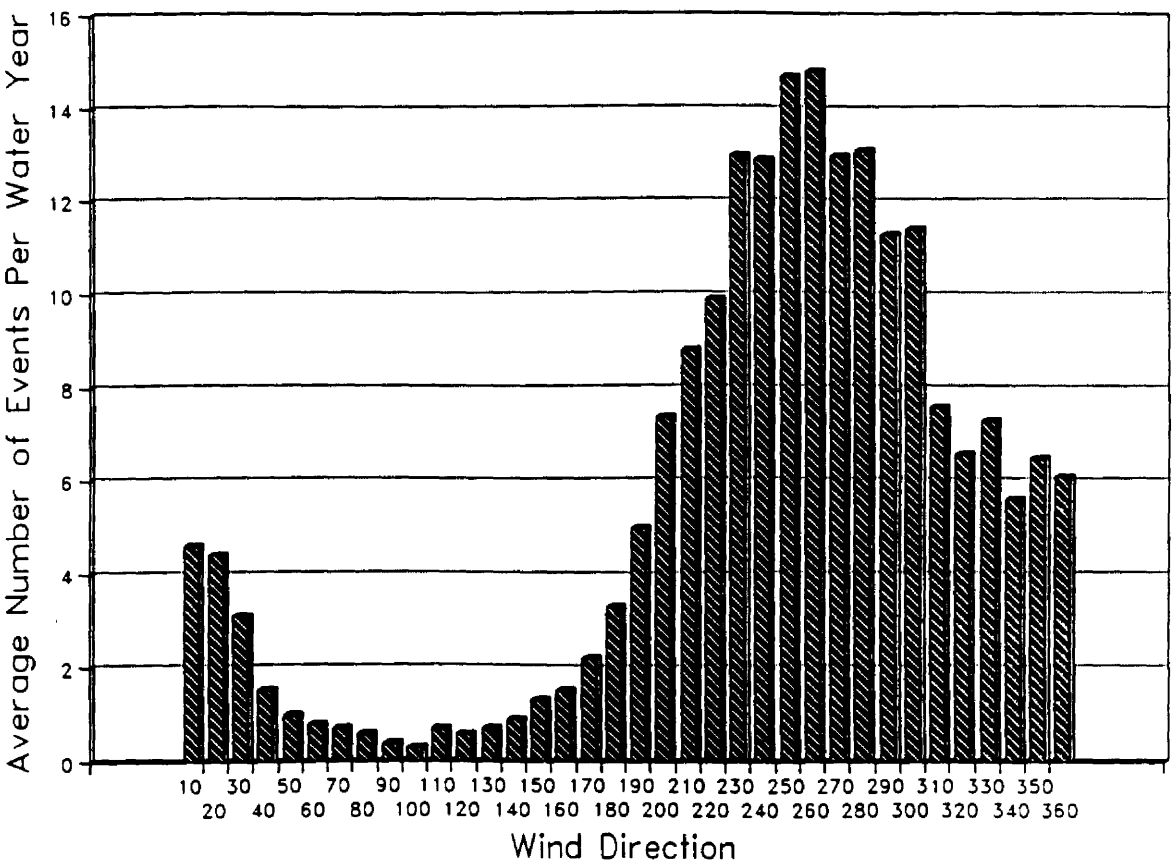

Figure 18. Distribution of average number of 12 hour precipitation episodes for each of the 36 grid classes

Precipitation amount, however, has a different dependence on wind direction. The distribution of the average precipitation amount for each event over the entire grid for all 36 directions is shown in Figure 19. Notice that the maximum is 103.3 inches for a direction of 200 degrees, and that this peak is shifted from the 260 degrees maximum in Figure 18. Also, a secondary maximum of 79.3 inches occurs at 100 degrees which is likely a reflection of deep "upslope" storms along the Front Range. The average percent of the total grid area precipitation for all directions for the 27 seasons, which is essentially a combination of Figures 18 and 19, is shown in Figure 20. Not surprisingly, the maximum value for this distribution occurs at 230 degrees with a value of 9.85 percent.

5.3 Comparison to Snowcourses

Observed water equivalent values (Feb 1, Mar 1, Apr 1, May 1) for 92 snowcourse sites located in the study area were obtained from the SCS. However, only the 79 stations with elevations greater than 9000 feet were used in the analysis since it is the snowpack from these high elevations that contribute the most significantly to the spring and summer runoff. Figure 21 shows the location of the snowcourse sites relative to the model 10km x 10km topography.

Three types of comparisons to snowcourse observations are described in this section: snowcourse group averages to integrated model precipitation; individual station values to the corresponding model point values; and temporal evolution of the individual site correlations. The group comparisons utilized snowcourses located within each of 15 model areas shown in Figure 22. Note that the two Western San Juan areas used by Rhea (1978) were combined into a single

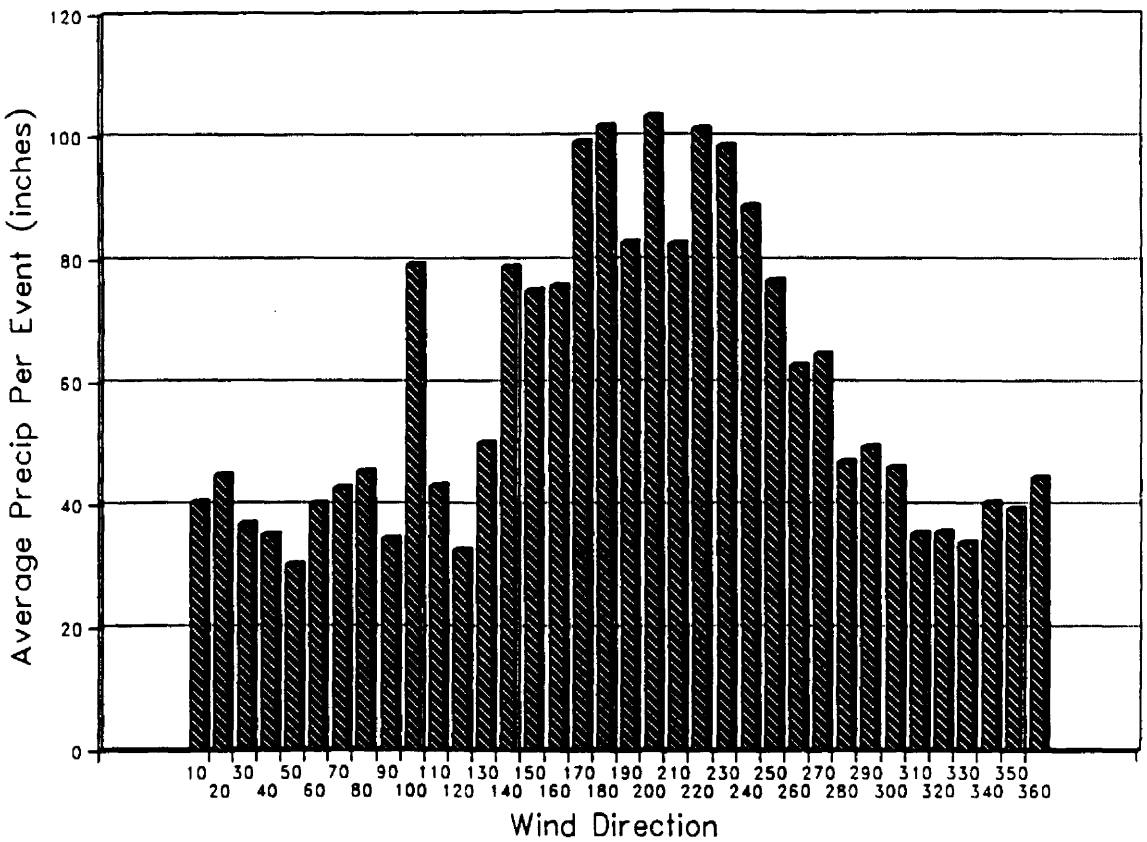

Figure 19. Distribution of average model grid total precipitation amount in each of the 36 grid classes

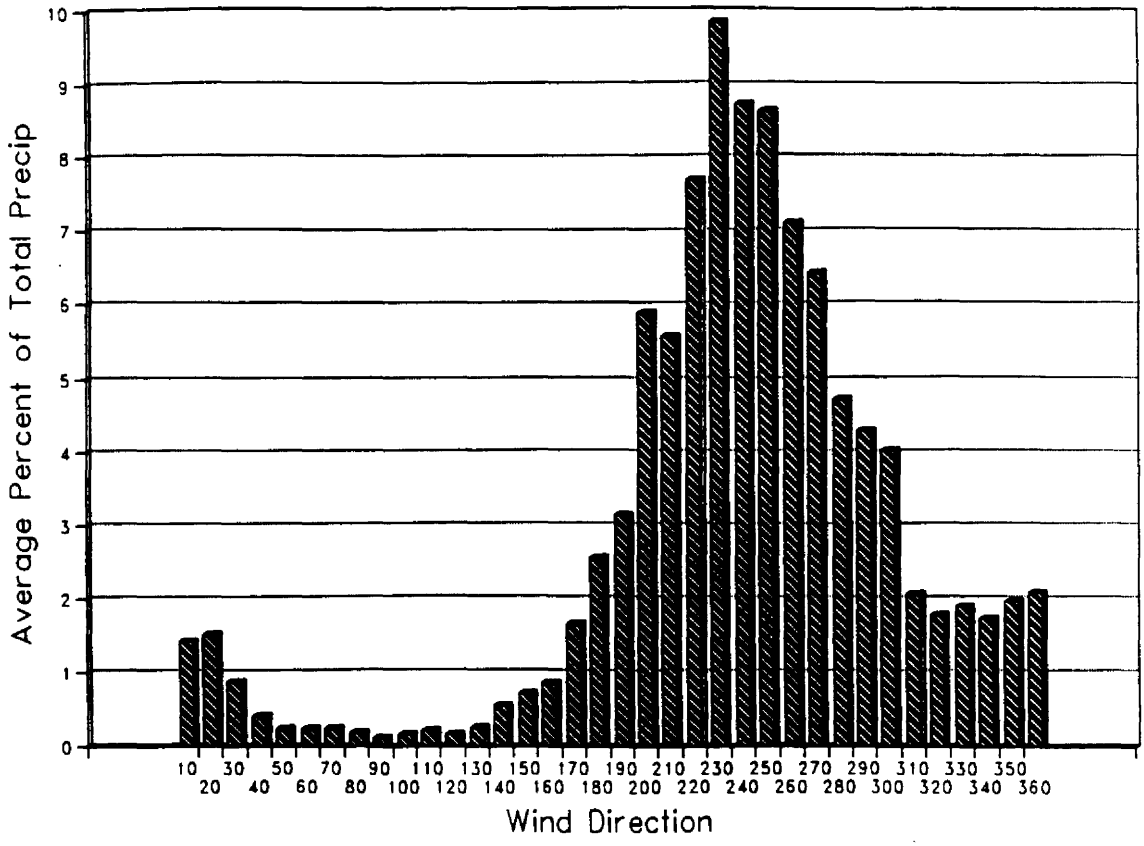

Figure 20. Distribution of average percentage of model grid total precipitation for each of the 36 grid classes

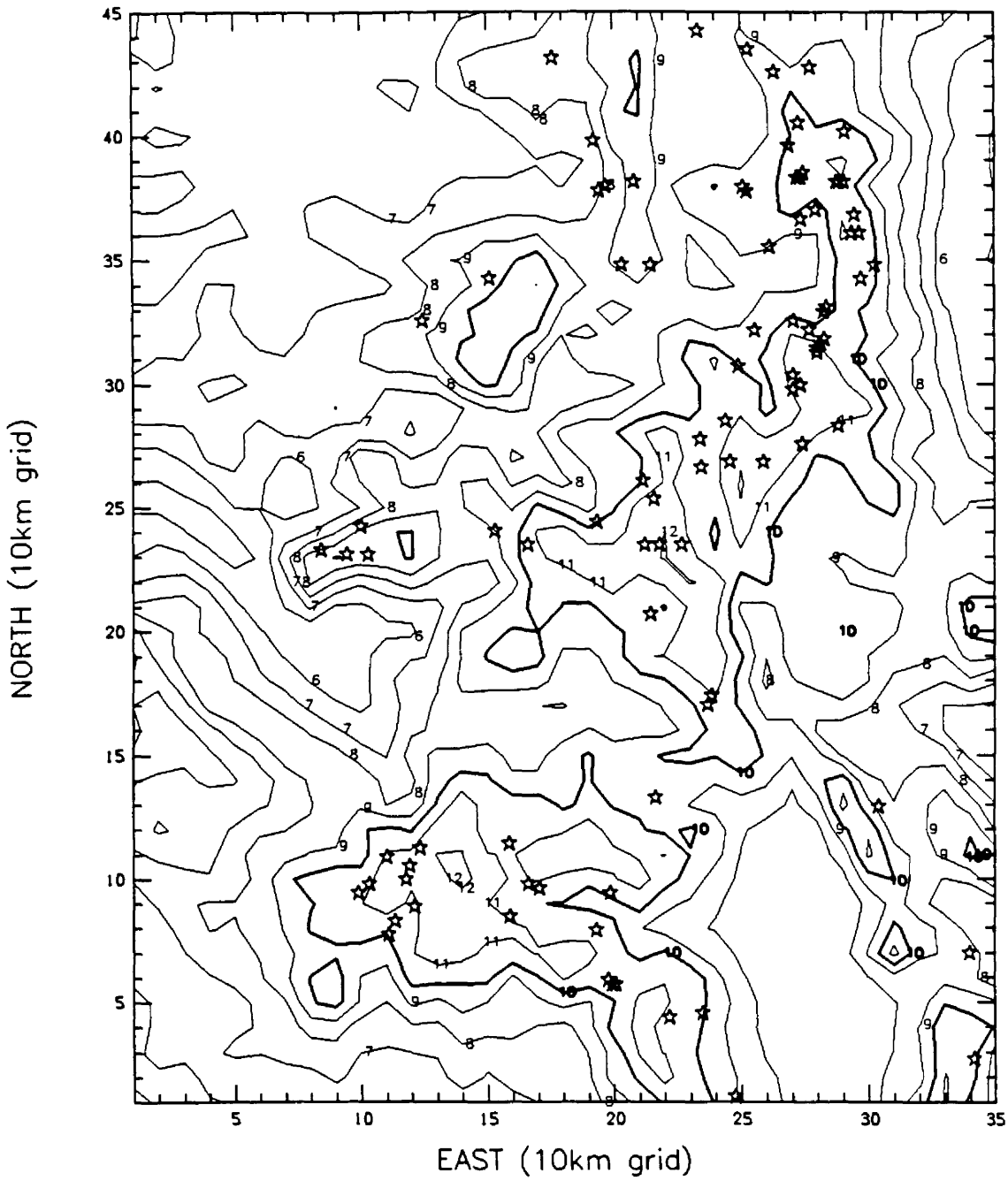

Figure 21. Elevation contour map of model domain with stars showing the location of the Soil Conservation Service snowcourses used for model evaluation. Numbers indicate elevation, kft MSL.

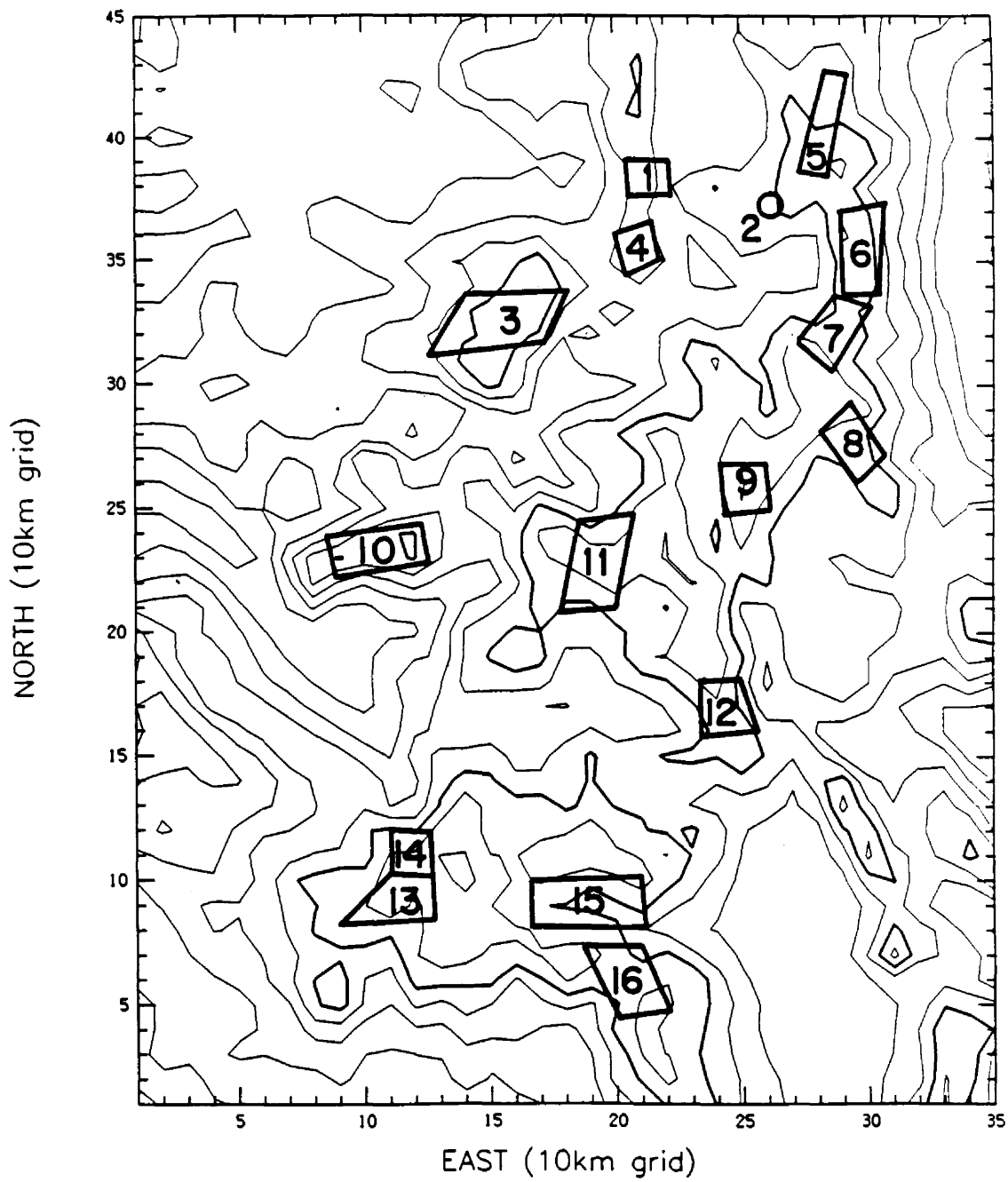

Figure 22. General location of the snowcourse areas used for model validation

area for this research. Plots of areally-integrated October 15 to April 30 model precipitation versus observed April 1 water equivalent values for four of the 15 areas are shown in Figures 23 through 26. Table 3 lists the statistical relationships for all 15 sites. The average correlation coefficient for all 15 areas is 0.72 with a standard deviation of 0.06. The average slope of the regression line is 0.88, which indicates that the model's integrated precipitation values are slightly lower than the corresponding observations of snowcourse water equivalent.

The above results demonstrate that the model has good agreement with snowcourse observations on a seasonal basis for areally integrated precipitation. However, a more detailed examination of snowcourse data is required to investigate the questions of temporal evolution and accuracy of the model precipitation at specific point locations during the course of the water year period. Determination of the latter is complicated by smoothing of the terrain using the 10km grid interval, which inhibits the ability of the model to adequately represent point values of precipitation at specific measurement sites, a particularly severe problem if the site resides in a locally low area surrounded by nearby higher ridges.

In an attempt to investigate these two issues, cumulative model precipitation for each site from October 15 up to the date of each observation (either Feb 1, Mar 1, Apr 1 or May 1) was compared to the corresponding observed water equivalent value (e.g., Oct 15 - Jan 31 cumulative model precipitation was compare with observed Feb 1 value). Example scatterplots of cumulative model precipitation versus observed water equivalent for each of the four months are shown for Milner Pass (Figures 27 through 30) and Independence Pass (Figures 31 through 34).

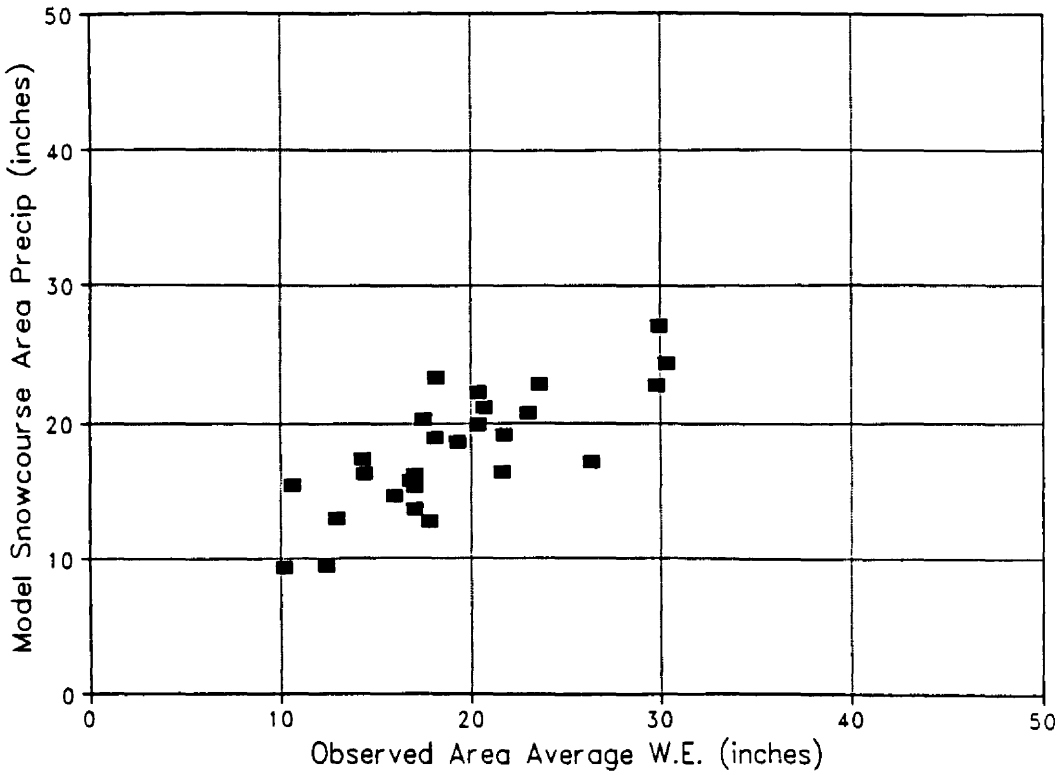

Figure 23. Comparison between October 15 - March 31 model precipitation and observed 1 April snowcourse values for the winter seasons 1961-62 through 1987-88 in snowcourse area no. 11

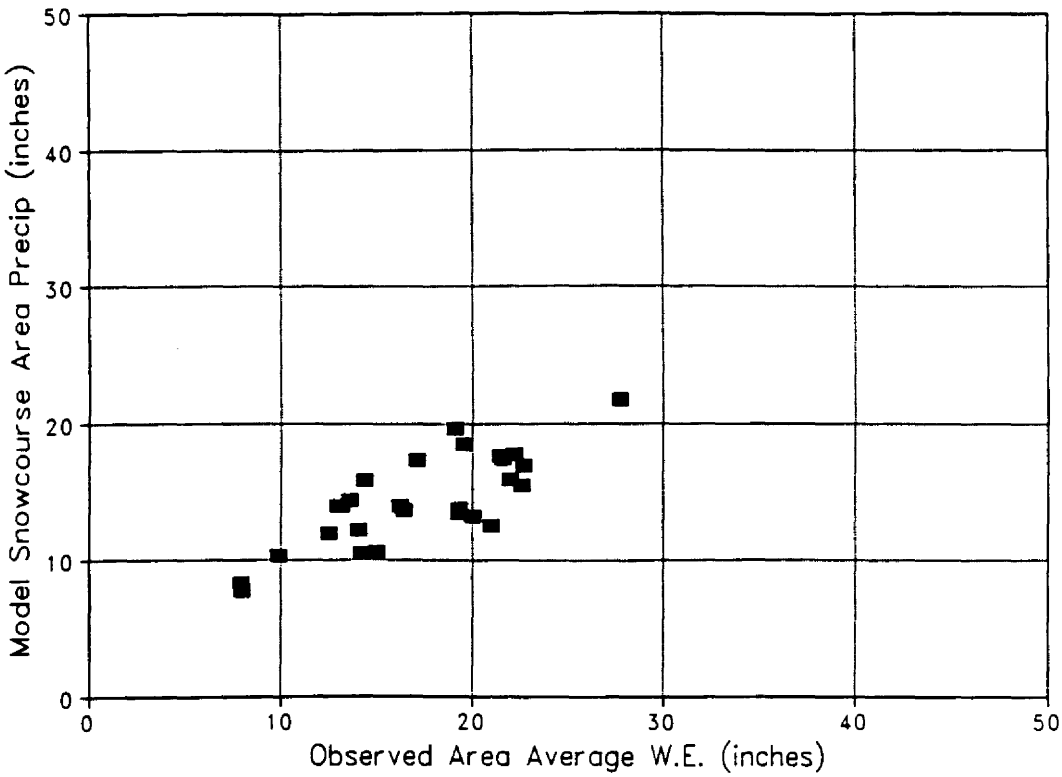

Figure 24. Comparison between October 15 - March 31 model precipitation and observed 1 April snowcourse values for the winter seasons 1961-62 through 1987-88 in snowcourse area no. 6

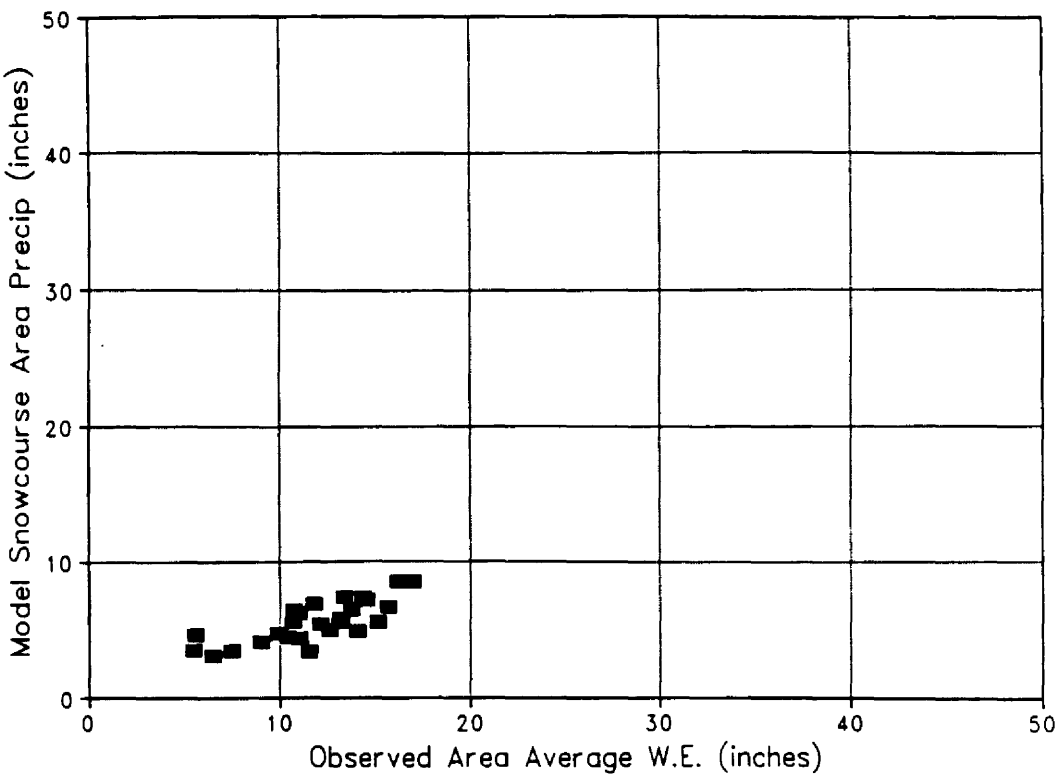

Figure 25. Comparison between October 15 - March 31 model precipitation and observed 1 April snowcourse values for the winter seasons 1961-62 through 1987-88 in snowcourse area no. 4

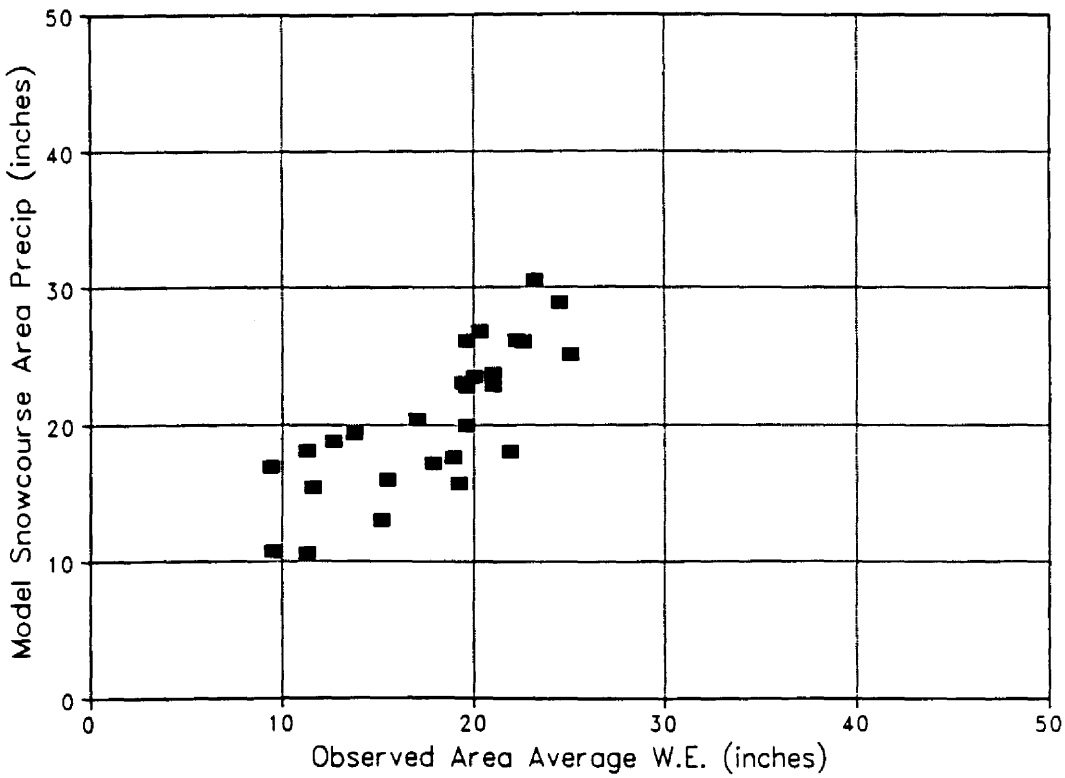

Figure 26. Comparison between October 15 - March 31 model precipitation and observed 1 April snowcourse values for the winter seasons 1961-62 through 1987-88 in snowcourse area no. 3

Table 3

Summary of Comparisons of Model Area Precipitation Calculations to Observed Snowcourse Water Equivalent Values for 27 Seasons (1961-62 to 1987-88)

Area Name	Area No.	Correlation Coefficient r	Regression Slope
Park Range	1	0.72	0.71
Willow Creek	2	0.62	1.12
Flat Tops	3	0.79	1.13
Gore-Lynx Pass	4	0.77	0.47
Cameron-Deadman	5	0.71	0.95
Indian-Lango Pass	6	0.79	0.82
Berthoud-Loveland	7	0.74	0.93
Kenosha-Geneva Park	8	0.62	0.71
Climax	9	0.70	1.13
Grand Mesa	10	0.77	0.64
Aspen-Crested Butte	11	0.78	0.91
Monarch Pass	12	0.71	0.83
Western San Juan	14	0.69	1.14
Upper Rio Grande Valley	15	0.59	0.62
Eastern San Juan	16	0.75	1.07
	Average	0.72	0.88

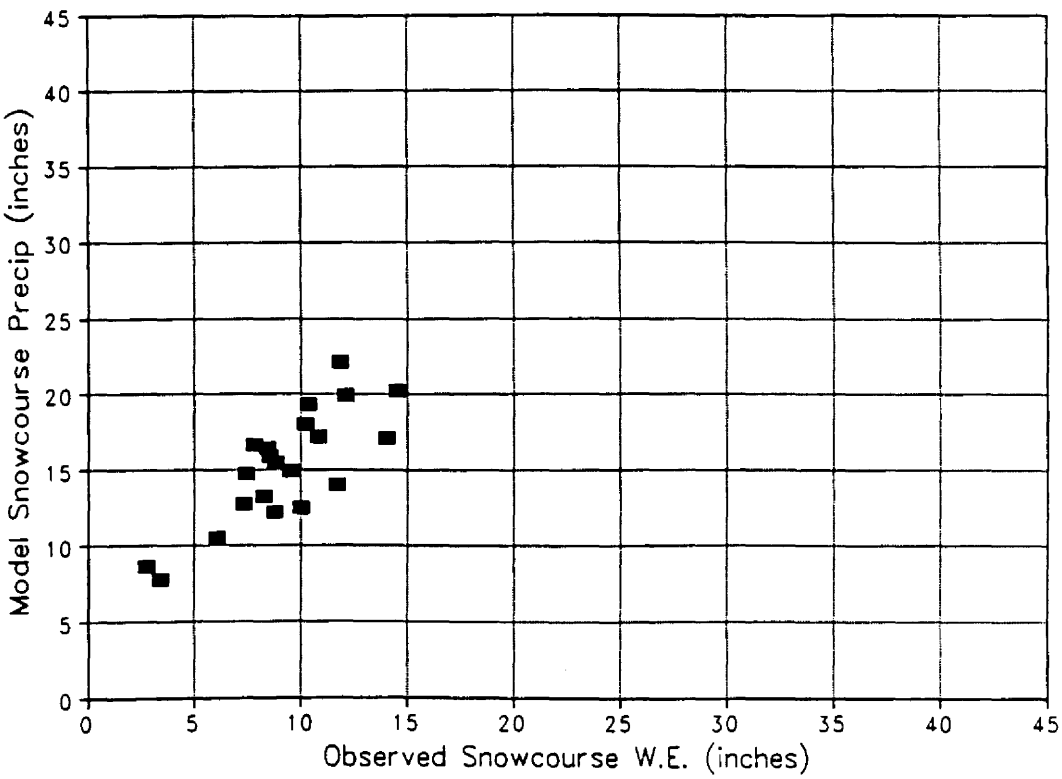

Figure 27. Comparison between model cumulative precipitation through January and observed Feb 1 snowcourse water equivalent values for the winter seasons 1961-62 through 1987-88 for Milner Pass

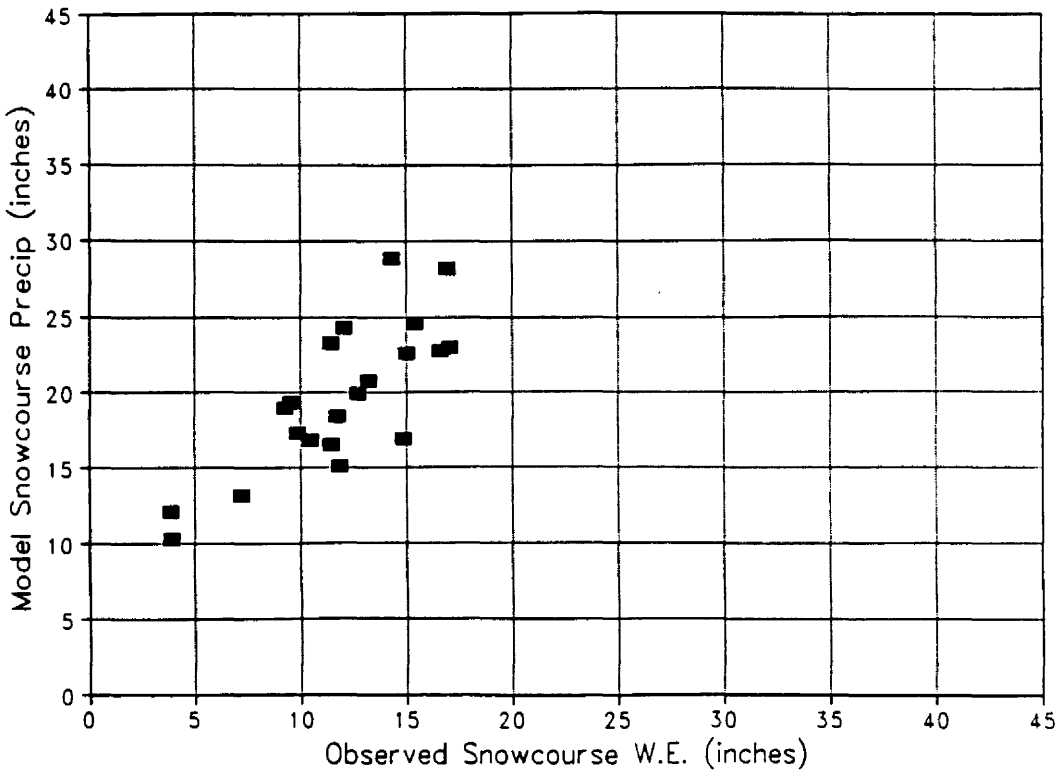

Figure 28. Comparison between model cumulative precipitation through February and observed Mar 1 snowcourse water equivalent values for the winter seasons 1961-62 through 1987-88 for Milner Pass

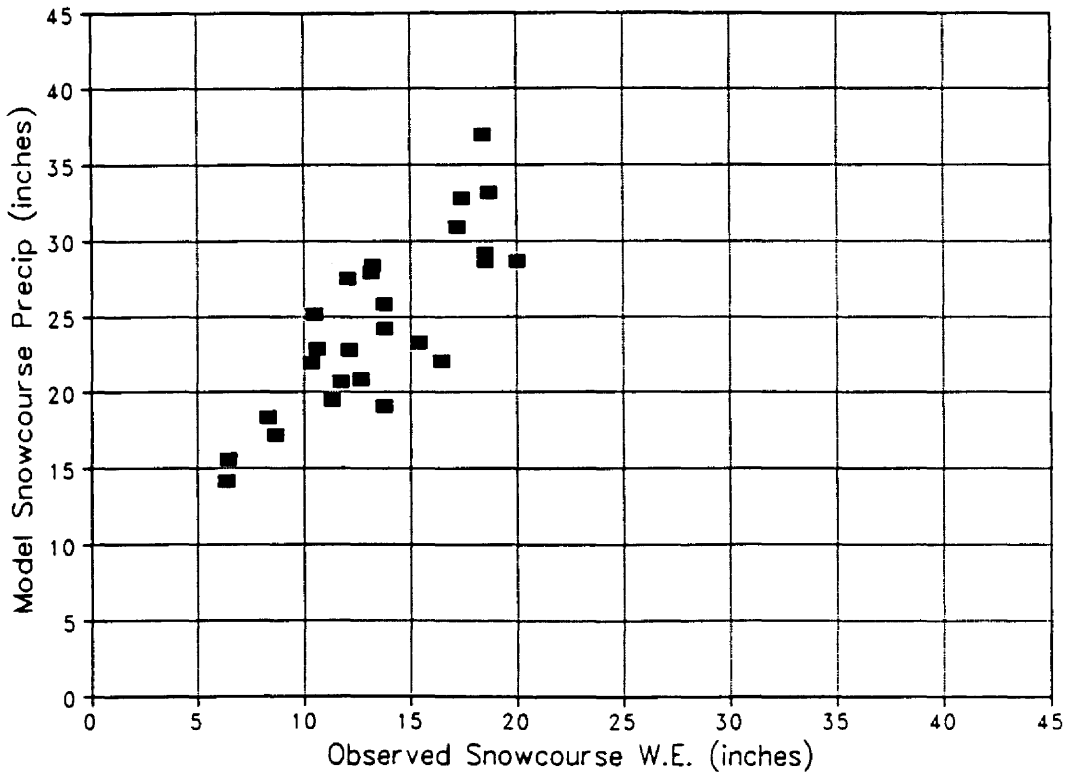

Figure 29. Comparison between model cumulative precipitation through March and observed Apr 1 snowcourse water equivalent values for the winter seasons 1961-62 through 1987-88 for Milner Pass

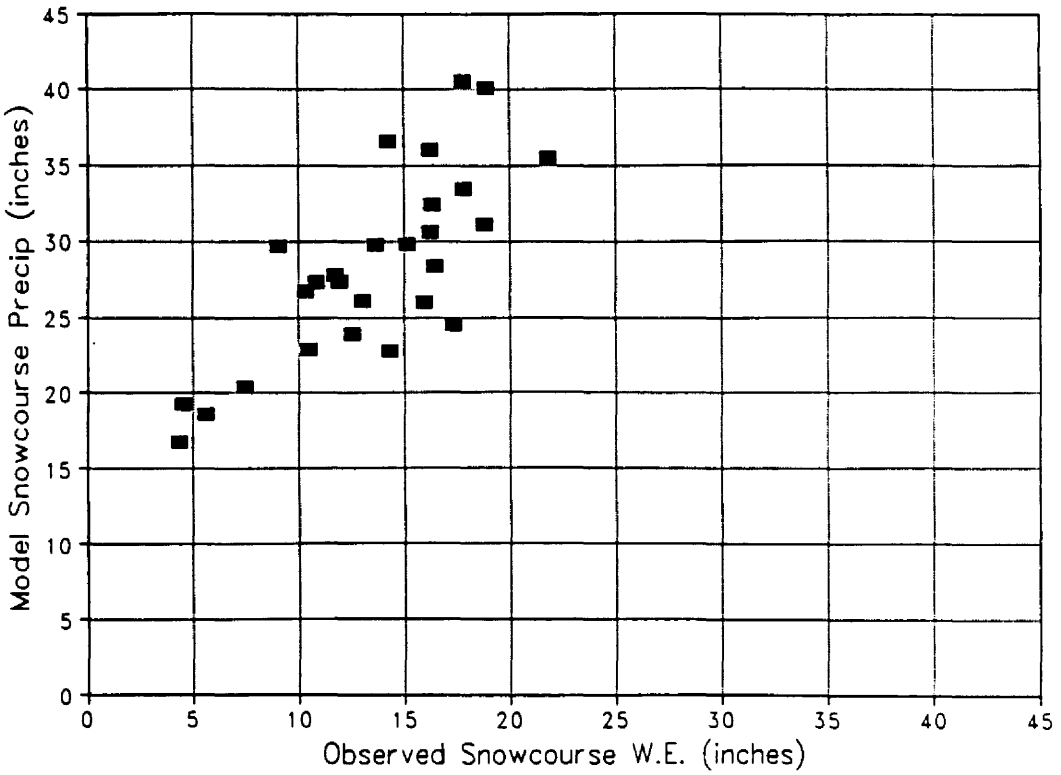

Figure 30. Comparison between model cumulative precipitation through April and observed May 1 snowcourse water equivalent values for the winter seasons 1961-62 through 1987-88 for Milner Pass

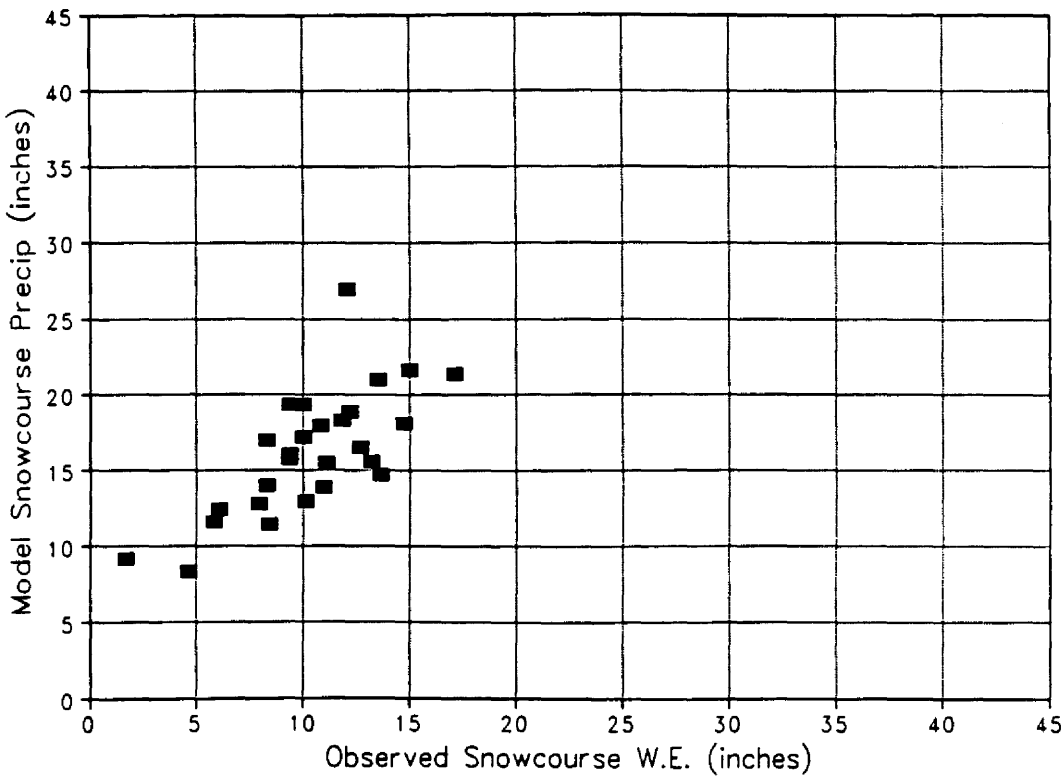

Figure 31. Comparison between model cumulative precipitation through January and observed Feb 1 snowcourse water equivalent values for the winter seasons 1961-62 through 1987-88 for Independence Pass

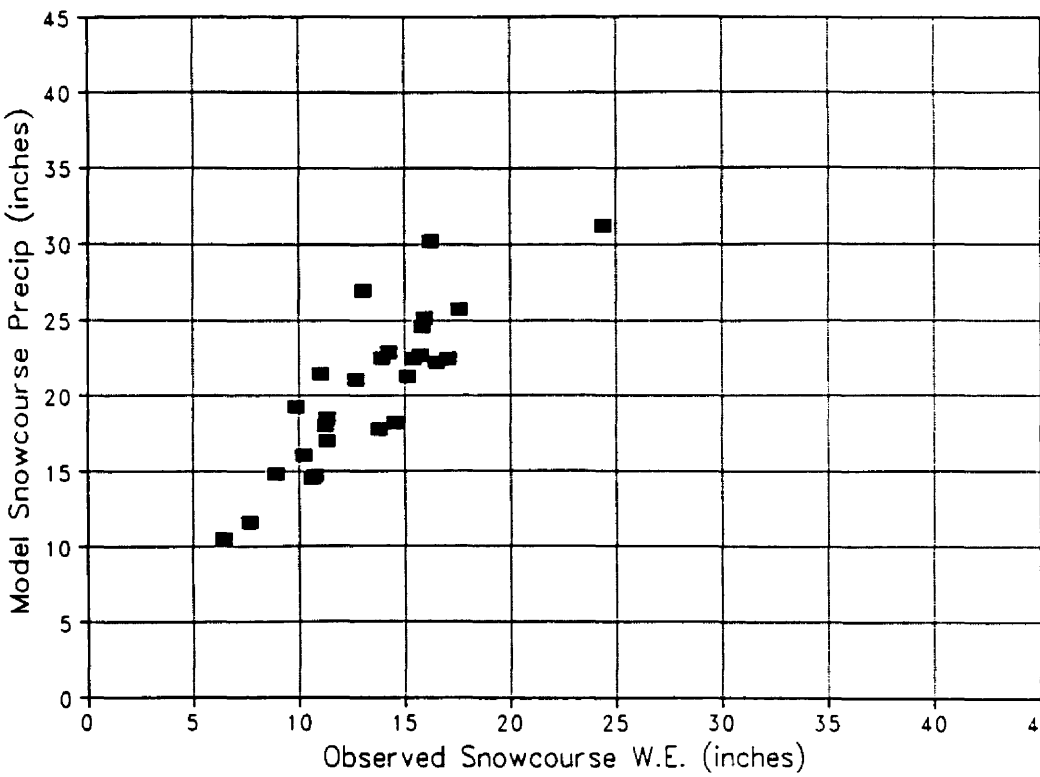

Figure 32. Comparison between model cumulative precipitation through February and observed Mar 1 snowcourse water equivalent values for the winter seasons 1961-62 through 1987-88 for Independence Pass

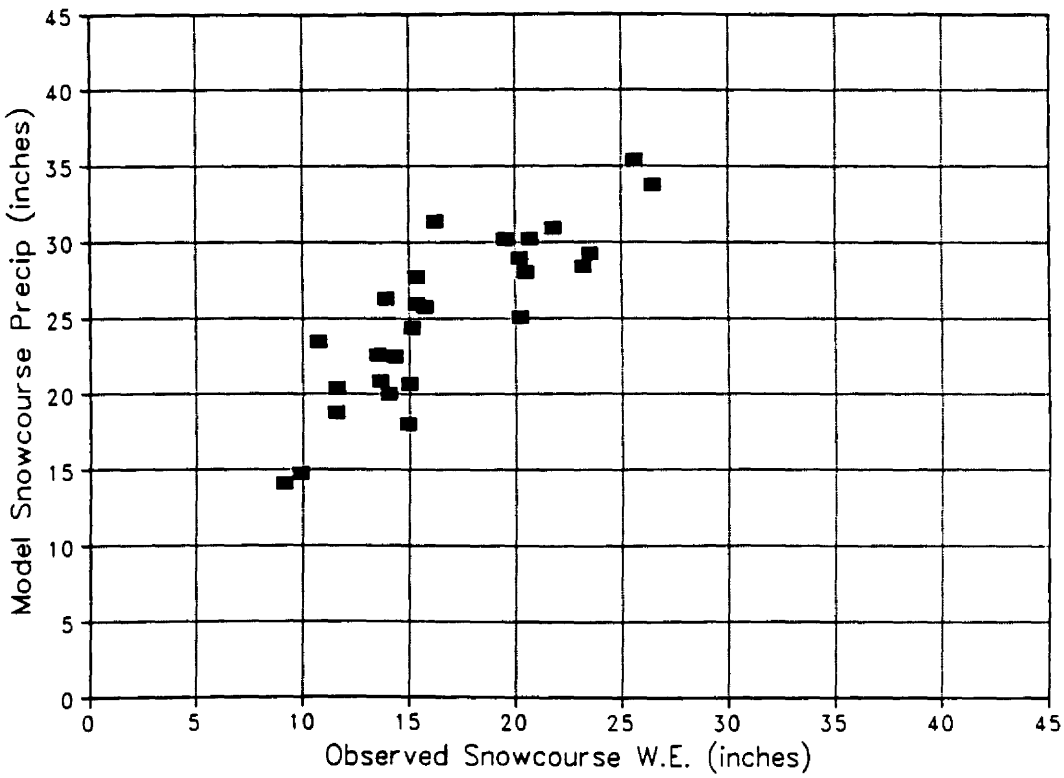

Figure 33. Comparison between model cumulative precipitation through March and observed Apr 1 snowcourse water equivalent values for the winter seasons 1961-62 through 1987-88 for Independence Pass

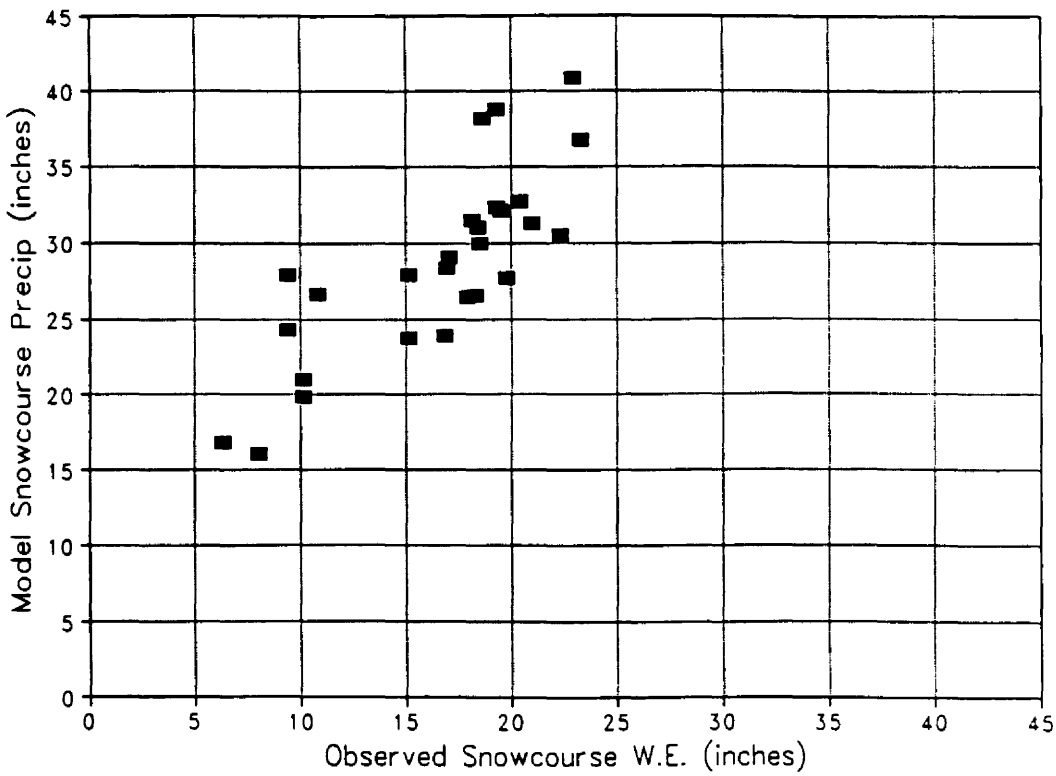

Figure 34. Comparison between model cumulative precipitation through April and observed May 1 snowcourse water equivalent values for the winter seasons 1961-62 through 1987-88 for Independence Pass

Table 4 shows the minimum, average and maximum linear correlation coefficient and slope values for all stations for each of the four months.

The average correlation coefficient for all sites is 0.64 for the February 1 data and increases to 0.68 for the March 1 and April 1 data. The average slope value is approximately 1.2 for these first three months, indicating a slight overprediction of water equivalent by the model. For the May 1 data, however, the average correlation coefficient decreases to 0.56 while the average slope value increases to 1.5. This is likely due to the warmer temperatures that often occur in April which effectively decreases the amount of snowpack. This effect is felt in the observations but not in the model calculated values, resulting in greater overprediction by the model than in the previous three months.

The most serious overestimations (i.e., highest slope values) occurred for narrow mountain valleys that are not adequately resolved by the model's 10km by 10km topography. The four sites with the highest slope values had elevations in the model topography that were on the order of 1000 feet higher than their actual elevations. The most serious underestimations occurred for broad, intermountain valleys such as Laveta Pass, Cochetopa Pass and Rabbit Ears Pass. Both of these results are consistent with Rhea (1978). Rhea theorized that the possible reasons for the underestimations in these areas were from the following limitations in the model: the non-orographic vertical motion fields are underestimated; the lack of representing mesoscale valley convergence fields from channeling; the delay of evaporation of falling precipitation until ice subsaturated instead of water subsaturated

Table 4

Summary of Comparisons of Model Point Precipitation Calculations to Observed Snowcourse Water Equivalent Values for 79 Sites for 27 Seasons (1961-62 to 1987-88)

Date	Correlation Coefficient r			Slope		
	min	avg	max	min	avg	max
FEB 1	0.21	0.64	0.82	0.27	1.20	3.35
MAR 1	0.31	0.68	0.85	0.26	1.22	3.46
APR 1	0.38	0.68	0.85	0.27	1.24	3.97
MAY 1	-0.21	0.56	0.81	0.35	1.51	4.91

conditions were achieved would have allowed additional precipitation over relatively low topography; and the extreme sensitivity of model precipitation at low altitudes as relative humidity changes from 85 percent to 100 percent, so underestimating the frequency of existing 100 percent relative humidity layers would lead to less precipitation.

Finally, there is a noticeable difference in the average April 1 slope values between the snowcourse areas (avg. = 0.88) and the individual sites (avg. = 1.24), even though the average correlation coefficients are approximately equal. This is probably best explained by noting that the snowcourse areas outlined over the model grid area not only encompass the locations of the observed snowcourse sites but also some surrounding grid points which are at lower relative elevations. These lower grid points often reside in preferred "rain-shadowed" areas where much less precipitation accumulates which effectively lowers the model average precipitation value for the snowcourse area.

5.4 Comparison to Streamflow Runoff

For the streamflow calculations, 18 of the original 20 small basins from Rhea (1978) were used (see Figure 35 and Table 5). Basin 20 was excluded due to a change in its flow regime (personal communication with Owen Rhea, 1989), and verification data were not available for the Piedra River (basin 7). Observed monthly runoff data were available through the 1985-86 winter season, so 25 of the 27 years were included in the calculations. For each of the 18 small basins, model basin volume precipitation was compared to observed runoff at the appropriate gauging station. The observed runoff due to only winter snowpack was estimated by taking the March through July values minus

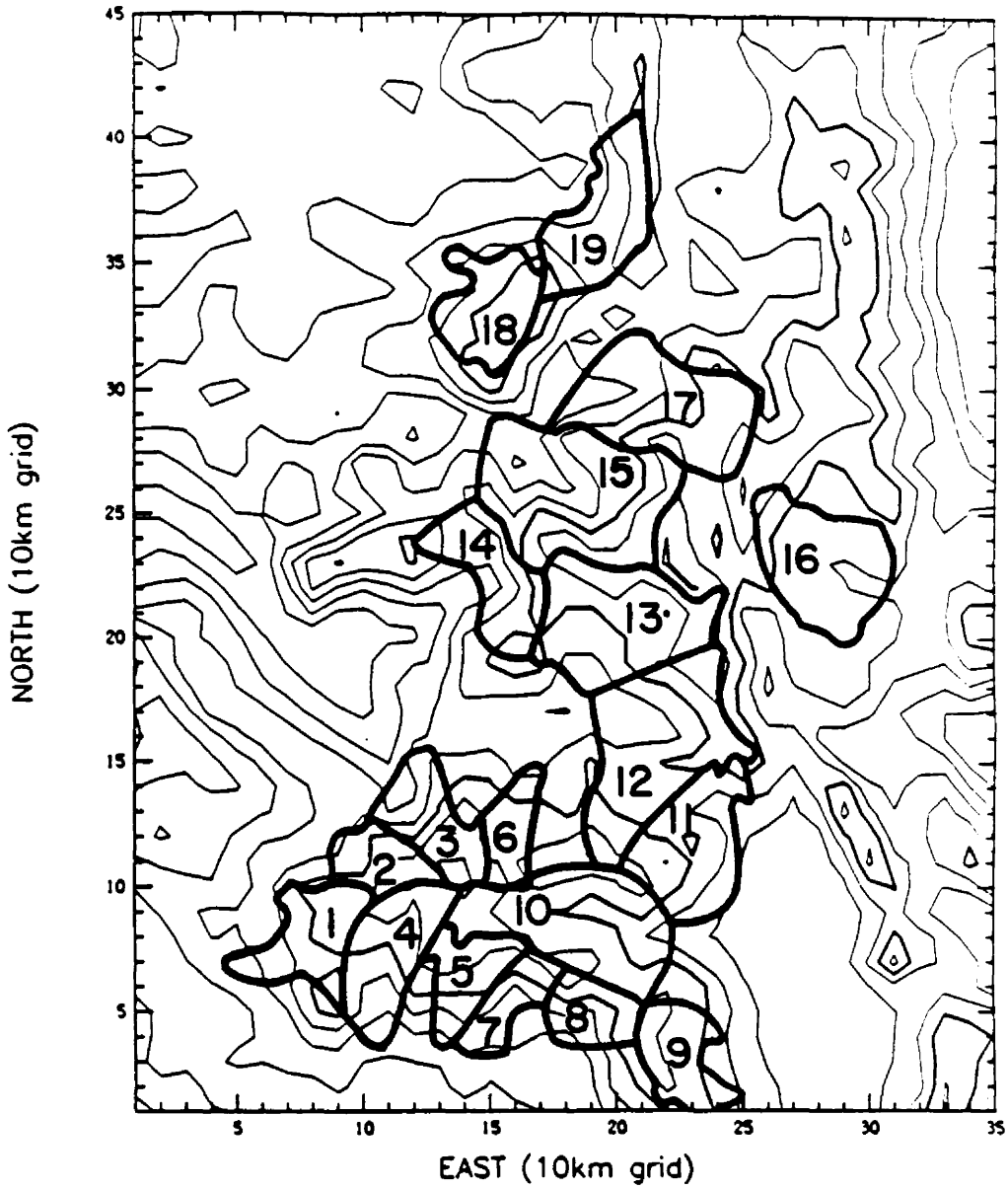

Figure 35. Locations of watersheds used for model evaluation

Table 5

List of Streamgauges Used for Model Validation

Basin #	Streamgauge Name
1	Dolores at Dolores
2	San Miguel at Placerville
3	Uncompahgre at Colona
4	Animas at Durango
5	Los Pinos near Bayfield
6	Lake Fork of Gunnison at Gateview
7	Piedra near Piedra
8	San Juan at Pagosa Springs
9	Conejos at Mogote and Alamosa above Terrace Resevoir
10	Rio Grande near Del Norte
11	La Garita Creek, Saquache Creek and Carnero Creek
12	Tomichi Creek at Gunnison
13	Gunnison near Gunnison
14	North Fork of Gunnison near Somerset
15	Roaring Fork below Glenwood
16	South Platte near Hartsel
17	Eagle below Gypsum
18	South Fork White and North Fork White near Buford
19	Yampa at Steamboat
20	Elk at Clark, Elkhead Creek at Elkhead and Slater Fork at Slater

five times the February value to roughly correct for the baseflow hydrograph component. Table 6 lists the statistical results for the 25 year period of record. The average correlation for the 18 small basins was 0.68.

Example scatterplots of the model versus observed streamflow are shown in Figures 36 and 37 for the Rio Grande River (small basin #10) and the Gunnison River (small basin #13), respectively. The correlation coefficients are 0.84 and 0.85, respectively. Note that the points in each of the figures do not lie along a 1:1 slope line as closely as in the snowcourse scatterplots. Instead, the model calculated basin precipitation values are on the order of twice the observed runoff for most of the 18 small basins. This is likely due to the effects of evapotranspiration and soil moisture recharge, which are not accounted for in the model. Also, as seen in the original dissertation results, variations occur in the regression slopes from one watershed to the next. This is in part due to the different basin runoff characteristics, which include vegetation, microclimatic conditions, soil characteristics and basin geology.

The streamflow comparison statistics were computed a second time with the omission of three "problem years". In 1961-62, the very cold and wet September of 1961 in the northern and central mountains of Colorado had a significant contribution to the seasonal snowpack, but model calculations did not commence until October 15. The 1972-73 season had heavy, convective October precipitation in the Grand Mesa and San Juan mountains, which is not adequately simulated by the model. Both of these years were noted in Rhea (1978). Also, the wind direction and speed values were missing from the upper air sounding

Table 6

Summary of Comparisons of Model Basin Precipitation Calculations to Observed Runoff for 25 Seasons (1961-62 to 1985-86)

Basin #	Correlation Coefficient r	Regression Slope
1	0.62	2.55
2	0.54	2.41
3	0.48	1.40
4	0.69	2.31
5	0.64	2.69
6	0.75	3.08
8	0.74	1.48
9	0.74	2.33
10	0.84	2.38
11	0.87	6.52
12	0.48	4.22
13	0.85	3.05
14	0.64	1.09
15	0.78	1.88
16	0.38	2.21
17	0.69	1.86
18	0.74	2.83
19	0.71	1.33
Average	0.68	2.53

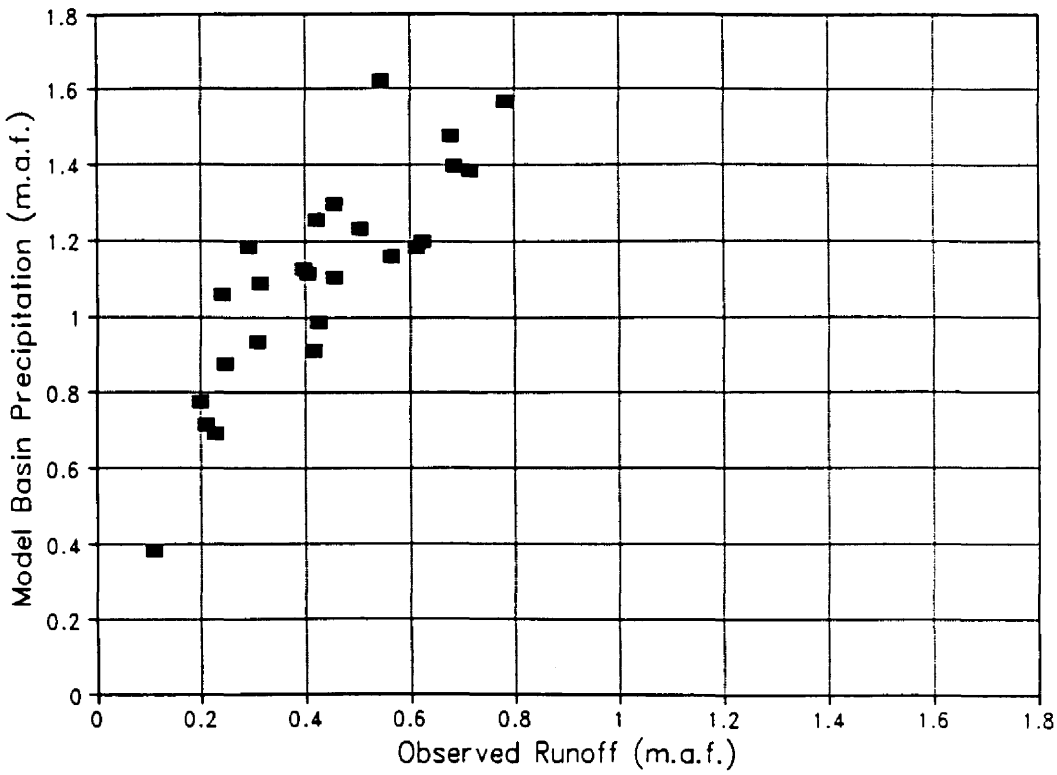

Figure 36. Example of model basin precipitation versus observed March through July (minus baseflow) runoff for the Rio Grande small basin for the winter seasons 1961-62 through 1985-86. Each point represents one water year. The correlation coefficient is 0.84. (m.a.f. = million acre-feet)

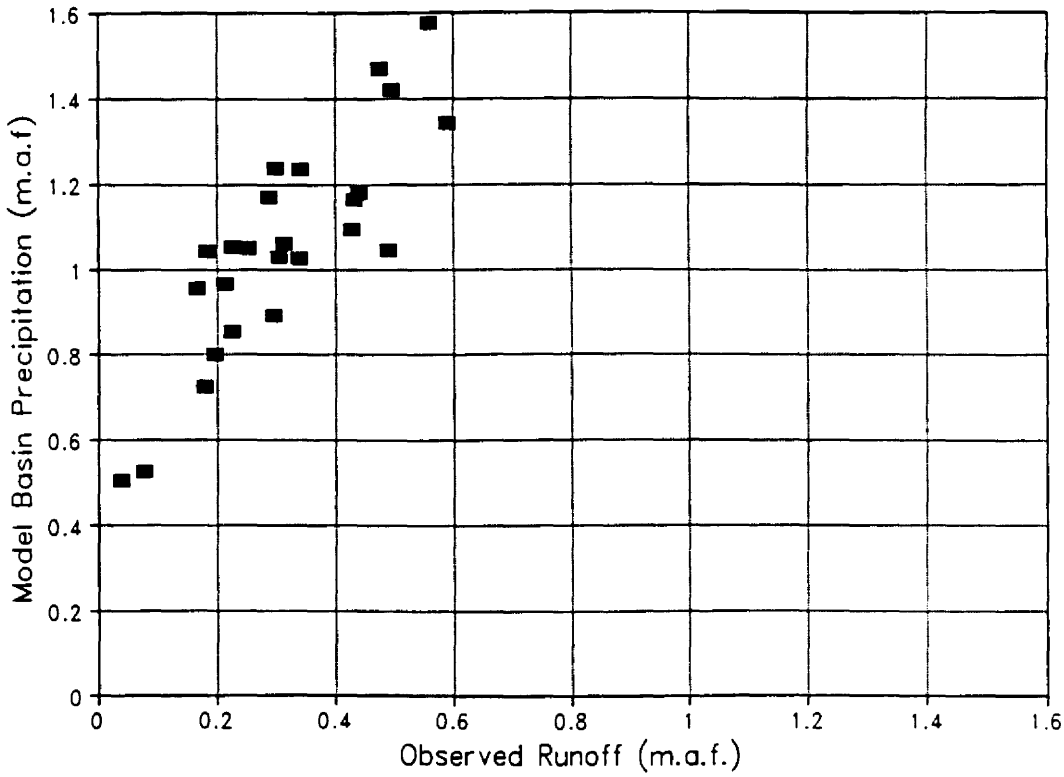

Figure 37. Example of model basin precipitation versus observed March through July (minus baseflow) runoff for the Gunnison small basin for the winter seasons 1961-62 through 1985-86. Each point represents on water year. The correlation coefficient is 0.85. (m.a.f. = million acre-feet)

data set for all six stations for the month of April, 1983. Correlation coefficients using the remaining 22 seasons are shown in Table 7. The average correlation coefficient for all 18 basins increases from 0.68 to 0.75 with the omission of these "problem years".

5.5 Comparison to Daily Precipitation Gauges

Observational data from 42 precipitation gauges located within the model domain were also compared with model calculations. Although daily precipitation gauges have a greater frequency of measurement than monthly snowcourses, few of the gauges are located at high elevations where most of the orographic precipitation falls. They are more often located along roads and in valleys.

As a first comparsion, model computations for cumulative October 15 through April 30 precipitation were correlated with the same period of observational record for each of the 42 sites. The average correlation coefficient for all 42 stations was only 0.43, but this average increases to 0.58 for the 7 stations which are above 9000 feet, and to 0.63 for the three stations located above 10,000 feet. Figure 38 is a scatterplot for Leadville, CO (elev. 10158 feet) for 17 seasons worth of data, and the correlation coefficient was 0.79. In general, the model calculated values displayed better agreement with observations for higher elevation precipitation stations.

Monthly and daily comparisons show a considerable amount of scatter, even for the highest located sites. Nevertheless, the model does quite well for the frequency distribution of events for daily precipitation categories, as can be seen in Figure 39. These comparative frequencies were taken from a compilation of four winter seasons of data for Berthoud Pass (1981-82 to 1984-85). The agreement

Table 7

Summary of Comparisons of Model Basin Precipitation Calculations to Observed Runoff for 22 Seasons (1961-62, 1972-73 and 1982-83 omitted)

Basin #	Correlation Coefficient r	Regression Slope
1	0.79	2.70
2	0.73	2.58
3	0.64	1.48
4	0.82	2.36
5	0.73	2.71
6	0.80	3.09
8	0.83	1.51
9	0.80	2.38
10	0.87	2.38
11	0.92	6.66
12	0.54	4.24
13	0.85	3.07
14	0.72	1.14
15	0.82	1.93
16	0.40	2.20
17	0.71	1.93
18	0.78	2.89
19	0.74	1.36
Average	0.75	2.59

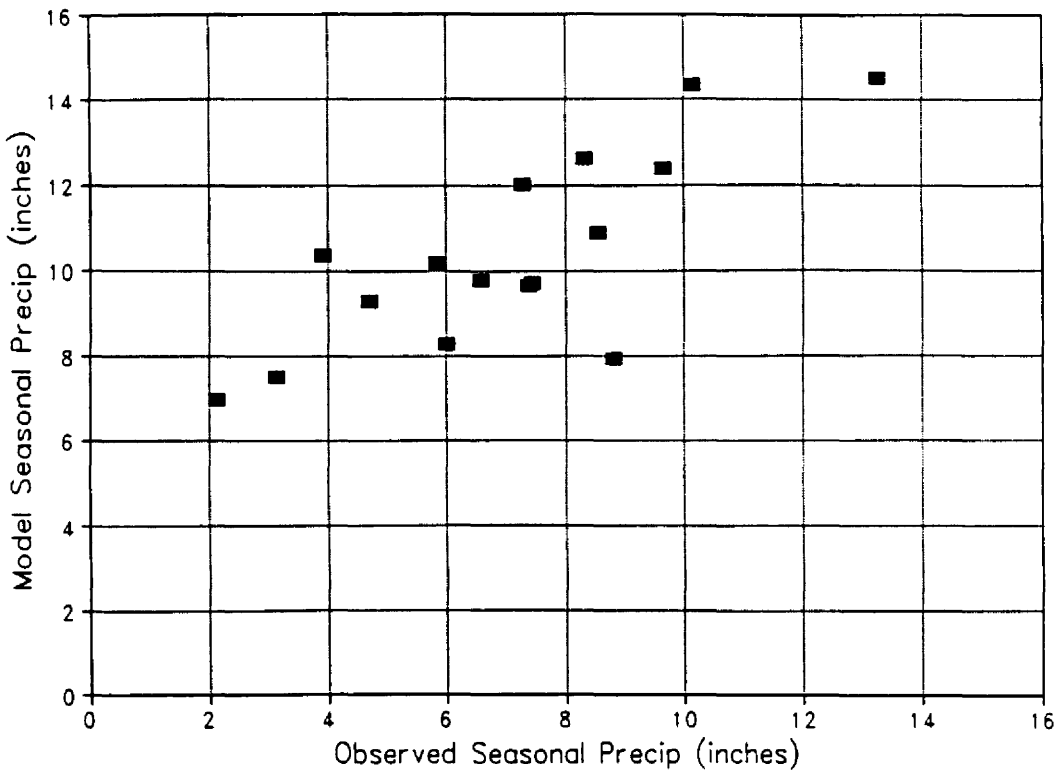

Figure 38. Comparison of model to gauge-measured seasonal precipitation at Leadville. Each point represents one water year. The correlation coefficient is 0.79.

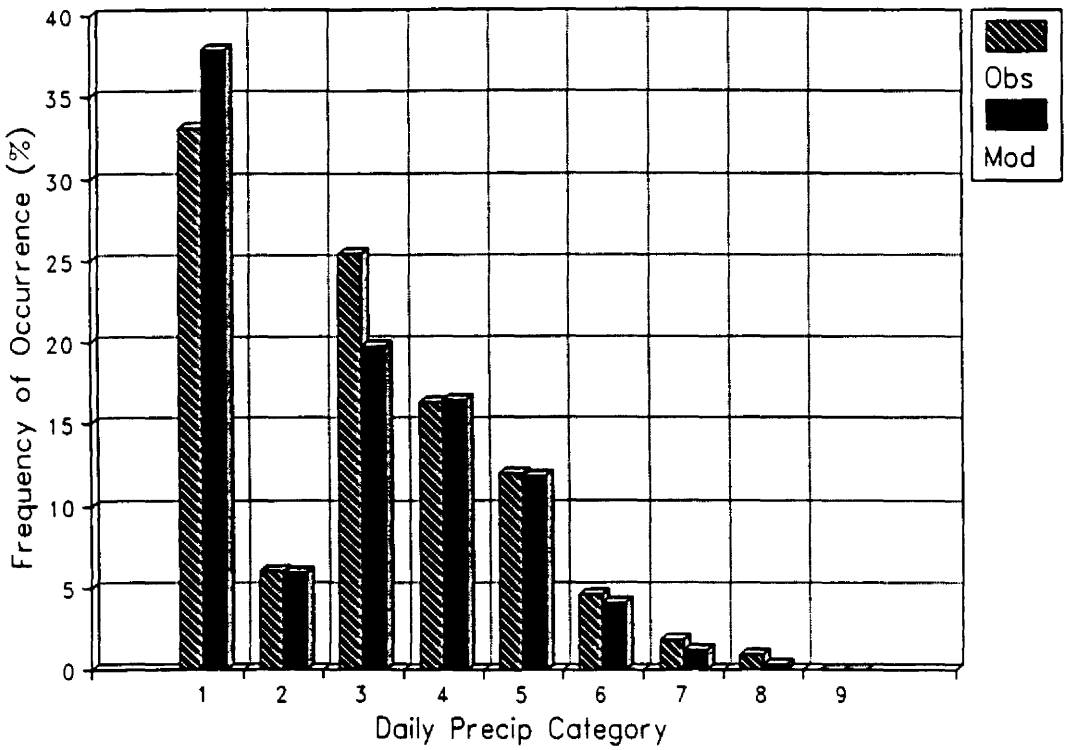

cat #	range (inches)
1	0.0
2	trace
3	0.01-0.10
4	0.11-0.25
5	0.26-0.50
6	0.51-0.75
7	0.76-0.99
8	1.00-1.99
9	>2.00

Figure 39. Comparison of model to observed frequency distribution of daily precipitation amounts for Berthoud Pass for four winter seasons (1981-82 to 1984-85) worth of data or approximately 793 days.

for most of the classes is remarkably equal with the exception of classes 1 (0.0") and 3 (0.01"-0.10"), where the model overpredicts for class 1 by about the same amount that it underpredicts for class 3.

5.6 Attempts to Improve Correlations to Observations

This section will describe the methods and results of two attempts to improve the correlations of model calculations to observations. The first method involved extending the time period of model calculations to include September and early October. The second method consisted of adding observed precipitation gauge data for the early fall and late spring/early summer to the original regression relationships between model basin precipitation and observed runoff for the 18 small basins.

5.6.1 Extension of Model Run Season

In section 5.4 it was shown that the correlations between model basin precipitation and observed runoff for the 18 small basins improved when three "problem years" were excluded from the statistical calculations. One of these years was 1961-62, when heavy September snows fell in the northern and central mountains. These early snows contributed significantly to the seasonal snowpack, but model calculations did not commence until October 15. This discrepancy suggested the possibility of improving the correlations by rerunning the historical calculations using a new, extended model run period of September 1 to April 30.

Accordingly, these calculations were performed for the 27 year historical period and comparisons to the three observational types (snowcourses, streamflow runoff and daily precipitation gauges) were recomputed. For the entire study area over the 27 year period, the model precipitation in September constituted 7.8% of the yearly total

on average while October's contribution was 10.8%. Precipitation data measured at the Berthoud Pass gauge for the years 1964 through 1984 showed that September contributed 8.1% of the observed seasonal precipitation while October contributed 8.8%. The fraction for the period September 1 through October 14 came to 11.9% of the season total.

Table 8 lists the correlation coefficients for model basin precipitation calculations for September 1 through April 30 to observed runoff for 23 seasons excluding 1972-73 and 1982-83. The average was 0.68. This compares with an average of 0.72 using the October 15 through April 30 model run period and removing all three "problem years" (see Table 7). For the precipitation gauges using all 27 years, the average correlation coefficient for all 42 sites increased from 0.43 to 0.54, and the average for the three sites located above 10,000 feet (Berthoud Pass, Climax and Leadville) increased from 0.63 to 0.71. For the snowcourses, the average correlation coefficient for the March 1 values decreased from 0.68 for the October 15 start to 0.58 using the September 1 start.

It is unclear as to why the correlation values increased for the precipitation gauges using the extended run period. Theoretically, the precipitation gauge values should give the best comparison to the model calculations because they directly measure the element that the model calculates, which is precipitation. Also, the observed precipitation values have an advantage over the snowcourse readings and runoff values because the frequency of their measurements is on the same approximate time scale as the model calculations. This is advantageous when the model season is extended to September 1 because the observed period of

Table 8

Summary of Comparisons of Model Basin Precipitation Setember 1 to April 30 Calculations to Observed Runoff for 23 Seasons (1972-73 and 1982-83 omitted)

Basin #	Correlation Coefficient r	Regression Slope
1	0.67	3.04
2	0.63	2.93
3	0.54	1.69
4	0.66	2.72
5	0.64	3.15
6	0.74	3.60
8	0.73	1.74
9	0.70	2.74
10	0.80	2.84
11	0.78	7.88
12	0.51	5.01
13	0.83	3.50
14	0.69	1.28
15	0.80	2.19
16	0.37	2.92
17	0.71	2.19
18	0.75	3.25
19	0.73	1.53
Average	0.68	2.59

record can be correspondingly lengthened to cover the same time frame. However, the precipitation gauge comparisons suffer from the major disadvantage of being located at comparitively low elevations relative to the areas of maximum orographic snowfall distribution, which are primarily the higher peaks. Thus, it is not surprising that the correlation coefficient values are low except for the higher elevation sites, but the rather substantial increase in the values using the extended model run period is unexpected.

On the other hand, it is easier to explain the possible reasons for the decrease in the snowcourse and streamflow runoff correlations when the September 1 to April 30 winter season is used. First of all, it is important to outline the advantages and disadvantages of using the snowcourse and streamflow readings as comparisons to model calculations as opposed to the use of precipitation gauges. Snowcourses are designed to measure the accumulated seasonal snowpack, which is as nearly a conserved quantity as the winter precipitation measured by rain gauges. The main differences are the decreases in the amount of the snowpack due to melting and evapotranspiration losses that can occur over the course of the winter season. These factors are not taken into account in the model. Additionally, snowcourse measurements are not taken as frequently as precipitation gauge measurements. Snowcourse readings are taken only four to five times during the winter season, generally once at the beginning of each month from February to May. However, snowcourses have a distinct advantage over precipitation gauges in that they are located by design in the higher mountainous areas and thus represent a more suitable comparitive data set for the model calculations. This factor is likely the main reason why the

snowcourse correlation values were much higher than the corresponding precipitation gauge values for both winter season periods that were studied.

The streamflow runoff correlations for the 18 small basins were also better than the precipitation gauge results and approximately equal to the snowcourse results on average. This result is not surprising since runoff is primarily governed in Colorado by the melting of the seasonal snowpack. An analysis of precipitation-runoff relationships in the San Juan Mountains as part of the Colorado River Basin Pilot Project showed that 90 percent of the spring and summer runoff in the Animas, Piedra, San Juan and Navajo Rivers is derived from the October through May precipitation (Crow, 1974).

The decrease in the snowcourse and runoff correlations to model calculations when the model's winter season is extended to include September and early October is likely due to the variable weather conditions that can occur during this period that are not taken into account in the model. The majority of the winter precipitation that occurs from mid-October through April falls as snow and the evapotranspiration losses to this accumulated snowpack are minimal. However, September and early October is a transitional period where a portion of the precipitation may fall in the form of rain and thus be lost to soil moisture recharge and evapotranspiration (Linsley, et al., 1975). Conversely, in an anomalous year, such as 1961, there may be significant snow amounts combined with cold temperatures during this period so that the precipitation would contribute heavily to the season snowpack and thus to the subsequent spring runoff. The model does not have the ability to differentiate these variable fall conditions and

simply accumulates all precipitation into the seasonal snowpack. Also, the model does not have the ability to adequately simulate convective showers, which are the primary mode of precipitation during this time of year. The result is substantially lower correlation coefficients between the snowcourse and streamflow runoff observations and model calculations.

5.6.1 Addition of Observational Data to Regression Relationships

A second attempt to improve the correlations to observations involved using observed precipitation data for the early fall period in place of the model calculated values. The first independent variable in the analyses was model small basin precipitation values accumulated for the October 15 to April 30 winter season. The other independent variable was observed September 1 through October 14 precipitation values for one or more gauges located within or near the small basin boundaries shown in Figure 35. In some cases only the September values were available. The dependent variable was the small basin observed runoff as formulated in section 5.4. Computations were made for 8 of the 18 small basins. Similar multiple regression calculations were made using May and June observed precipitation values as the additional independent variable(s) to study the effect of post-model period precipitation.

Table 9 below summarizes the results. In general, the improvement of the relations as compared to the values obtained in Table 6 was modest, but it is also apparent that the correlation coefficients did not decrease as occurred when the model season was lengthened. The addition of the May and June observed values to the regression relationships seemed to have a greater positive impact than the use of

Table 9

Summary of Comparisons of Model Basin Precipitation Calculations Combined with Observed Precipitation Values to Observed Runoff for 25 Seasons (1961-62 to 1985-86)

Type 1 = Model Oct15-Apr30 Basin Precip
Type 2 = Model Oct15-Apr30 Basin Precip + Obs Sep1-Oct14 Precip
Type 3 = Model Oct15-Apr30 Basin Precip + Obs May Precip
Type 4 = Model Oct15-Apr30 Basin Precip + Obs May Precip + Obs Jun Precip

Basin #	Gauge	Correlation Coefficients (r) Type 1	Type 2	Type 3	Type 4
1	Rico	0.62	0.69	0.70	0.71
2	Ames	0.54	0.54	0.57	0.57
	Telluride	0.54	0.62	0.60	0.79
3	Ouray	0.48	0.55	0.51	0.65
4	Tacoma	0.69	0.69	0.73	0.70
	Durango	0.69	0.69	0.71	0.70
	Silverton	0.69	0.67	0.73	0.70
11	Saguache	0.87	0.89	0.88	0.89
	Del Norte	0.87	0.87	0.87	0.87
13	Taylor Park	0.85	0.86	0.88	0.89
17	Eagle	0.69	0.69	0.77	0.81
19	Steamboat Springs	0.71	0.71	0.71	0.71

the September/early October values. This is likely due to the fact that the main snow melt period occurs during May and June, so most of the ground surface is wet and consequently any precipitation during these months is added directly to the snowpack runoff (Crow, 1974). However, as discussed above, the contribution of the September/early October precipitation to the subsequent runoff was not as straightforward.

6.0 1989-90 REAL-TIME SNOWPACK MONITORING RESULTS

The good correlations obtained for model calculated precipitation to observations suggested the possibility of using the model to monitor the current year's snowpack on a real-time basis. For this real-time study, new larger drainage basins were defined to cover the entire model domain. These basins correspond to those defined by the SCS. Calculations were made for only those grid points in each basin located above 9000 feet. This stipulation was included because observational studies have shown that the precipitation which enters streams and reservoirs as runoff is collected from areas primarily located above 9,000 feet (Crow 1967).

The model was run for the 1989-90 winter season for the period October 15 to April 30, as was done for the previous 27 year study. Radiosonde data was obtained from Mountain States Weather, Fort Collins, CO. Monthly reports were prepared describing the model's cumulative precipitation estimates through the end of January, February, March and April. Plots showing the current amount of model calculated precipitation for each of the 13 basins relative to the average, minimum and maximum values determined from the 27 year historical period were included.

The final 1989-90 results for all 13 basins are shown in Figure 40. All of the basins finished below the model averages, with the lowest values occurring for the two southwest basins San Miguel/Dolores and San Juan/Animas. An example of a time series plot for the Colorado

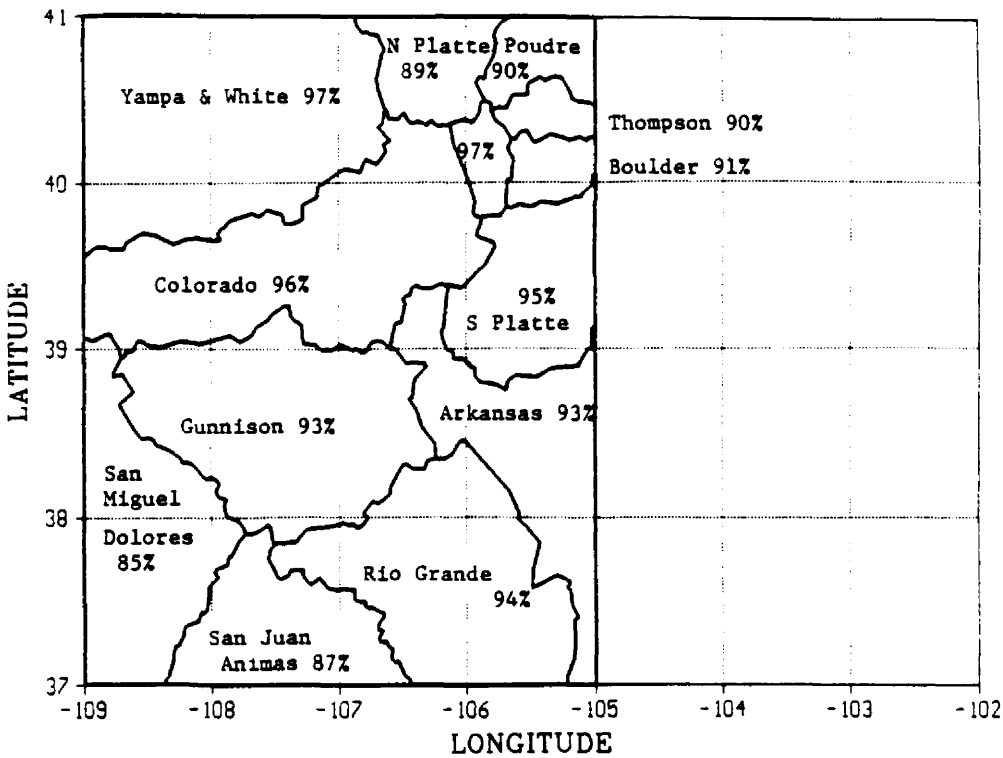

Figure 40. Location and 1989-90 results for the 13 large basins. Values indicate the 1989-90 seasonal total as a percentage of the 27 year historical average for each basin.

Basin is shown in Figure 41. Note that a new minimum basin precipitation value was established for the model near the end of November, an indication of the extreme dryness of the early months.

The monthly reports were designed to coincide with monthly snowpack reports issued by the SCS. Comparison of model calculated values versus observed snowcourse measurements as reported by the SCS through April 30 are shown in Table 10. Generally, the model percentage values exceed the SCS values, especially for the southwest basins.

The isohyetal plot for the model cumulative grid total precipitation is shown in Figure 42. Compared to the model averages based on the 27 year historical period, the individual monthly grid total precipitation was below average for October/November, December and January and above average for February, March and April. The season total was 12,002 inches, which was slightly below the average of 13,048 inches.

In section 5.2, it was shown that the correlation of cumulative monthly grid total precipitation to the season total value increases with time during the course of the winter season. Regression relationships based on these correlations were developed to predict the grid total precipitation at April 30 based on the monthly values. These equations along with their predictions for the 1989-90 season are shown in Table 11.

The equations naturally underpredict the season total due to the below average early season months of October/November and December. In fact, the October/November model precipitation would rank as the 3rd driest if it were included as the 28th year of historical computations.

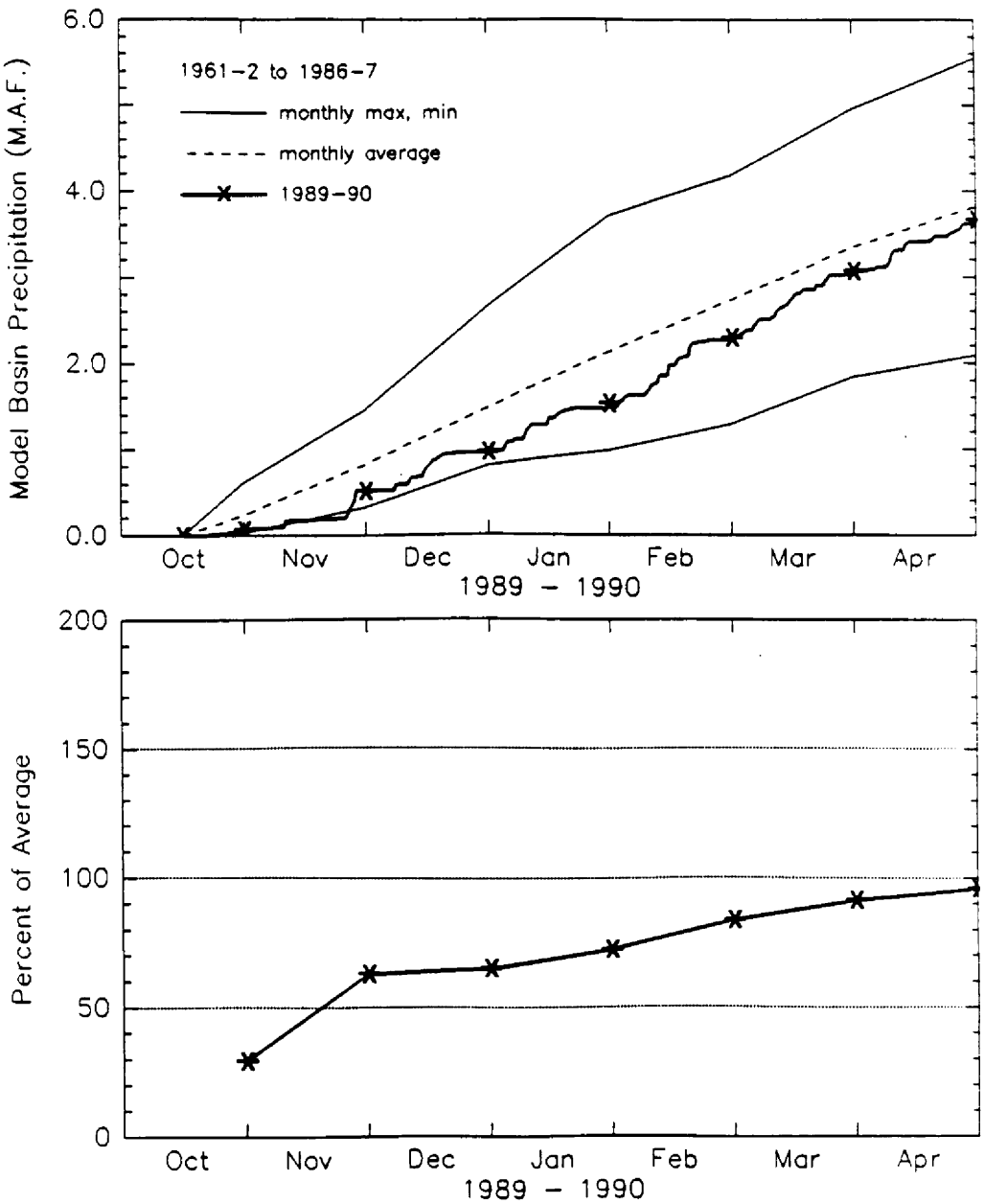

Figure 41. Model basin precipitation time series plot for the Colorado River basin grid points located above 9000 feet

Table 10

Comparison of Percentage of Average Values Between Model Basin Precipitation Calculations to Observed Average Snowcourse Water Equivalent Values for 1989-90

Basin	Model % of Average	SCS Observed % of Average
UPPER GUNNISON	93	65
UPPER COLORADO	96	74
NORTH PLATTE & LARAMIE	89	89
YAMPA & WHITE	97	57
UPPER ARKANSAS	93	82
UPPER RIO GRANDE	94	66
SAN JUAN & ANIMAS	87	68
SAN MIGUEL & DOLORES	85	49
UPPER SOUTH PLATTE	95	80
BIG THOMPSON	90	96
BOULDER CREEK	91	134
CACHE LA POUDRE	90	94
GRAND COUNTY	97	--

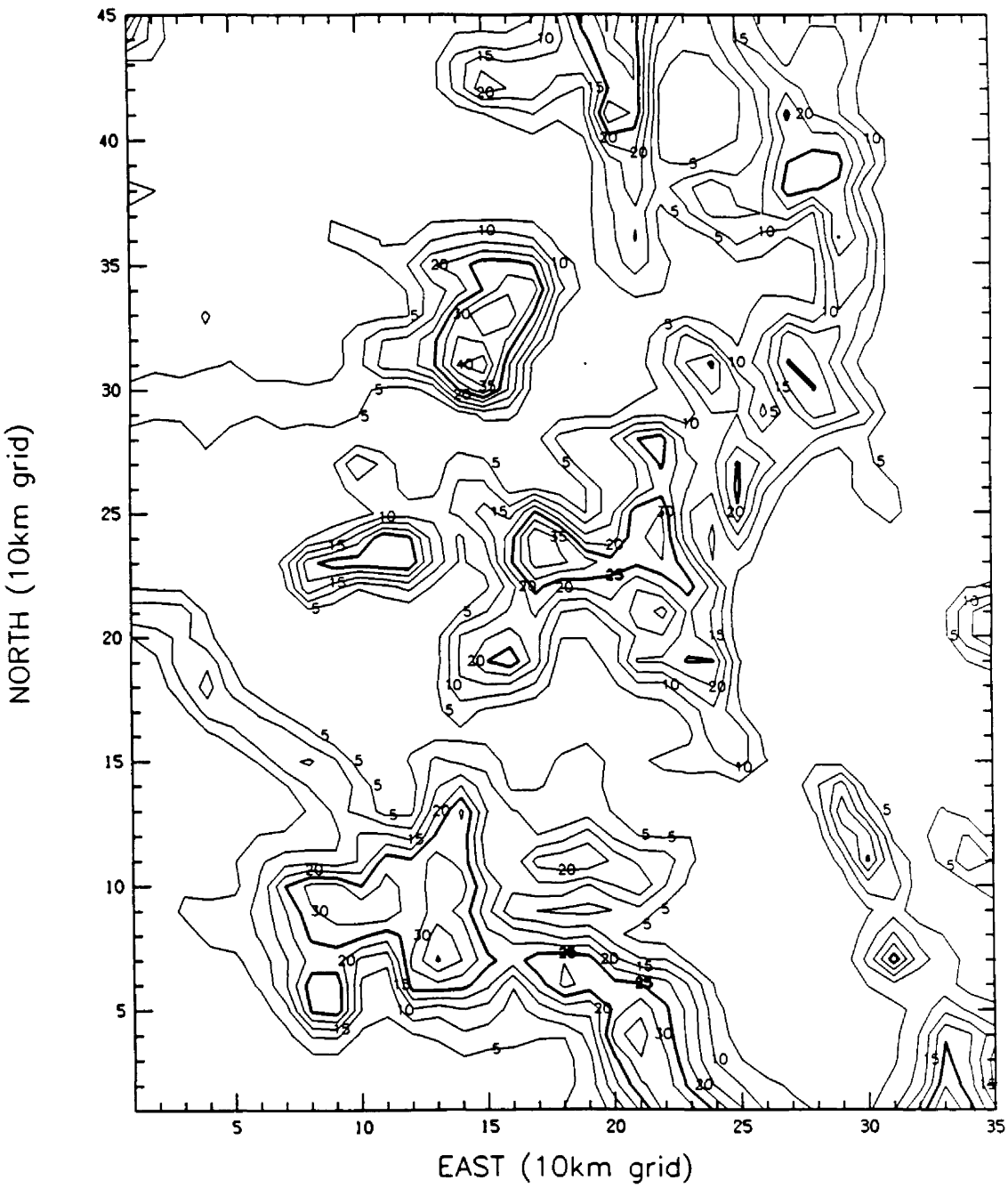

Figure 42. Isohyetal map of model precipitation for the 1989-90 winter season (inches)

Table 11

Predictions for 1989-90 Model Grid Total Precipitation Using Cumulative Monthly Totals

Month	Equation	Prediction	% Average
OCT/NOV	APR = 7597.6 + 1.87*(OCT/NOV)	10353"	79
DEC	APR = 6237.2 + 1.31*(DEC)	9702"	74
JAN	APR = 3217.0 + 1.36*(JAN)	9254"	71
FEB	APR = 2436.0 + 1.15*(FEB)	10526"	81
MAR	APR = 431.2 + 1.11*(MAR)	11333"	87

The December amount would be the 7th driest on record, and the cumulative October 15 through December precipitation amount would be the 2nd driest to the 1976-77 value, which ended up being the driest season overall of the historical period (see Figure 9).

7.0 NGM GRIDDED DATA RUNS

Another way of running the model in a "real-time" fashion is in a predictive sense with National Meteorological Center (NMC) gridded forecast data for input. A special version of the model was designed to ingest NGM or Limited Fine-Mesh Model (LFM) gridded data as input instead of upper air sounding data.

NGM gridded data initialized on February 19, 1987 at 0000 UTC was used as a case study. Data are available for pressure height, temperature and relative humidity in the proper format. For use by the model, the wind data are ingested in zonal and meridional components and converted to direction and speed. Each parameter is available at 850mb, 700mb, 500mb, 400mb and 300mb and the values are first horizontally interpolated to the 10 border points followed by vertical interpolation to 50mb increments. In addition, the fields for vertical velocity at 700mb and 500mb were ingested and averaged to produce large-scale vertical motion estimates.

The resulting precipitation patterns of the predicted gridded fields at 12 hours (870219, 1200 UTC) and 24 hours (870220, 0000 UTC) along with the corresponding patterns produced by the upper air sounding data are shown in Figures 43 through 46, respectively. Fairly good agreement is evident for both cases. The spatial distribution of the precipitation over the study area for a given sounding period is primarily a function of the directional grid used, which is chosen by the interpolated 700mb wind direction at the center of the study area.

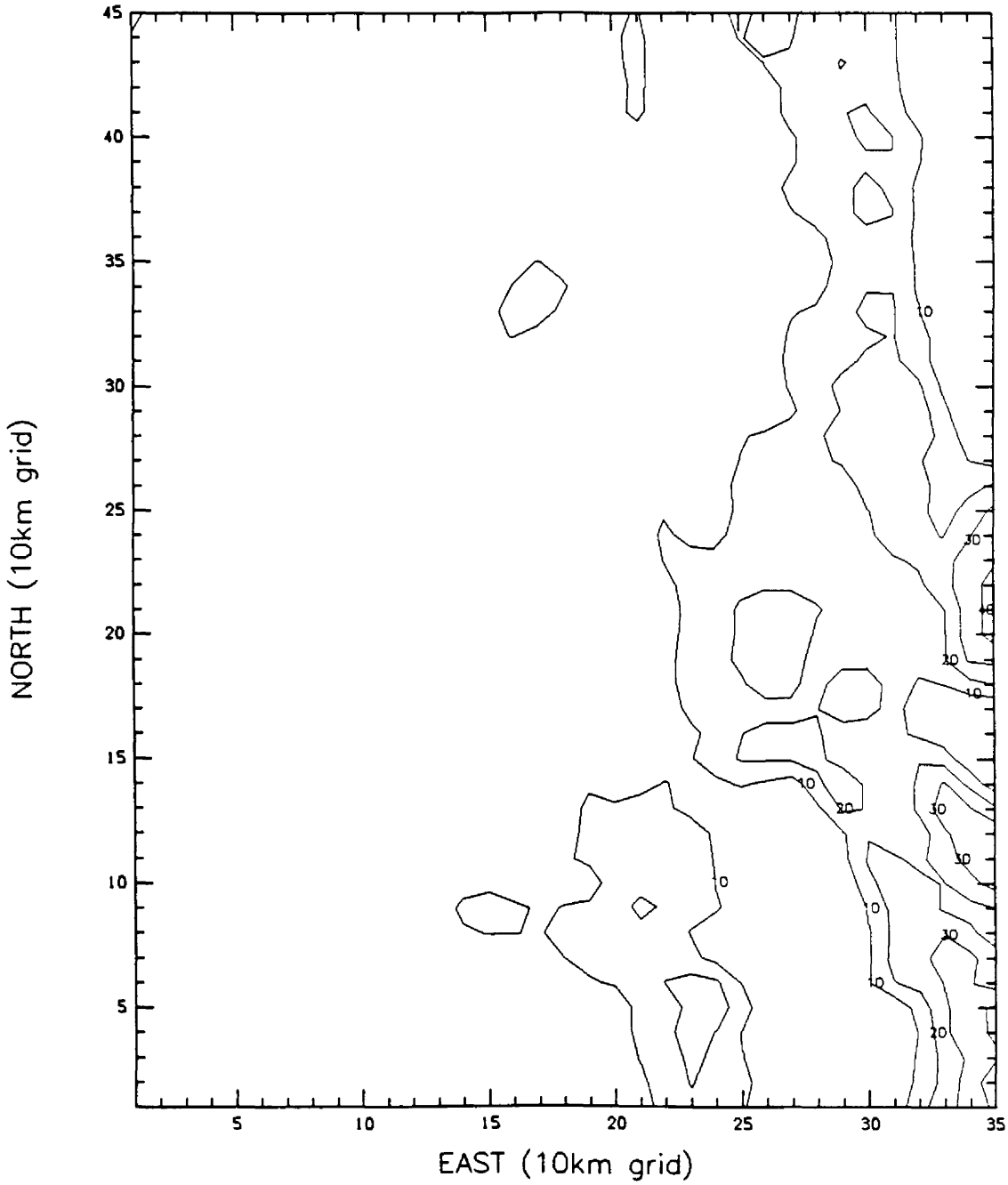

Figure 43. Isohyetal plot of model precipitation using NGM 12 hour forecasted gridded data valid for 1200 UTC on February 19, 1987 (inches*100)

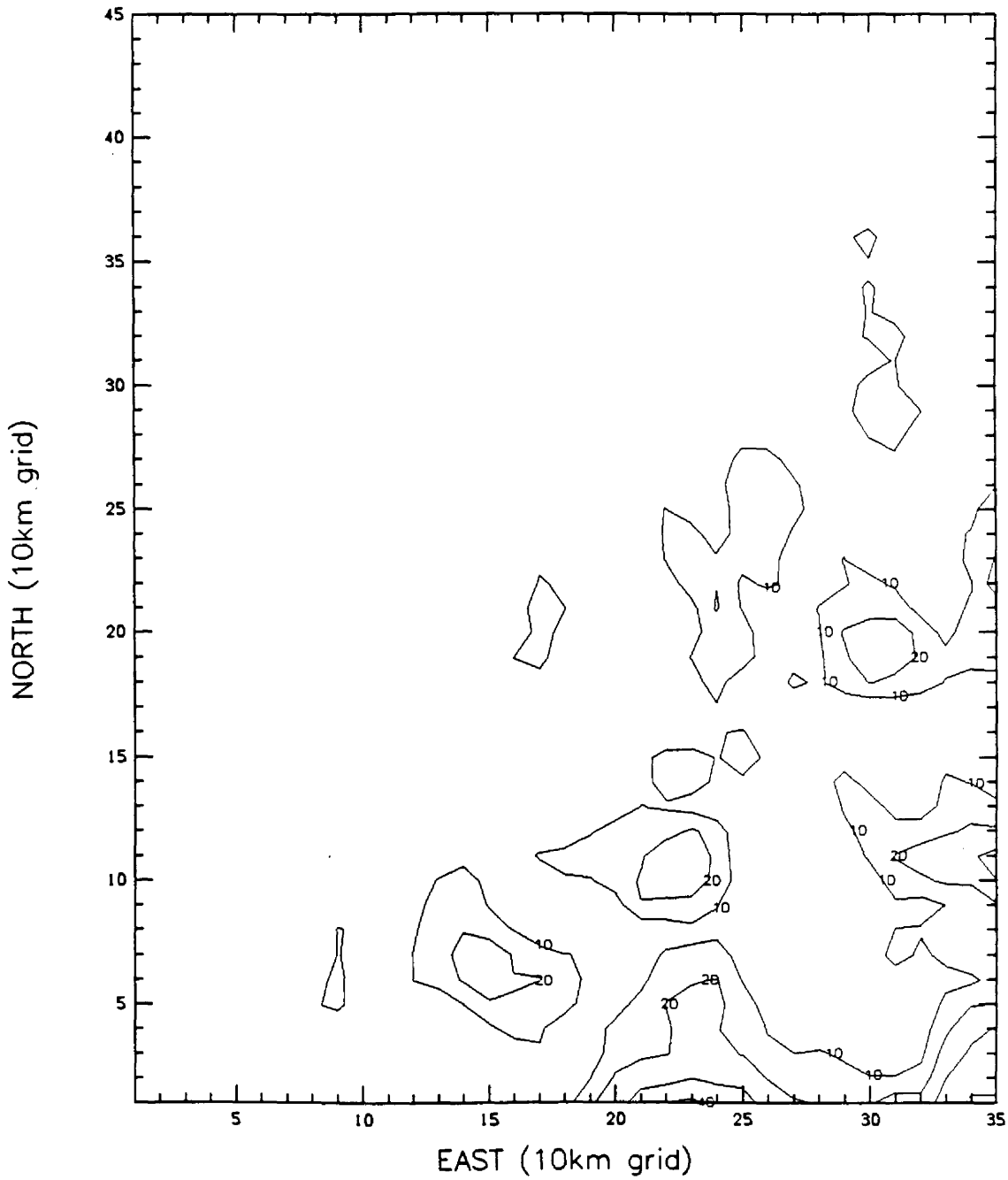

Figure 44. Isohyetal plot of model precipitation using upper air sounding data valid for 1200 UTC on February 19, 1987 (inches*100)

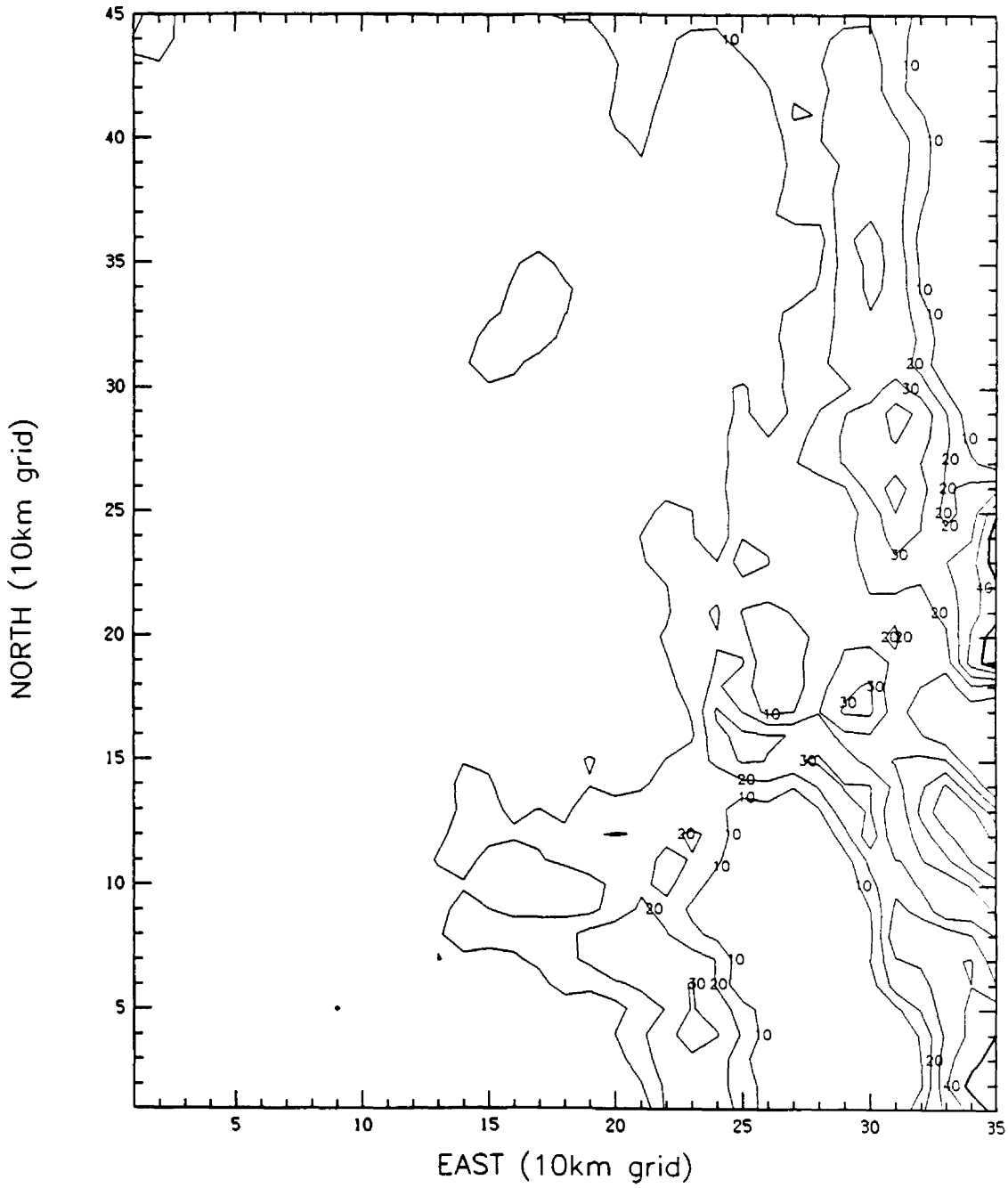

Figure 45. Isohyetal plot of model precipitation using NGM 12 hour forecasted gridded data valid for 0000 UTC on February 20, 1987(inches*100)

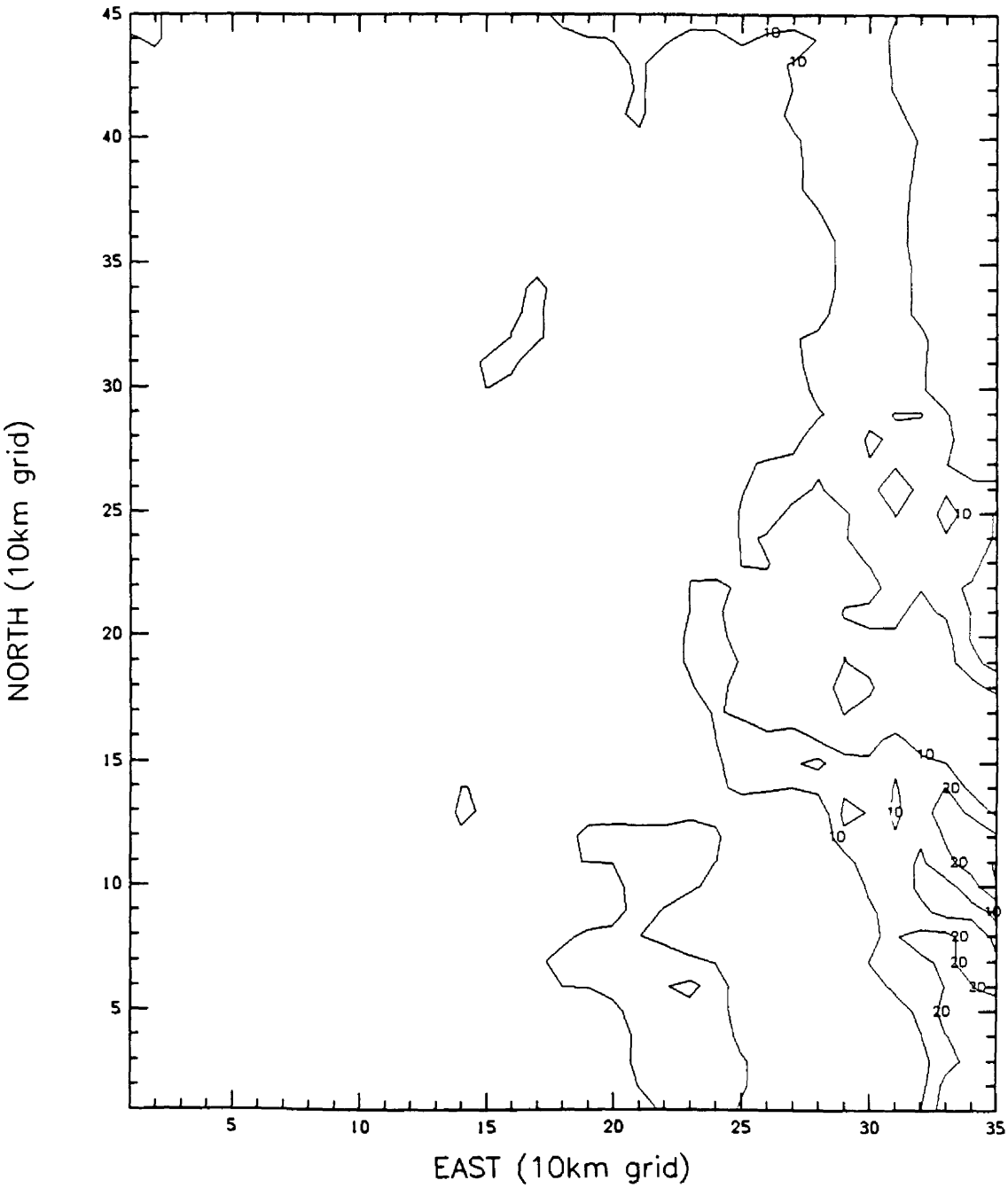

Figure 46. Isohyetal plot of model precipitation using upper air sounding data valid for 0000 UTC on February 20, 1987 (inches*100)

The sounding data for these two periods resulted in the relatively rare cases of southeasterly and easterly flow, with the model employing the 140 degree grid for the February 19 1200 UTC event and the 70 degree grid for the February 20 0000 UTC event. The NGM data duplicated these flow characteristics fairly well, using the 90 degree grid for the February 19 12z event and the 80 degree grid for the February 20 0000 UTC event. The overall precipitation amounts are higher for the NGM data, a result which is likely attributable to the coarser vertical resolution available for the thermodynamic variables and the overestimation of the relative humidity values, which is typical of the NGM in the Rocky Mountain region.

Figure 47 shows the observed daily precipitation amounts for May 19, 1987 for 32 available gauges. The observed amounts showed agreement with both the NGM and the sounding data results in that most of precipitation was confined to the southern and eastern portions of the study area. However, the observed amounts were generally lighter than achieved with either of the model runs. Again, this comparison is hampered by the limited number of high elevation precipitation gauges and the lack of any gauges available in the extreme eastern portion of the study area, which is where the highest amounts were predicted by both model runs. More case studies with gridded data which would cover more of the typical southwesterly flow events are certainly needed to fully test the model's potential predictive ability.

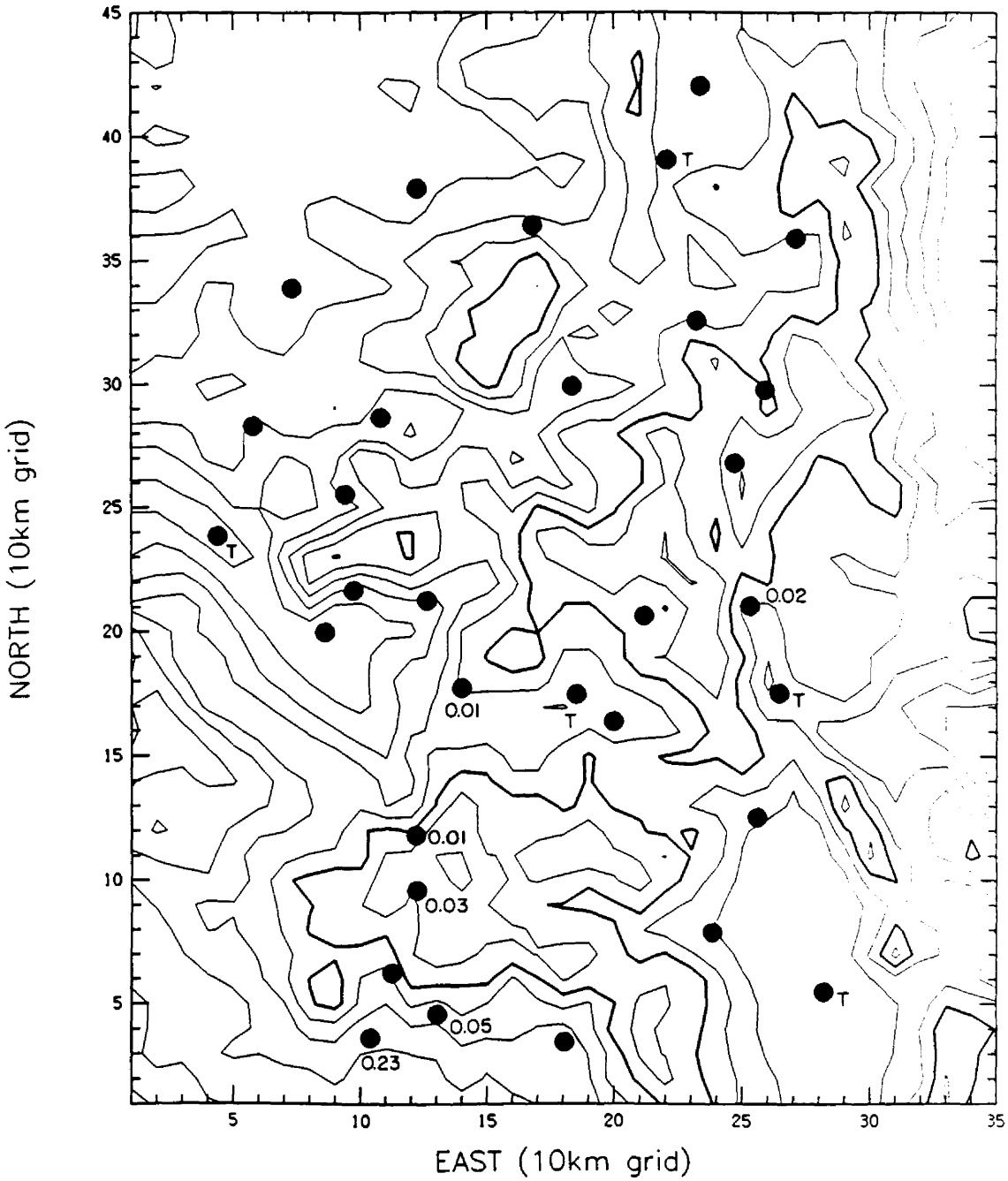

Figure 47. Observed precipitation data (inches) for 32 available gauges for February 19, 1987. (T = trace)

8.0 SUMMARY AND CONCLUSIONS

The main objective of the research described in this paper was to attempt to improve the scientific understanding and diagnostic capabilities of predicting winter orographic precipitation. A current version of the Rhea winter orographic precipitation model was successfully installed on a VaxStation 2000 workstation. Upper air sounding data for the six input stations (Denver, CO; Grand Junction, CO; Lander, WY; Salt Lake City, UT; Albuquerque, NM; and Winslow, AZ) were obtained from the NCAR data archives for a 27 year period. Historical computations were performed for the 1961-62 winter season through the 1987-88 season and the resulting precipitation values were compared to observed values of snowcourse water equivalent, runoff and precipitation gauge data. For the 1989-90 winter season, the model was run on a continuous basis throughout the year, and monthly reports were compiled coinciding with Soil Conservation Water Supply Outlooks to monitor the snowpack status. In addition to these studies, an attempt to improve the statistical comparisons to observations was investigated as well as a study into the model's potential use a forecast product using Nested-Grid Model (NGM) gridded data as input.

The results of the research on the specific objectives listed in Chapter 2 are as follows:

1) Comparison of model precipitation computations to observations results in good positive correlations. Correlation coefficients between model area integrated precipitation and observed snowcourse

water equivalent values ranged from 0.61 to 0.79. Comparisons between model point precipitation calculations and individual snowcourse values for 79 sites show an average correlation coefficient of 0.64 for the February 1 data. This average increases to 0.68 for the March 1 and April 1 data, but decreases to 0.56 for the May 1 data. These data also show that the model's most serious overestimations occur for narrow mountain values and the most serious underestimations occur for broad intermountain valleys. Basin model precipitation was also compared to observed spring and summer runoff, and the correlation coefficients ranged from 0.38 to 0.87 with an average of 0.68. With the removal of three problem years, the average increases to 0.75.

2) Analysis of the model's precipitation distribution for the 27 seasons showed that the average precipitation over the entire study domain is 13,048 inches and that 51.4 percent of the sounding events produce at least 0.01 inches of precipitation. Distribution of all precipitation events by wind direction showed a dominance for southwesterly flow events, with an average of 50.8 percent of all precipitation-producing events occurring between 180 and 270 degrees. The peak occurred for a flow direction of 260 degrees. The distributions of average precipitation amount and percentage of total grid precipitation were likewise skewed toward southwesterly flow directions. Also, the average duration of a precipitation event for the 27 seasons in terms of number of consecutive 12 hour sounding periods that produce at least 0.01 inches of precipitation over the entire grid was 4.1 events, or approximately 48 hours. Good agreement to observations was observed when number of occurrences of long

duration storm events was compared to the relative water year precipitation.

3) Extending the model computational period to September 1 through April 30 did not significantly alter the correlations between model and observed values. The streamflow runoff comparisons for the 18 small basins decreased slightly. The snowcourse sites showed a slight decrease in correlation coefficient values, although the precipitation site values did increase. However, the use of observed fall and spring precipitation data in multiple correlations with model calculated precipitation values increased the correlations to observed small basin streamflow runoff in most cases.

4) The exploratory use of the model to monitor the snowpack in "real-time" indicated that this application is quite feasible, even with modest computing and analysis resources. Monthly reports outlining the precipitation amounts with respect to historical averages for 13 new drainage basins were issued to coincide with SCS Water Supply Outlook Reports. For the 1989-90 winter season, the model computed slightly below normal values for all basins with the substantially lower values for the southern locations. SCS averaged snowcourse May 1 values also showed the southwest basins as the driest, but their values were lower on average compared to the model's. Regression equations for seasonal snowpack developed using the historical data underpredicted the season grid total snowpack due to extremely dry conditions which occurred in the first two and a half months of the 1989-90 model run period.

5) A preliminary study of the use of the model as a forecast product was promising. Model runs using NGM gridded data for one case

study produced predicted 12 and 24 hour precipitation patterns that were similar to the patterns produced from upper air sounding data input.

9.0 SUGGESTIONS FOR FUTURE RESEARCH

The results of this study suggest the following potential utilizations of the model in the future:

1) Continued use as a current year ("real-time") snowpack monitoring tool. Although the 1989-90 results have yet to be compared to observations, the historical results presented in this paper show good correlations to observed spring and summer runoff and the simplistic model design allows for quick and easy processing of the sounding data on a daily basis.

2) Further case studies into the model's use as a predictive aid using NGM or LFM gridded data. Again, the feasibility of this utility is made possible by the fast running time of the model code, which can process a series of forecasts out to 48 hours using gridded data in less than 10 minutes.

3) Interfacing the model precipitation calculations with a hydrological model for better runoff estimates. The precipitation calculations from the snowpack model could be used as input to hydrological model which would take into account such factors as vegetation, slope and aspect, soil moisture conditions and the surface energy budget. Plans were underway at the time of this writing for a joint study with such a hydrological model currently in use by the USGS.

4) Converting the model to run with 5 x 5 km topographical grids. As described in Rhea (1978), both 5 x 5 km and 10 x 10 km grids were

originally developed from the 2.5km grids. Rhea used the 10 x 10 km grids because the marginal gain in overall areal-total precipitation accuracy with 5 x 5 km grids was offset by the quadrupled running time. This is no longer as great a problem due to the increased computer power that is now available.

5) Adapting the model to other mountainous areas, such as Utah or Wyoming. This had already been done for the Atlas Mountains of Morocco (El Majdoub, 1989), the Mogollon Rim of Arizona (Medina, 1991) and the Delaware River basin (Medina, 1991) with considerable success.

6) Use of the model in climate change research. The U.S. Bureau of Reclamation is currently working to link large-scale general circulation models (GCMs) used in global climate simulations at NCAR to mesoscale and local-scale models such as the Rhea model to better simulate the possible impacts of global climate change upon precipitation, evapotranspiration and streamflow in the western United States (Matthews et al., 1991).

Additionally, certain additions to or refinements in the model physics might yield useful results or insights. Some possible areas of study might include redefining the precipitation efficiency function; consideration of three-dimensonal airflow effects, such as channeling; inclusion of a more complete parameterization of convection; and consideration of such phenomena as mesoscale banded precipitation features and short waves. Also, better input radiosonde resolution along with an improved interpolation scheme could vastly improve the results (Rhea, 1981)

In fact, an investigation into improving the precipitation efficiency parameterization was done as part of this study. As

discussed in section 4.4.6, the current scheme originally developed by Rhea (1978) is solely a function of the unlifted cloud top temperature. Rhea expressed in his dissertation the desire for more research aimed at a better understanding into the nature of this parameter. However, only a few studies have been conducted since the development of the model in 1978.

In general, these studies obtained good estimates of precipitation efficiency values for orographic clouds, but they did not explicitly determine the macrophysical and/or microphysical variables upon which the efficiency term must surely depend. Leverson et al. (1979) computed condensation supply rates from upwind rawinsondes in the Park Range of Colorado and compared these to hourly precipitation measurements. The resulting values ranged from 7 to 20 percent for 8 of the 9 storm periods studied. The other period had a value of 49 percent but may have been contaminated by a research cloud seeding project. A similar study by Hindman (1986) utilized the same method also in the Park Range and obtained values ranging from 6 to 14 percent. A field study conducted by the Utah Division of Water Resources and NOAA in the Tushar mountains of Utah from January to March, 1985 incorporated C-band Doppler radar data in conjunction with radiosonde data to measure the water release rates in the cloud (Long, 1986). These rates were compared to hourly precipitation rates to compute the precipitation efficiencies. For the case study of February 8-9, 1985, the resulting efficiency values ranged from 5 percent to 25 percent and seemed to be directly related to the synoptic conditions (prefrontal, frontal passage, postfrontal).

Hopefully, future studies of the precipitation efficiency

parameter in orographic clouds will yield a definition that can be utilized in the Rhea model. However, a new efficiency scheme or any other change in the model physics will likely need to be based on meteorological variables that are contained in the model. Extreme parameter sensitivity is not desirable considering the crudeness of the input data as verified in previous sensitivity studies, where more complex precipitation efficiency parameterizations based on microphysical quantities did not yield better results (Rhea, 1978). The operationally-oriented nature of the model which was achieved by its simplistic design and sole reliance on upper air data as input should remain the paramount consideration with regard to any future modifications.

REFERENCES

Bellamy, J.C., 1949: Objective calculations of divergence, vertical velocity, and vorticity. Bull. Amer. Meteor. Soc., 30, 45-49.

Chappell, C.F., 1970: Modification of cold orographic clouds. Ph.D. Dissertation, Colorado State University, Atmospheric Science Paper No. 173.

Colton, D.E., 1975: Precipitation analysis for operational streamflow forecasting - the use of mesoscale numerical modeling to enhance estimation of precipitation in mountainous areas. Proceedings of AGU Conference on Precipitation Analysis for Hydrologic Modeling, Davis, California, June.

Colton, D.E., 1976: Numerical simulation of the orographically induced precipitation distribution for use in hydrologic analysis. J. Appl. Met., 15, 1241-1251.

Cotton, W.R., G.J. Tripoli, R.M. Rauber, and E.A. Mulvihill, 1986: Numerical simulation of the effects of varying ice crystal nucleation rates and aggregation processes on orographic snowfall. J. Clim. Appl. Met., 25, 1658-1680.

Crow, L.W., 1967: Report on major sub-basin target areas for weather modification in Upper Colorado River Basin. Rep. No. 53, Denver.

Crow, L.W., 1974: Preliminary analysis of precipitation-runoff relationships during summer in the San Juan Mountains, Weather Modification - A Pilot Project, Appendix D, 42 pp.

El Majdoub, A., 1989: Adaptation of the Rhea winter orographic precipitation model to Morroco. Master's Thesis, North Dakota School of Mines and Technology.

Elliott, R.D., 1969: Cloud seeding area of effect numerical model: Aerometric Research, Inc., Report to Fresno State College Foundation, Aerometric Research, Inc., Goleta, California.

Elliott, R.D., and E.L. Hovind, 1964: On convective bands within Pacific Coast storms and their relation to storm structure. J. Appl. Met., Vol. 1, 218.

Elliott, R.D., and R.W. Shaffer, 1962: The development of quantitative relationships between orographic precipitation and airmass parameters for use in forecasting and cloud seeding evaluation, J. Appl. Met., Vol. II, 143-228.

Fraser, A.B., R.C. Easter, and P.V. Hobbs, 1973: A theoretical study of the flow of air and fallout of solid precipitation over mountainous terrain, Part I, Airflow Model: J. Atm. Sci, Vol. 30, No. 5, 801-812.

Hartzell, C.L. and L.W. Crow, 1976: WSSI final report for the Colorado River Basin Project. Fort Collins, 251 pp.

Hindman, E.E., 1986: An atmospheric water balance over a mountain barrier. J. Clim. Appl. Met., 25, 180-183.

Hindman, E.E., 1981: The influence of the Colorado Rockies on precipitation for "wet" and "dry" winters. Colorado State University, 13 pp.

Hurley, P.A., 1972: Colorado Pilot Project: design hydrometeorology. J. Hydraulics Div., 98, 811-826.

Hjermstad, L.M., 1970: The influence of meteorological parameters on the distribution of precipitation across central Colorado mountains. Master's Thesis, Colorado State University, Atmospheric Science Paper No. 163.

Klazura, G.E., 1983: Description of winter precipitation characteristics in the upper Colorado River basin, 16th Conference on Agriculture and Forest Meteorology, Fort Collins, CO.

Leverson, V.H., E.E. Hindman and L.O. Grant, 1979: The precipitation efficiency of winter Colorado mountain clouds, presented at the 3rd WMO Scientific Conference on Weather Modification, Clermont-Ferrand, France, July, 1980.

Linsely, R.K., M.A. Kohler and J.L.H. Paulhus, 1975: Hydrology for Engineers. Second Edition, McGraw-Hill, Inc., 274-281.

Long, A.B., 1986: On the precipitation efficiency of a winter mountain storm in Utah. Atmospheric Sciences Center, Desert Research Institute, Reno, Nevada.

Matthews, D., F. Giorgi and G. Bates, 1991: Modeling regional controls of watershed precipitation for climate change studies. Preprints, Second Symposium on Global Change Studies, 14-18 January, New Orleans, LA, 63-67.

Medina, J.G., 1991: Application of a simple local-scale numerical model in the study of altered climate impacts on watershed precipitation. Preprints, Second Symposium on Global Change Studies, 14-18 January, New Orleans, LA, 68-73.

Meyers, M.P., 1989: An evaluation of the factors affecting wintertime quantitative precipitation forecasts in an explicit cloud model over mountainous terrain. Master's Thesis, Colorado State University, Atmospheric Science Paper No. 450.

Myers, V.A., 1962: Airflow on the windward side of a ridge. J. Geophy. Res., 67, 4267-4291.

Nickerson, E.D., C.F. Chappell, and E.L. Magaziner, 1976: Effects of cold orographic clouds, Atm. Physics and Chemistry Lab Report, NOAA, Boulder, Colorado.

Nielsen, B.C., 1966: A technique for forecasting the rate of snowfall at Alta, Utah. Alta Avalanche Study Center, Project D, Progress Report No. 1, U.S. Dept. of Agriculture, Forest Service, Wasatch National Forest, 15 p.

O'Brien, J.J., 1970: Alternative solutions to the classical vertical velocity problem, J. Appl. Meteor., 9, 197-203.

Panofsky, H.A., 1949: Objective weather map analysis, J. Meteor., 6, 386-392.

Peck, E.L., and M.J. Brown, 1962: An approach to the development of isohyetal maps for mountain areas. J. Geophy. Res., Vol. 67, 681-694.

Peck, E.L., and P. Williams, Jr., 1962: Terrain influences on precipitation in the intermountain west as related to synoptic situations. J. Appl. Met., Vol. 1, 343-347.

Plooster, M.N., and N. Fukuta, 1974: Numerical model of seeded orographic snowfall. AMS Proceedings of Fourth Conference on Weather Modification, Fort Lauderdale, Florida, Novermber.

Rauber, R.M., 1981: Microphysical processes in two stably stratified orographic cloud systems, Master's Thesis, Colorado State University, Atmospheric Science Paper No. 337.

Rhea, J.O., V.H. Leverson, L.O. Grant and J.L. LeCompte, 1981: Utility of special rawinsonde observations in weater modification programs for the Upper Colorado River basin, Final Report to the Bureau of Reclamation, 71 pp.

Rhea, J.O., P. Willis and L.G. Davis, 1969: Park Range atmospheric water resources program. Final report to Bureau of Reclamation (Contract No. 14-06-D-5640), EG&G, Inc., Boulder, Colorado.

Rhea, J.O., 1973: Interpreting orographic snowfall patterns. Colorado State University, Atmospheric Science Paper 192, January, 74 pp.

Rhea, J.O. and L.O. Grant, 1974: Topographic influences on snowfall patterns in mountainous terrain, Advanced Concepts and Techniques in the Study of Snow and Ice Resources, Nat'l Academy of Sci., Washington, D.C., pp 182-192.

Rhea, J.O., 1978: Orographic Precipitation Model for Hydrometeorological Use, Colorado State University, Atmospheric Paper 287, March, 198 pp.

Rogers, C.F., 1970: A mountain precipitation study, Master's Thesis, University of Nevada, Reno.

Sarker, R.P., 1967: Some modifications in a dynamical model of orographic rainfall, Monthly Weather Review, Vol. 95, No. 10, 673-684.

Schermerhorn, V.P., 1967: Relations between topography and annual precipitation in western Oregon and Washington. Water Resources Research, 707-711.

Spreen, W.C., 1947: A determination of the effect of topography upon precipitation, American Geophysical Union Trans., Vol. 28, No. 2, 285-290.

United States Department of Agriculture, 1986: Colorado Annual Data Summary - Water Year 1986, Soil Conservation Service.

United States Department of Agriculture, 1987: Colorado Annual Data Summary - Water Year 1987, Soil Conservation Service.

Willis, P., 1970: A parameterized numerical model of orographic precipitation, Report to the U.S. Bureau of Reclamation, Contract 14-06-D-5640, EG&G, Inc., Environmental Service Operation, Boulder, Colorado.

Wilson, J.W., and M.G. Atwater, 1972: Storm rainfall variability over Conneticut. J. Geophy. Res., 77, (21), 3950-3956.

Young, K.C., 1974: A numerical simulation of wintertime orographic precipitation: Part I. Description of the model microphysics and numerical techniques. J. Atm. Sci., 31, (7), 1735-1748.